A TURBULENT COMBUSTION NOISE MODEL

by

Arun Nathani

Thesis submitted to the Faculty of the

Virginia Polytechnic Institute and State University

in partial fulfillment of the requirements for the degree of

Master of Science

in

Mechanical Engineering

APPROVED:

J. R. Mahan, Co-Chairman

L. A. Roe, Co-Chairman

R. J. Roby

May 1989

Blacksburg, Virginia

A TURBULENT COMBUSTION NOISE MODEL

by

Arun Nathani

J. R. Mahan, Co-Chairman

L. A. Roe, Co-Chairman

Mechanical Engineering

(ABSTRACT)

A turbulent combustion noise model based on first principles is developed in this thesis. The model predicts (1) the pressure time series, (2) Sound Pressure Level (SPL) spectrum, (3) Over-All Sound Pressure Level (OASPL), (4) the thermoacoustic efficiency, (5) the peak frequency, and (6) the sound power of combustion generated noise. In addition, a correlation for sound power is developed based on fundamental burner and fuel variables known to affect the acoustic characteristics of turbulent combustion. The predicted pressure time series exhibits consistency with reality in that it has no steady component. It also confirms speculation in the literature that the predominant noise mechanism in open turbulent flames results from a "transition burning" phenomenon at the flame front. The predicted Sound Pressure Level spectrum, Over-All Sound Pressure Level, and the thermoacoustic efficiency are in excellent agreement with the results available in the literature. The shifts in the peak frequency with basic burner and fuel parameters are consistent with experimental observations from the literature. The disagreements between the predicted and the observed exponents of fuel and burner parameters for sound power are shown to be well within the standard deviation of the experimental observations. Certain areas for further analytical research on the combustion noise mechanism are identified.

Acknowledgements

The author would like to express his sincere appreciation to Drs. J. R. Mahan and L. A. Roe for their guidance, help and encouragement throughout this work. The author would also like to thank Dr. R. J. Roby for serving on his advisory committee.

Finally, the author would like to thank his parents, Mr. and Mrs. and all his family members, for their financial support and more importantly for their never-ending love and motivation.

Table of Contents

List of Illustrations

List of Tables

List of Symbols

a_0, a_n, b_n	Fourier series coefficients
a, b, c, d	Constants in the transition burning expression
b	Order of the 1/3-octave band
c	Velocity of sound in air (m/s)
d	Distance of the field point from source (m)
D	Burner Diameter (m)
E	Expansion ratio (-)
f	Frequency (Hz)
f_c	Frequency of the maximum radiated sound power (Hz)
F	Fuel mass fraction (-)
H	Heat release rate (kJ/s)
n	The effective number of noise sources
$\dot{n}$	The production rate of noise sources (s^{-1})
OASPL	Over-All Sound Pressure Level (dB)
OAPWL	Over-All Sound Power Level (dB)
p	Acoustic pressure (N/m^2)

P	Nondimensional acoustic pressure (-)
q	Source of the sound field (kg $m^{-3}s^{-2}$)
Q	Volumetric flow rate (m^3/s)
R	Radius of the spherical cell (m)
r	Instantaneous radius of the spherical cell (m)
S	Surface area (m^2)
S_L	Laminar flame speed of the fuel (m/s)
S_P	Sound Power (W)
SPL	Sound Pressure Level (dB)
t	time (s)
t_i	Fuel injection time (s)
U	Convective velocity of the fuel (m/s)
V	Volume (m^3)
z	Nondimensional cell diameter (-)

Greek Letters

β	Quantity used to nondimensionalize d^2V/dt^2 (m^3/s^2), Eq. (4.32)
δ	Three-Dimensional Delta Function (m^{-3})
ε	Nondimensional transition time (-)
η	Thermoacoustic efficiency (-)
γ	Quantity used to nondimensionalize acoustic pressure (N/m^2), Eq. (4.34)
ρ	Density of air (kg/m^3)

τ	Nondimensional time (-)

Subscripts

b	Refers to the order of the frequency band
bl	Refers to the quantities associated with the lower frequency of the "b" band
bu	Refers to the quantities associated with the upper frequency of the "b" band
c	Refers to the central burning process
i	Refers to the initial value of the corresponding quantities
n	Refers to the order of frequency
s	Refers to the surface burning process
tr	Refers to the transition burning process
tt	Refers to the complete process of burning

1.0 Introduction

Direct combustion noise occurs when turbulent eddies result in local concentrations of combustible mixture which subsequently are ignited and burn. The complex and random nature of the fluctuations in a turbulent flame produces a noise spectrum which is difficult to predict. It is typical of the type associated with jet noise, containing no discrete peaks, and it extends over about ten octaves. Perhaps, the most significant characteristic of combustion noise detected in the far-field is its predominately low frequency (500 Hz octave band) content.

Turbulent flames are prevalent in a variety of industrial and commercial burners, not to mention propulsion applications. Because a turbulent flame is relatively short and efficient, it has a definite edge over the use of a laminar flame in chemical processing and heating applications. It is somewhat surprising that a predictive ability does not exist for the noise production mechanism in such extensively encountered flames. Many theoretical and experimental investigations have been undertaken during the past 25 years in an attempt to identify the combustion noise mechanism together with its variation with relevant geometric and flow parameters. Many of the theories developed to date are based on, or have been influenced by, experimental correlations. Hence, while

almost all of them successfully predict some particular aspect of the noise production mechanism, their range of applicability is still quite limited. The need for an analytical model that properly reflects the physics of the noise generation process cannot be overstated. The availability of such an analytical model, based entirely on first principles, would subsequently facilitate:

- Development of technology that may be applied to suppress engine core noise in gas turbine power plants,
- Development of acoustic diagnostic techniques to monitor burner combustion performance.

The goal that has been chosen in the present study, then, is the development of such a first-principle model. Complete combustion has been assumed for the development of expressions in this thesis. Also, the destructive interference effects between different compact noise sources in the turbulent flame are not accounted for by the theory.

2.0 Literature Review

Combustion noise may be generally classified as either direct or indirect. Direct combustion noise occurs when local nonuniformities in combustible mixture concentration caused by turbulent mixing of fuel and oxidizer, are ignited and burned. Indirect combustion noise occurs when the local hot spots created by the burning of turbulent eddies are convected through pressure gradients associated with flow restrictions downstream of the burner. Indirect combustion noise also occurs due to the perturbation of the local flow field caused by the increase in volume of the products of combustion. In a ducted configuration there are other complicating factors; for example, direct combustion noise may be modified by the acoustic characteristics of the enclosure. Furthermore, the combustion process itself may be responsive to reflected pressure waves, as is obvious when one considers the sensitivity of reaction rate to, say, pressure. It appears, therefore, that the problem of combustion noise is a complex one, with its study requiring knowledge of combustion, turbulence and acoustical phenomena. The foregoing remarks are summarized in Fig. 1, from Strahle [1]. Lines drawn with question marks indicate interactions which are not currently understood.

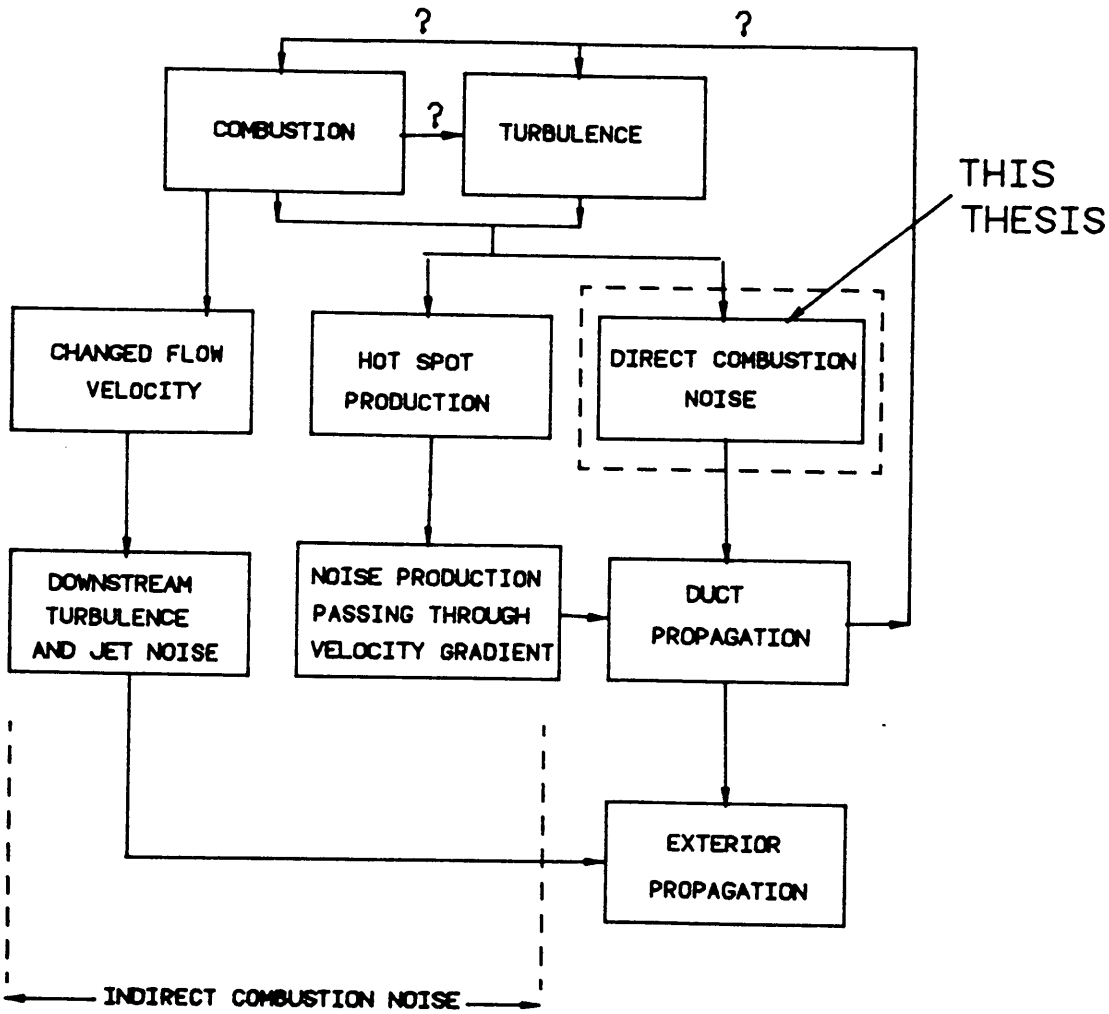

Fig. 1. Relation Among Combustion Noise Mechanisms [1].

The body of experimental and theoretical literature on combustion noise is extensive, and so this review is restricted to those investigations which are directly related to this thesis. Primary emphasis has been placed on past theoretical and semi-empirical attempts to predict or explain observed direct combustion noise characteristics of open, turbulent, gaseous fuel flames. Treatment of indirect combustion noise and the noise generated from ducted burners is excluded. Investigations into various sources of indirect combustion noise can be found in Refs. 2 through 5. A thorough treatment of the combustion noise mechanism in ducted burners can be found in Refs. 6 through 12. The interested reader is referred to Mahan's NASA Contractor Report [13] for a more extensive review of the combustion noise literature. To obtain a greater amount of coherence, the present review is presented in chronological order of publication of the papers cited.

Although much research has been done on combustion noise in the past 25 years, conflicting theories about the dominant generating mechanism still exist. In 1953, Gayden and Wolfhard [14] discussed briefly the generation of flame noise or "combustion roar". However, a decade passed before Bragg [15] enlarged upon their suggested line of thought in a paper that appeared to include all pertinent elements. Bragg's paper, perhaps, was the first attempt to make a fundamental study of the noise produced by a simple turbulent flame. He reasoned that if a small element of air-fuel mixture burns at a constant pressure, and if the heat evolved causes the products to expand, an equivalent volume of the surrounding gases must be displaced. Such a displacement leads to the radiation of a pressure wave, which begins its movement away from the element as soon as burning begins. The pressure wave is followed by an expansion wave which eventually brings the surroundings to rest again when the burning is complete. This wave exhibits a general characteristic of a monopole noise source, namely that the total energy radiated and the intensity at any point both depend on the time rate of

change of the rate of volume evolution (d^2V/dt^2), rather than on the rate of volume evolution (dV/dt) itself. In a steady laminar flame, the rate of fuel consumption everywhere is constant, so d^2V/dt^2 is everywhere zero and the process is theoretically noiseless. In a turbulent flame, on the other hand, although the overall rate of consumption of fuel may be constant, the local rate at a point varies with time. For a small volume element then, $d^2V/dt^2 \neq 0$ and noise is produced. Bragg's rudimentary theoretical analysis suggested that the noise radiated from the expansion of burning fuel might amount to one millionth of the energy released. His treatment was general enough to cover both premixed and diffusion flames, but without experimental data, he could not verify his conclusions nor modify his equation as might be required.

In a published discussion [16] of Bragg's paper, Weinberg suggested the idea of "informed listening" to flames for the possible evaluation of the parameters of turbulence. Bragg replied that a much more detailed mathematical analysis would be needed to answer this question but he had hopes that once this was done noise analysis could indeed be used as a diagnostic tool for investigating flames.

Later that same year, Smith and Kilham [17] performed an experimental study to provide fundamental data on the acoustic energy released by combustion processes. Based on their experimental observations, they relate the sound power S_P radiated by a premixed open turbulent flame to the various geometric and flow parameters,

$$S_P \propto U^2 D^2 S_L^2 , \tag{2.1}$$

where U is the mixture flow velocity, D is the burner port diameter, and S_L is the laminar flame speed. They show that this relationship is similar to the basic equation for the acoustic power output of a monopole source, and go on to conclude that the sound radiated may be considered to arise from a statistical distribution of monopole sources throughout the combustion zone. The combustion noise spectra were found to be typ-

ical of the type associated with jet noise, containing no discrete peaks, extending over many octaves, and rising to a single broad maximum. The major difference between the combustion noise spectrum and that of jet noise was that the former was found to contain a much higher proportion of high frequency components. The 20-dB bandwidth of the combustion noise spectrum can be shown to be about 10 octaves as compared with 6.5 octave for jet noise.

In 1966 Thomas and Williams [18] followed up on the theory of Smith and Kilham. They made an extensive study of the noise produced by a flame developing in a spherical volume of homogeneous premixed combustible gas confined within a soap bubble and ignited by a spark. Such a spherically expanding flame was shown to act as a monopole source of sound, the pressure waveform being dependent on the time rate of change of the rate of increase of volume (that is, d^2V/dt^2) of the gas during combustion. The rate of volume increase was proportional to the burning velocity of the combustible mixture multiplied by the flame area. The pressure in the sound wave emitted by the burning soap bubble was recorded as a function of time and of a fixed distance d from the source. They also derived expressions for the acoustic pressure a distance d from the center of a bubble as a function of its instantaneous radius, for both center and surface ignited bubbles. While they were unable to test the theory for the case of surface ignition, their experimental results for central ignition are in excellent agreement with their theory.

In 1970, Giammar and Putnam [19] suggested that there should be a cancellation effect of the flame noise as the quarter wavelength of the sound approaches the flame length. The reason is that this results in decreased efficiency of the flame as a noise source.

In 1972, Arnold [20] gave an analytical description of the noise produced by burning fuel-air mixtures. He showed that the combustion noise results when the heat release rate of the mixture passing through the reaction zone is variable with time. His argu-

ments and examples suggest that combustion noise from a turbojet engine is caused by random temporal fluctuations in the instantaneous space-integrated area of the flame front in the combustion space. His observations indicate that the combustion noise can be controlled by suppressing the fluctuations. He concluded by suggesting that the benefits other than sound control to be derived from a relatively quiet combustion system include alleviation of sonic fatigue problems, reduction of combustion-induced mechanical vibration, (probably) more stable combustion, and the possibility of higher combustion efficiency.

In 1973 Roberts and Leventhall [21] offered evidence that the major source of noise in open turbulent gaseous premixed flames is fluctuation in the flow velocity reaching the flame front. This gives rise to pressure pulses, whereas discrete turbulent eddies of combustible gas igniting and generating pressure pulses as they burn are not a major contribution to noise in practical applications.

In 1973, Shivashankara, *et al.* [22] extended the results of Smith and Kilham by considering flames with flow velocities to 600 fps, burner sizes to one inch in diameter, and by using several microphone locations. These experiments produced sound power to 10^{-1} W, and thermoacoustic efficiencies as high as 10^{-6}.[1] The scaling law developed, valid for hydrocarbon-air fuel-lean flames anchored on burner tubes, is

$$S_P = 4.54 \times 10^{-5} U^{2.69} D^{2.84} S_L^{1.36} F^{0.4}. \tag{2.2}$$

where F is the fuel mass fraction in the premixed gas and S_P is in watts. The convective velocity and the flame speed are measured in feet per second and the diameter is measured in feet. The standard deviation of these results is 37 percent. Equation (2.2) sug-

[1] Thermoacoustic efficiency (η) is defined as the fraction of the chemical heat release in the combustion process which appears as the acoustic energy in the far-field of burner.

gests that another variable, the fuel mass fraction F, should be considered independently of the flame speed S_L. For fuel-rich flames Shivashankara, *et al.* obtained

$$S_P \propto U^3 D^2 \,. \tag{2.3}$$

The scaling law generated for the frequency of maximum radiated sound power is

$$f_c = 12.57 U^{0.18} D^{-0.08} S_L^{0.52} F^{-.69} \text{ Hz} \,. \tag{2.4}$$

The standard deviation of this result is 13.2 percent. Figures 2 and 3 show the various combustion noise spectra obtained by Shivashankara, *et al.*. The peak frequency is shown to increase with increasing convective velocity, increasing laminar flame speed, and decreasing burner diameter. Their results also indicate that the role of the directivity in combustion noise is insignificant, as evident in Figs. 4 and 5, in which the directivity is shown to be slight, less than 4 dB of variation, with the peak shifting towards the downstream with increasing flow velocity and decreasing port diameter. The authors interpreted these results as consistent with the idea of monopole sources being convected downstream with the flow. In the same paper, the authors also report experimental observations of the thermoacoustic efficiency for premixed open turbulent flames burning in an anechoic chamber. Their regression gives values of the thermoacoustic efficiency between 10^{-8} and 10^{-6}.

On the basis of additional measurements, Strahle [23] in 1975 presented new correlations to replace Eqs. (2.2) and (2.4). The "new" scaling law developed, valid for hydrocarbon-air fuel-lean flames anchored on burner tubes, is

$$S_P = 0.625 \text{ X } 10^{-5} U^{2.67} D^{2.81} S_L^{1.83} F^{-0.26} \,, \tag{2.5}$$

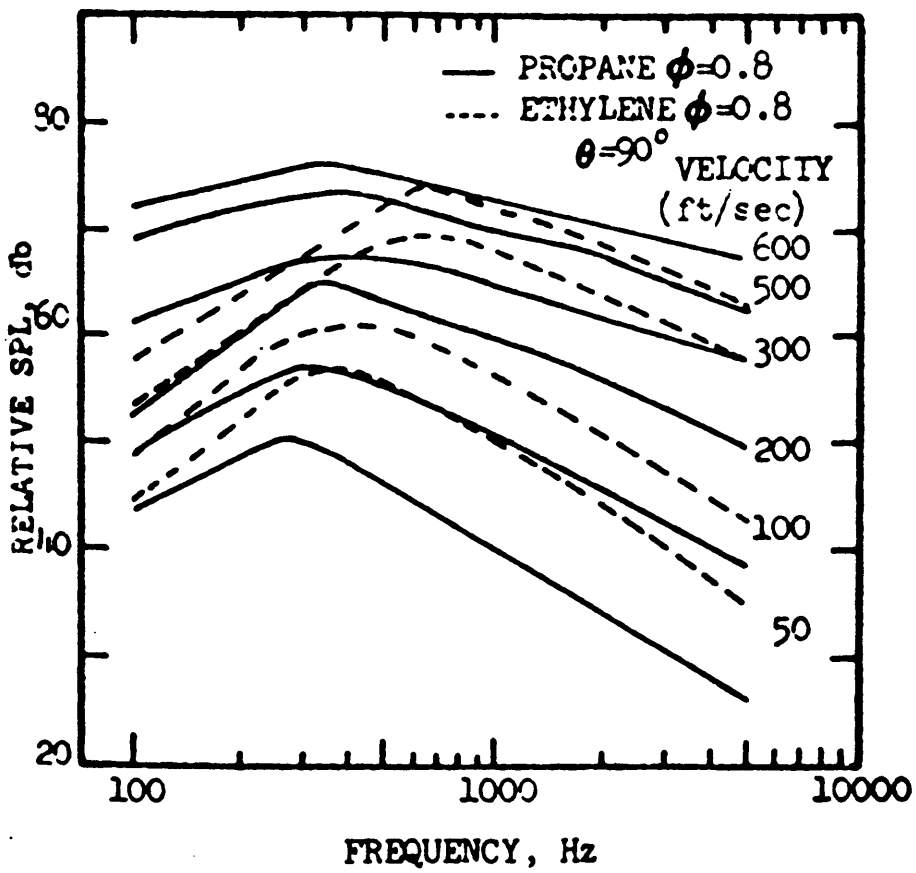

Fig. 2. Effects of Velocity and Laminar Flame Speed on the Frequency Spectra of Premixed Flames [22]

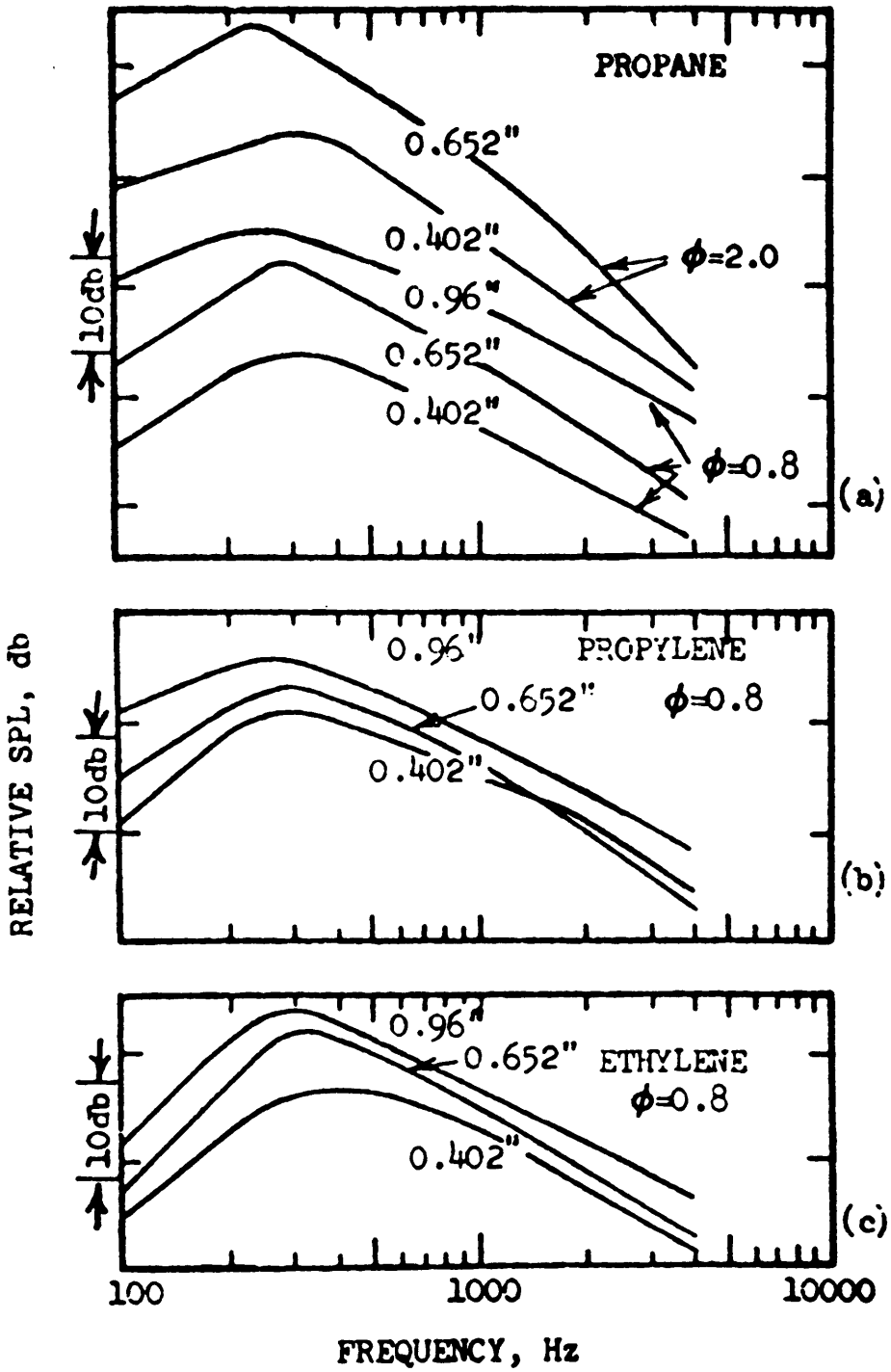

Fig. 3. Effects of Burner Diameter on the Frequency Spectra of Premixed Flames [22]

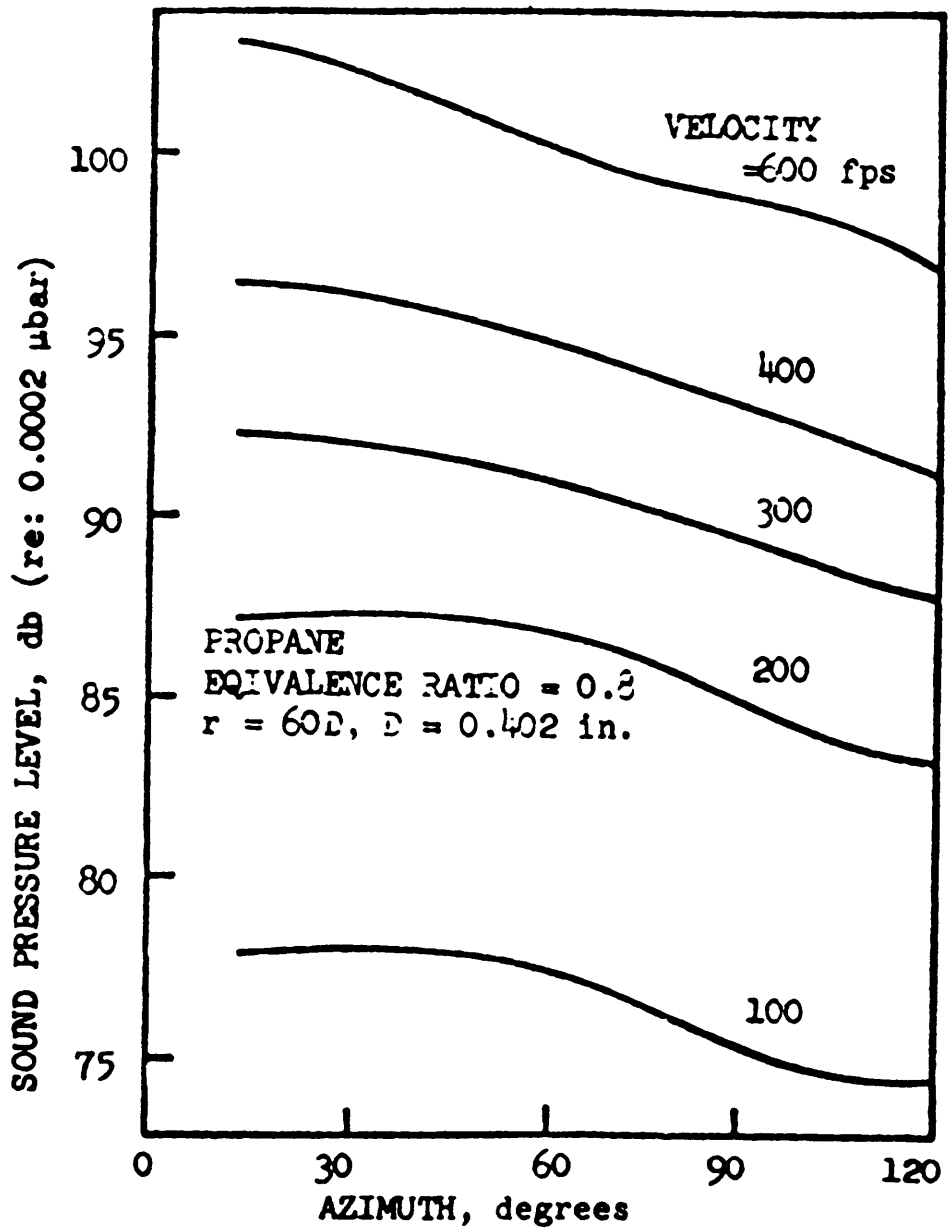

Fig. 4. Directivity as a Function of Flow Velocity in a Typical Open Flame [22]

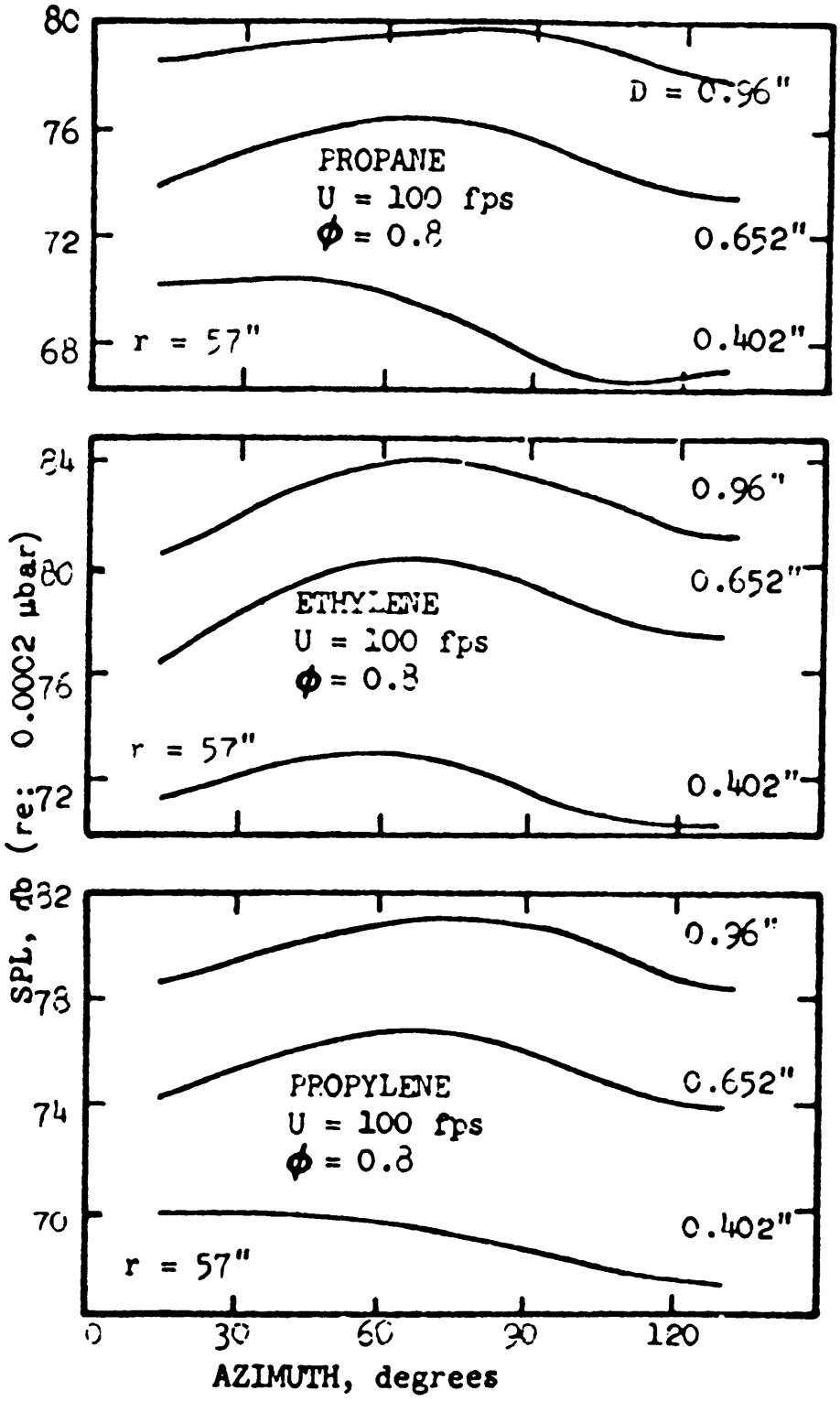

Fig. 5. Directivity as a Function of Burner Diameter in a Typical Open Flame [22]

where the convective velocity and the flame speed are in feet per second, the diameter is in feet and the sound power is in watts. The standard deviation of these results is 43 percent. The revised scaling law developed for the frequency of maximum radiated sound power is

$$f_c = 0.966 U^{0.13} D^{-0.59} S_L^{0.78} F^{-1.1} \text{ Hz} . \tag{2.6}$$

The standard deviation of these results is 23 percent.

In 1979, Ramohalli [24] explored the feasibility of inferring information regarding turbulence and combustion details in turbulent combustion zones through knowledge of the acoustic field. Untill then, the vast majority of the researchers had been investigating the noise radiation from the flame with the view of characterization and suppression of noise. Ramohalli's paper, reminiscent of Weinberg's earlier suggestion [16], raised the question of the inverse possibility, that of utilizing the acoustic field as a valuable tool to diagnose the combustion and turbulence phenomena.

In 1983, Ramachandra and Strahle [25] developed a nonintrusive acoustic technique to obtain the fluctuating heat release distribution in an open premixed turbulent flame. An attempt was made to extract information about the heat release rates with the acoustic spectra as the input. The computed results were qualitatively verified by the emission study of C_2 radicals. The experimentally observed correspondence between mean and rms C_2 emission intensity implied that the shape of the mean heat release rate distribution can, in principle, be deduced by the acoustic technique.

In 1986, Seshan [26] analysed acoustic emission spectra for open nonpremixed turbulent flames. A section of Seshan's spectra is given in Fig. 6. These spectra were analysed for identification of a "predictable" frequency range that is most responsive to, and readily correlated with, combustion efficiency. He also discussed the dependence of the most responsive frequency range on the various Reynolds numbers associated

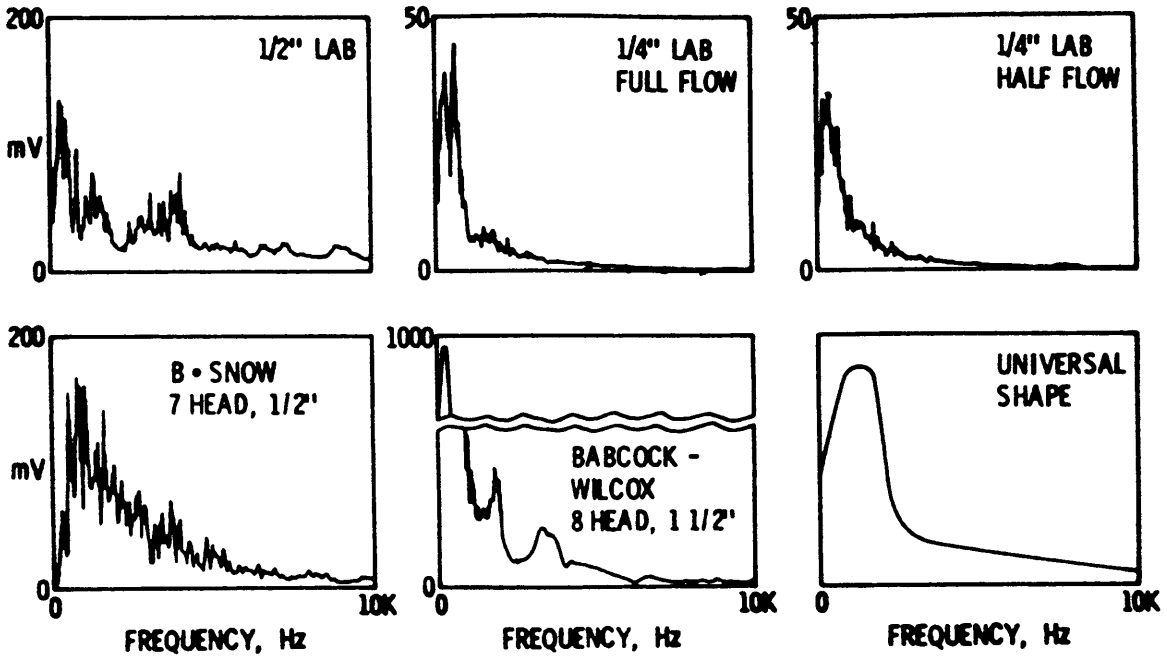

Fig. 6. Behavior of Non-premixed Jet Flames in an Anechoic Chamber [26]

with turbulent jets. He suggested that these results could form a basis for the development of an algorithm to monitor and control gas-fired industrial furnaces through inexpensive, nonintrusive acoustic measurements.

In 1987, Mahan [27] followed up Thomas and William's [18] theoretical development for the surface ignition of isolated bubbles of mixture. His approach to formulating a direct combustion noise model was to assume that the flame is a statistically stationary compact noise source. This implies a physical model in which a stream of turbulent eddies of varying size enters the combustion zone in a random order, but with a statistical size distribution. Mahan assumed that the initial diameters of the eddies were normally distributed about a specified mean value with a specified standard deviation. He then performed a Fourier analysis of the pressure time series produced by a continuous stream of these eddies entering the flame zone and subsequently burning after surface ignition. The resulting line spectrum was then converted into a 1/3 octave band sound pressure spectrum. When representative values of flame speed and reasonable eddy size distributions are introduced into the model, a spectral shape typical of those observed for actual open turbulent flames is obtained.

3.0 Theoretical Background

3.1 Development of a General Acoustic Pressure Expression

In this chapter a general expression for the sound pressure produced by a point source is developed. This expression provides the foundation upon which a more rigorous expression for combustion generated noise is developed in subsequent chapters.

The acoustic wave equation may be written

$$\left(\frac{1}{c^2} \frac{\partial^2}{\partial t^2} - \nabla^2 \right) \frac{f(t - d/c)}{d} = 0 \,, \tag{3.1}$$

where $f(t - d/c)/d$ is the general solution of the wave equation, c is the velocity of propagation of sound in the medium through which the wave propagates, d is the distance of the field point from the source, t is time, and $(t - d/c)$ is the retarded time.

Equation (3.1) does not hold for $d = 0$, which is a point of singularity. Also, at points near the singularity this equation takes a different form. Figure 7 shows a surface S of area $4\pi\varepsilon^2$ surrounding a spherical volume V enclosing points near the singularity $d = 0$. In Eq. (3.1),

$$\frac{1}{c^2}\frac{\partial^2}{\partial t^2}\left(\frac{f(t-d/c)}{d}\right) \to 0 \quad \text{as} \quad d \to 0 .$$

Hence the left-hand side of the wave equation is reduced to the Laplacian operation, $\nabla^2[f(t-d/c)/d]$. Integration of the Laplacian over a vanishingly small volume surrounding the origin may be accomplished with the aid of Gauss' theorem,

$$\int_V \nabla^2\left(\frac{f(t-d/c)}{d}\right)dV = \int_S \frac{\partial}{\partial n}\left(\frac{f(t-d/c)}{d}\right)dS$$

$$= 4\pi\varepsilon^2\left\{\frac{-f(t-\varepsilon/c)}{\varepsilon^2} + \frac{1}{\varepsilon}\frac{\partial}{\partial d}[f(t-\varepsilon/c)]\right\}$$

$$= 4\pi f(t) \quad \text{as} \quad \varepsilon \to 0 . \tag{3.2}$$

The three-dimensional delta function is defined such that it integrates to unity over a vanishingly small volume surrounding the origin. The delta function is denoted by $\delta(x)$, and its dimensions are L^{-3}. It is defined

$$\int_V \delta(\mathrm{x})dV = 1, \quad \text{if V includes x} = 0 ; \tag{3.3a}$$

otherwise,

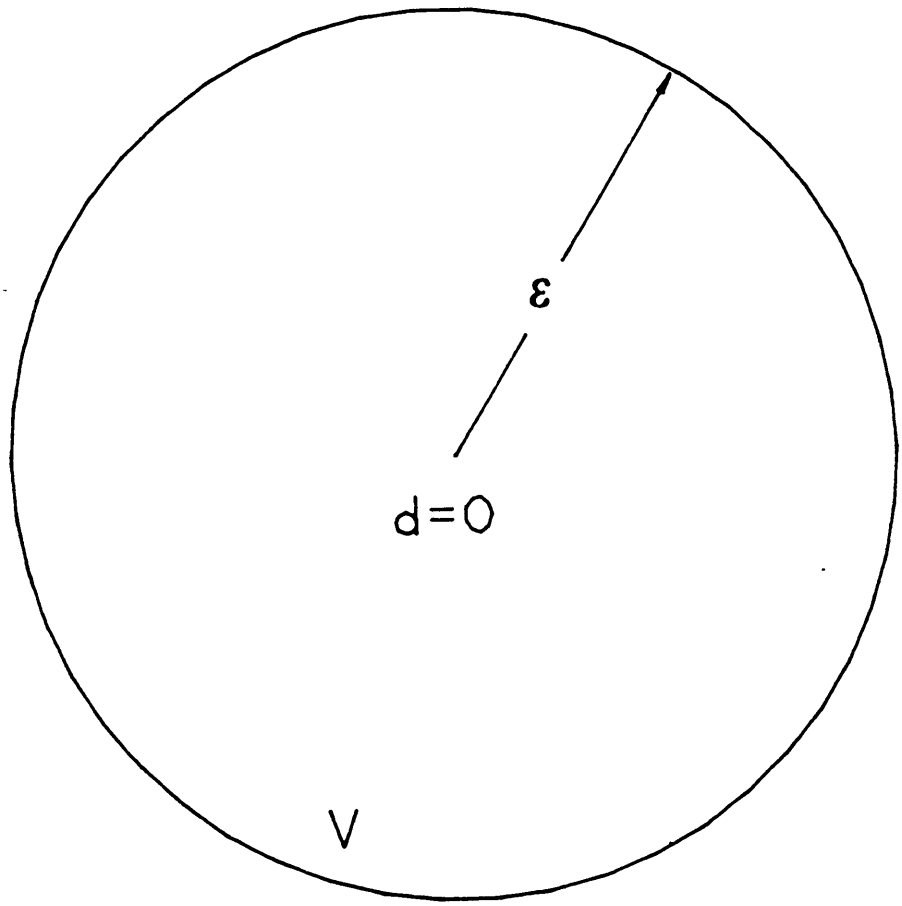

Fig. 7. Representation of the Region Near a Point of Singularity.

$$\int_V \delta(\mathrm{x})dV = 0 \,. \tag{3.3b}$$

That is, $\delta(\mathrm{x}) = 0$ when $\mathrm{x} \neq 0$, but near $\mathrm{x} = 0$ it is sufficiently large so that it's integral over any volume enclosing the origin is unity. Multiplying Eq. (3.3a) by $4\pi f(t)$ yields

$$4\pi f(t)\int_V \delta(\mathrm{x})dV = 4\pi f(t) \,. \tag{3.4}$$

Comparing this result with Eq. (3.2), it follows that

$$\left(\frac{1}{c^2}\frac{\partial^2}{\partial t^2} - \nabla^2\right)\frac{f(t-d/c)}{d} = 4\pi f(t)\delta(\mathrm{x}) \,. \tag{3.5}$$

Equation (3.5) is the basic building block in determining the solutions of practical problems of sound generation.

Sound is defined as a very weak disturbance in a material medium at rest. Such disturbances must conform to the wave equation,

$$\frac{1}{c^2}\frac{\partial^2 p}{\partial t^2} - \nabla^2 p = q \,, \tag{3.6}$$

where $p = p(\mathrm{x},t)$ is the pressure of the sound field and $q = q(\mathrm{x},t)$ is the source of the sound field. In Eq. (3.6), $q = 0$ in the sound field (to satisfy the homogeneous acoustic wave equation), and $q \neq 0$ in the source region V.

Figure 8 shows that the sound emitted at y is heard by the observer at x at a time $|\mathrm{x}\text{-}\mathrm{y}|/c$ after emission. Thus, the expression for $q(\mathrm{x},t)$ is

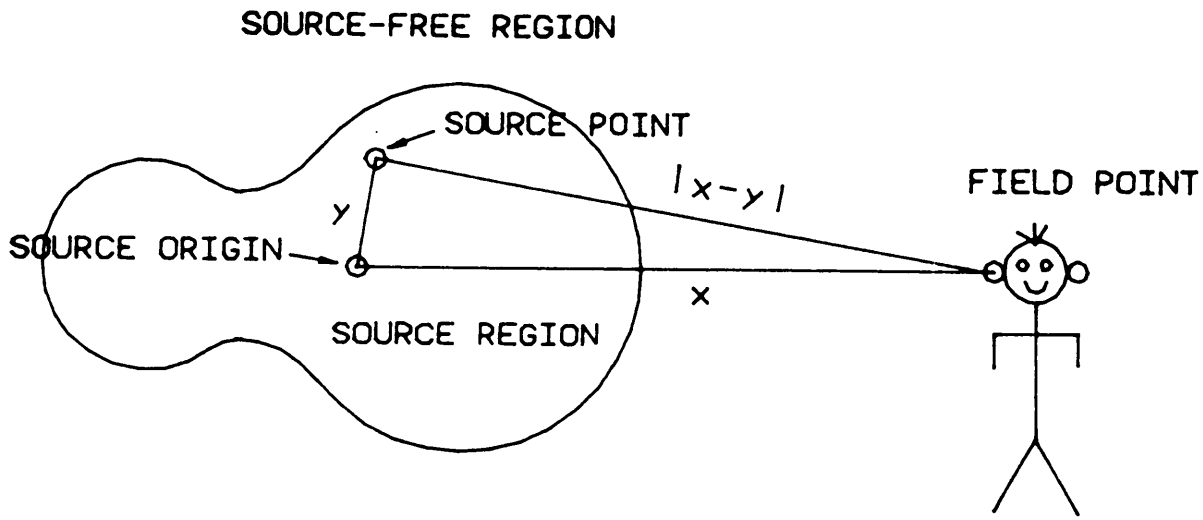

Fig. 8. Time Delay Between the Emission and Observation of Sound.

$$q(\mathrm{x},t) = \int_V q(\mathrm{y},t)\delta(\mathrm{x}\text{-}\mathrm{y})d^3\mathrm{y} \ . \tag{3.7}$$

Comparing Eq. (3.7) with Eq. (3.5), f may be identified with q here, and $\delta(\mathrm{x})$ may be identified with $\delta(\mathrm{x}\text{-}\mathrm{y})$. Therefore, Eq. (3.5) can be rewritten as

$$\left(\frac{1}{c^2}\frac{\partial^2}{\partial t^2} - \nabla^2\right)\frac{q(\mathrm{y},t-d/c)}{d} = 4\pi q(\mathrm{y},t)\delta(\mathrm{x}\text{-}\mathrm{y}) \ , \tag{3.8}$$

where $d = |\mathrm{x}\text{-}\mathrm{y}|$. Integrating this equation over the source volume V, there results

$$\int_V \left(\frac{1}{c^2}\frac{\partial^2}{\partial t^2} - \nabla^2\right)\frac{q(\mathrm{y},t-|\mathrm{x}\text{-}\mathrm{y}|/c)}{|\mathrm{x}\text{-}\mathrm{y}|}d^3\mathrm{y} = \int_V 4\pi q(\mathrm{y},t)\delta(\mathrm{x}\text{-}\mathrm{y})d^3\mathrm{y} \ ,$$

or

$$\left(\frac{1}{c^2}\frac{\partial^2}{\partial t^2} - \nabla^2\right)\int_V \frac{q(\mathrm{y},t-|\mathrm{x}\text{-}\mathrm{y}|/c)}{4\pi|\mathrm{x}\text{-}\mathrm{y}|}d^3\mathrm{y} = \int_V q(\mathrm{y},t)\delta(\mathrm{x}\text{-}\mathrm{y})d^3\mathrm{y}$$

$$= q(\mathrm{x},t) \ . \tag{3.9}$$

Upon comparison of Eq. (3.9) with Eq. (3.6), it may be concluded that

$$p(\mathrm{x},t) = \int_V \frac{q(\mathrm{y},t - |\mathrm{x}\text{-}\mathrm{y}|/c)}{4\pi|\mathrm{x}\text{-}\mathrm{y}|}\, d^3\mathrm{y} \,. \tag{3.10}$$

For a *compact source*, that is, one which is concentrated near a point and is very far from the field point, it can be assumed

$$|\mathrm{x}\text{-}\mathrm{y}| \sim |\mathrm{x}| \sim d \,.$$

Upon substitution of this approximation into Eq. (3.10), there results

$$p(\mathrm{x},t) = \int_V \frac{q(\mathrm{y},t - d/c)}{4\pi d}\, d^3\mathrm{y} \,. \tag{3.11}$$

In the compact source region, the distance d of the observation point from the source point becomes very small. Thus, neglecting d/c compared to t in the compact source region reduces Eq. (3.11) to

$$p(x,t) = \frac{1}{4\pi d} \int_V q(y,t) d^3y \,, \tag{3.12}$$

where q is the volumetric sound source strength. The value of $\int_V q(y,t)d^3y$ yields the effective strength of the region.

3.1.1 Sound Generation in Combustion

In combustion, noise is generated by "turbulent eddies" which, as they burn, generate a pressure wave due to the expansion of the hot products of combustion, and so act as monopole sources of sound. The strength of such an ideal monopole source is $\rho(d^2V/dt^2)$, where ρ is the density of the medium through which the sound is propagating, and d^2V/dt^2 is the rate of change of volume evolution of the source. Replacing $\int_V q(y,t)d^3y$ by $\rho(d^2V/dt^2)$ in Eq. (3.12), the equation for acoustic pressure in combustion takes the form,

$$p(x,t) = \frac{\rho}{4\pi d}\left(\frac{d^2V}{dt^2}\right). \tag{3.13}$$

Based on this expression, a solution for the acoustic pressure at a distance d from the burning source can be obtained.

3.2 The Burning Sphere

A differential equation for the acoustic pressure as a function of the rate of change of increase in volume of a monopole source was developed in the previous section. In this section, this expression, Eq. (3.13), will be used to obtain expressions for the acoustic pressure for the case of a burning sphere. Most of the results presented in this section are consequence of Thomas and William's [18] and Mahan's [27] work.

Consider a sphere of combustible gas. Separate expressions are developed for: (1) ignition at the surface, and (2) ignition at the center. Subscript s denotes the case of surface ignition, while subscript c represents the case of central ignition.

3.2.1 Ignition at the Surface

Assume that a sphere of combustible gas of initial radius R_s is ignited at the surface and that an infinitely thin flame propagates radially inwards toward its center. This process is assumed to take place at constant pressure, and so the sphere expands during the process, as shown in Fig. 9. Let the ratio of volume occupied by burned gas to that occupied by the same gas before burning be denoted by E. For an instantaneous radius r_s of the unburned mixture sphere, the volume occupied by the burned gas *before* it was burned is given by

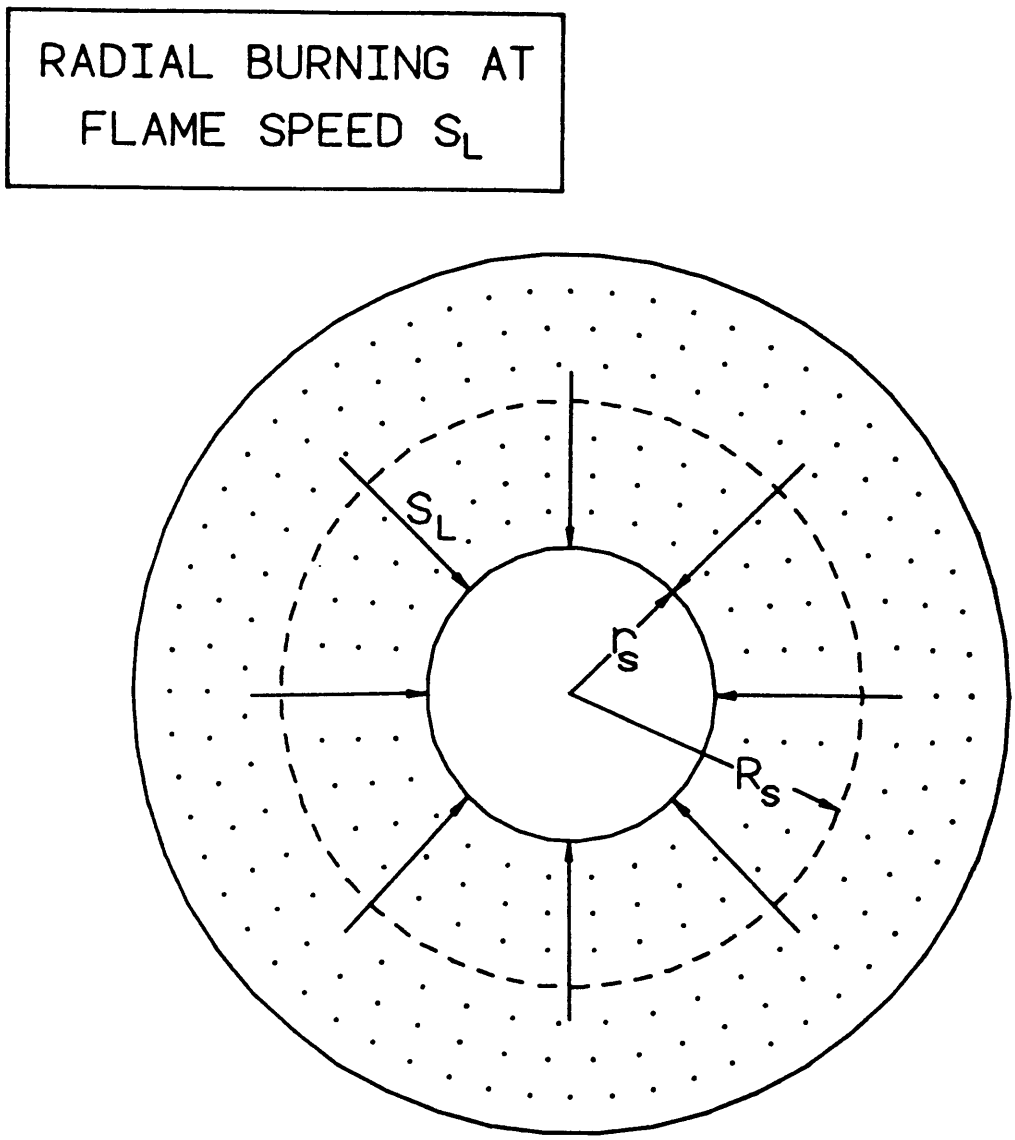

Fig. 9. Increase in Volume of a Surface Ignited Sphere.

$$V_{ub} = \frac{4}{3}\pi(R_s^3 - r_s^3) .$$

At the moment depicted in Fig. 9 this gas now occupies a volume

$$V_b = E\left[\frac{4}{3}\pi(R_s^3 - r_s^3)\right] .$$

Therefore, the increase in volume on burning is given by

$$\Delta V = V_b - V_{ub} = (E-1)\left[\frac{4}{3}\pi(R_s^3 - r_s^3)\right] .$$

The rate of increase in volume is given by

$$\frac{dV}{dt} = \frac{d}{dt}(\Delta V)$$

$$= \frac{d}{dt}\left\{(E-1)\left[\frac{4}{3}\pi(R_s^3 - r_s^3)\right]\right\}$$

$$= -\frac{4}{3}\pi(E-1)3r_s^2\frac{dr_s}{dt}$$

$$= -4\pi(E-1)r_s^2\frac{dr_s}{dt} . \qquad (3.14)$$

Upon substitution of Eq. (3.14) into Eq. (3.13), there results

$$p_s = \frac{\rho}{4\pi d}\frac{d}{dt}\left(\frac{dV}{dt}\right)$$

$$= \frac{\rho}{4\pi d}\left\{-4\pi r_s^2\frac{d^2r_s}{dt^2} - 8\pi r_s\left(\frac{dr_s}{dt}\right)^2\right\}(E-1)$$

$$= -\frac{\rho}{d}\left\{r_s^2\frac{d^2r_s}{dt^2} + 2r_s\left(\frac{dr_s}{dt}\right)^2\right\}(E-1)\,. \qquad (3.15)$$

If S_L is the constant flame front velocity (that is, the laminar flame speed), then

$$S_L = -\frac{dr_s}{dt} = \text{constant.} \qquad (3.16)$$

Thomas and Williams [18] in their development of Eq. (3.16) overlooked the "minus" factor in the expression. This mistake was later corrected by Mahan [27]. The total burning time, t_s, is given by

$$t_s = \frac{R_s}{S_L}\,. \qquad (3.17)$$

Upon substitution of Eq. (3.16) into Eq. (3.15), there results

$$p_s = -\frac{2\rho r_s}{d}(E-1)S_L^2\,. \qquad (3.18)$$

The instantaneous radius at any time is given by

$$r_s = R_s - S_L t\,. \qquad (3.19)$$

Upon substitution of Eq. (3.19) into Eq. (3.18), there results

$$p_s = -\frac{2\rho(R_s - S_L t)}{d}(E-1)S_L^2\,,$$

or,

$$\left(\frac{d}{D_s}\right)\left(\frac{p_s}{\rho S_L^2(E-1)}\right)=\left(\frac{S_L}{R_s}t-1\right), \tag{3.20}$$

or finally,

$$z_s P_s = \tau_s - 1 , \tag{3.21}$$

where

$$z_s = \frac{d}{D_s},$$

$$P_s = \frac{p_s}{\left[\rho S_L^2(E-1)\right]} ,$$

and

$$\tau_s = \frac{t}{t_s} = \frac{S_L t}{R_s} .$$

Equation (3.21) which was first derived by Mahan [27], differs from Thomas and Williams' incorrect result, which was

$$z_s P_s = 1 - \tau_s .$$

3.2.2 Ignition at the Center

Assume that a sphere of initial radius R_c is ignited at the center and that an infinitely thin flame propagates radially outward toward its surface. This process is, like the pre-

vious one, assumed to take place at constant pressure, and so the sphere expands during the process, as shown in Fig. 10. For a radius r_c of burned gas, the volume of burned gas is given by

$$V_b = \frac{4}{3}\pi r_c^3 .$$

This gas, unburned, had occupied a volume of

$$V_{ub} = \frac{4}{3}\pi r_c^3 / E .$$

Therefore, the increase in volume on burning is given by

$$\Delta V = V_b - V_{ub} = \frac{4}{3}\pi r_c^3 \left(1 - \frac{1}{E}\right) .$$

The rate of increase of volume is given by

$$\frac{dV}{dt} = \frac{d}{dt}(\Delta V)$$

$$= \frac{d}{dt}\left\{\frac{4}{3}\pi r_c^3 \frac{E-1}{E}\right\}$$

$$= 4\pi r_c^2 \left(\frac{E-1}{E}\right)\frac{dr_c}{dt} . \qquad (3.22)$$

Upon substitution of Eq. (3.22) into Eq. (3.13), there results

$$p_c = \frac{\rho}{4\pi d}\frac{d}{dt}\left(\frac{dV}{dt}\right)$$

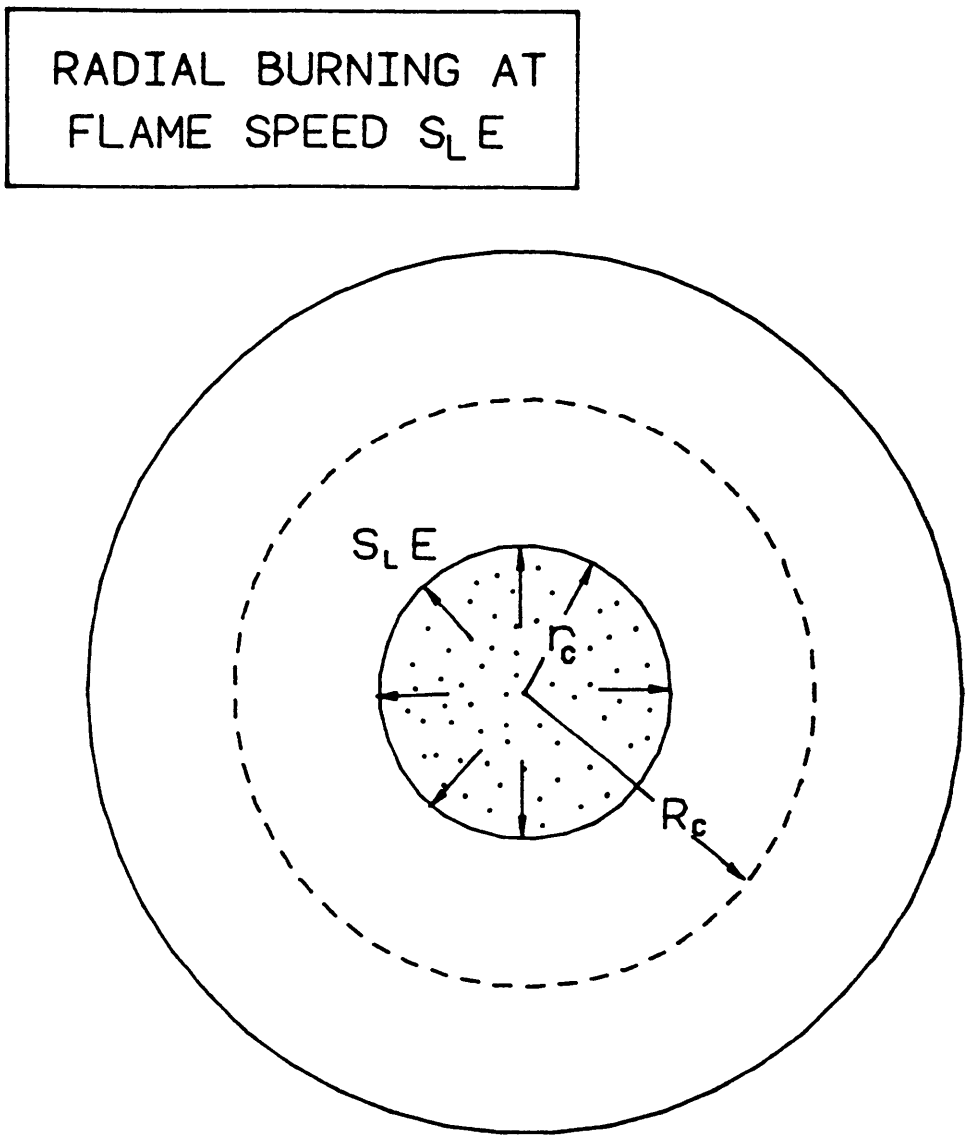

Fig. 10. Increase in Volume of a Center Ignited Sphere.

$$= \frac{\rho}{4\pi d}\left\{4\pi r_c^2 \frac{d^2 r_c}{dt^2} 8\pi r_c\left(\frac{dr_c}{dt}\right)^2\right\}\frac{E-1}{E}$$

$$= \frac{\rho}{d}\left\{r_c^2 \frac{d^2 r_c}{dt^2} + 2r_c\left(\frac{dr_c}{dt}\right)^2\right\}\frac{E-1}{E} \,. \tag{3.23}$$

If S_L is the constant flame speed, then

$$S_L = \frac{dr_c}{dt} = \text{constant} \,. \tag{3.24}$$

Upon substitution of Eq. (3.24) into Eq. (3.23), there results

$$p_c = \frac{2\rho r_c}{d}\left(\frac{E-1}{E}\right)S_L^2 \,. \tag{3.25}$$

The instantaneous radius r_C is given by

$$r_c = S_L E t \,. \tag{3.26}$$

Upon substitution of Eq. (3.26) into Eq. (3.25), there results

$$p_c = \frac{2\rho}{d}(E-1)S_L^3 t \,. \tag{3.27}$$

If R_C' is the final radius of the burned gases, then

$$\frac{4}{3}\pi R_c'^3\left(1-\frac{1}{E}\right) = \frac{4}{3}\pi(R_c'^3 - R_c^3) \,,$$

or,

$$R_c' = R_c E^{1/3} \,. \tag{3.28}$$

If t_C is the total burning time, then

$$R_c' = S_L E t_c \,. \tag{3.29}$$

Upon substitution of Eq. (3.29) into Eq. (3.28), there results

$$t_c = \frac{R_c E^{-2/3}}{S_L} \,. \tag{3.30}$$

Finally, upon substitution of Eq.(3.30) in Eq.(3.27), there results

$$p_c = \frac{2\rho}{d}(E-1)S_L^3 \frac{t}{t_c}\left(\frac{R_c E^{-2/3}}{S_L}\right),$$

$$\left(\frac{d}{D_c}\right)\left(\frac{p_c}{\rho(E-1)S_L^2 E^{-2/3}}\right) = \left(\frac{t}{t_c}\right),$$

or

$$z_c P_c = \tau_c \,, \tag{3.31}$$

where

$$z_c = \frac{d}{D_c} \,,$$

$$P_c = \frac{p_c}{\rho(E-1)S_L^2 E^{-2/3}} \,,$$

and

$$\tau_c = \frac{t}{t_c} \ .$$

The development of Eq. (3.31) follows of Thomas and Williams' [18] and leads to the same result when their equation is nondimensionalized.

3.3 *Mahan's Model for a Surface Ignited Sphere*

Mahan [27] argued that surface ignition, rather than central ignition, was a more plausible model to describe the burning of a turbulent eddy in the combustion zone. This section is devoted to his solution of the acoustic pressure expression, Eq. (3.21), for the case of a surface ignited sphere. His approach to formulating a direct combustion noise model was to assume that the flame is a statistically stationary compact noise source where a single continuous stream of spherical cells enters the flame zone and subsequently burns after surface ignition. A "single continuous stream of burning cells" means that only one cell burns at a time. After the fuel content of this cell is completely consumed, the next cell enters the combustion zone, and so on.

The nondimensional acoustic pressure equation for a surface ignited sphere, derived in the previous section, is

$$z_s P_s = \tau_s - 1 \ , \tag{3.32}$$

where Eq. (3.32) is defined only for $0 < \tau_S \leq 1$, so that $z_S P_S \leq 0$. Remember that for $\tau_S < 0$, the bubble volume is constant, and so $dV/dt = 0$. Then at time $\tau_S = 0$ (ignition), the volume suddenly begins to change and dV/dt suffers a discontinuity. The mathematical consequence of this is that the second derivative of V with respect to t is a half Dirac delta function; that is,

$$z_s P_s(0) = \frac{1}{2}\,\delta(0)\ . \tag{3.33}$$

The line spectrum produced by a continuous train of such burning cells may be obtained by computing the Fourier series of the periodic function of period $\tau_s = 1$. The result is a line spectrum corresponding to the Fourier series

$$z_s P_s = a_0 + \sum_{n=1}^{\infty} a_n \cos(2\pi n\tau_s)d\tau_s + \sum_{n=1}^{\infty} b_n \sin(2\pi n\tau_s)d\tau_s\ . \tag{3.34}$$

The corresponding time series for Eq. (3.34) is

$$z_s P_s(\tau_s) = \frac{1}{2}\,\delta(\tau_s), \quad \tau_s = 0, 1, 2,\ldots\ ,$$

$$z_s P_s(\tau_s) = \tau_s - 1, \quad 0 < \tau_s < 1, \quad 1 < \tau_s < 2,\ldots\ . \tag{3.35}$$

Evaluation of the Fourier constants a_0, a_n and b_n, results in

$$a_0 = 2\int_0^1 z_s P_s(\tau_s)d\tau_s$$

$$= 2\int_0^{\varepsilon} \delta(\tau_s)d\tau_s + 2\int_{\varepsilon}^{1} (\tau_s - 1)d\tau_s$$

$$= 1 + 1 - 2$$

$$= 0\ . \tag{3.36}$$

$$a_n = 2\int_0^1 z_s P_s(\tau_s)\cos(2\pi n\tau_s)d\tau_s$$

$$= 2\int_0^{\varepsilon} \delta(\tau_s)\cos(2\pi n\tau_s)d\tau_s + 2\int_{\varepsilon}^1 (\tau_s - 1)\cos(2\pi n\tau_s)d\tau_s \, .$$

Upon integration of the above equation, there results

$$a_n = \frac{2\cos(0)}{2} + 2\left(\frac{1}{2\pi n}\right)^2[\cos(2\pi n) - \cos(0) + 2\pi n \sin(2\pi n)]$$

$$-\left(\frac{2}{2\pi n}\right)[\cos(2\pi n) - \cos(0)]$$

$$= 1 + 2\left(\frac{1}{2\pi n}\right)^2(1 - 1 + 0) - \frac{1}{n\pi}(1 - 1) \, ,$$

or finally,

$$a_n = 1, \quad n = 1,2,3,\ldots,\infty \, . \tag{3.37}$$

$$b_n = 2\int_0^1 z_s P_s(\tau_s)\sin(2\pi n\tau_s)d\tau_s$$

$$= 2\int_0^{\varepsilon} \delta(\tau_s)\sin(2\pi n\tau_s)d\tau_s + 2\int_{\varepsilon}^1 (\tau_s - 1)\sin(2\pi n\tau_s)d\tau_s \, ,$$

which upon integration, yields

$$b_n = \frac{2\sin(0)}{2} + 2\left(\frac{1}{2\pi n}\right)^2[\sin(2\pi n) - \sin(0) - 2\pi n\cos(2\pi n)]$$

$$-\left(\frac{2}{2\pi n}\right)[-\cos(2\pi n) + \cos(0)]$$

$$= 1 + 2\left(\frac{1}{2\pi n}\right)^2(0 - 0 - 2\pi n) - \frac{1}{n\pi}(1 - 1)\,,$$

or finally,

$$b_n = -1/n\pi, \quad n = 1,2,3,\ldots,\infty\,. \tag{3.38}$$

The nondimensional pressure amplitude corresponding to the Fourier series given by Eq. (3.34) is

$$|z_s P_s| = \sqrt{a_n^2 + b_n^2}\,,$$

or

$$|z_s P_s| = \sqrt{1 + \left(\frac{1}{n\pi}\right)^2}\,, \quad n = 1,2,3,\ldots,\infty\,. \tag{3.39}$$

This result was first derived by Mahan [27]. The corresponding function of the rate of change of volume is shown in Fig. 11, the corresponding acoustic pressure in Fig. 12, and the line spectrum for the nondimensional pressure amplitude in Fig. 13.

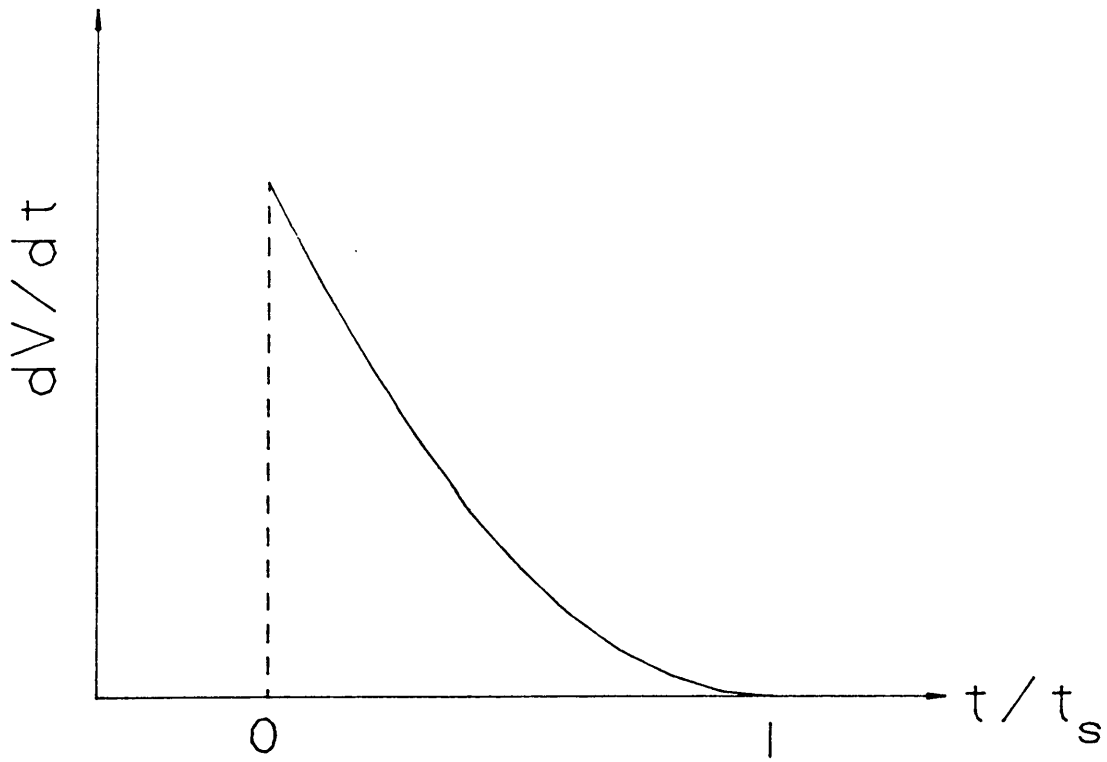

Fig. 11. The Quantity dV/dt Versus Time for a Surface Ignited Sphere.

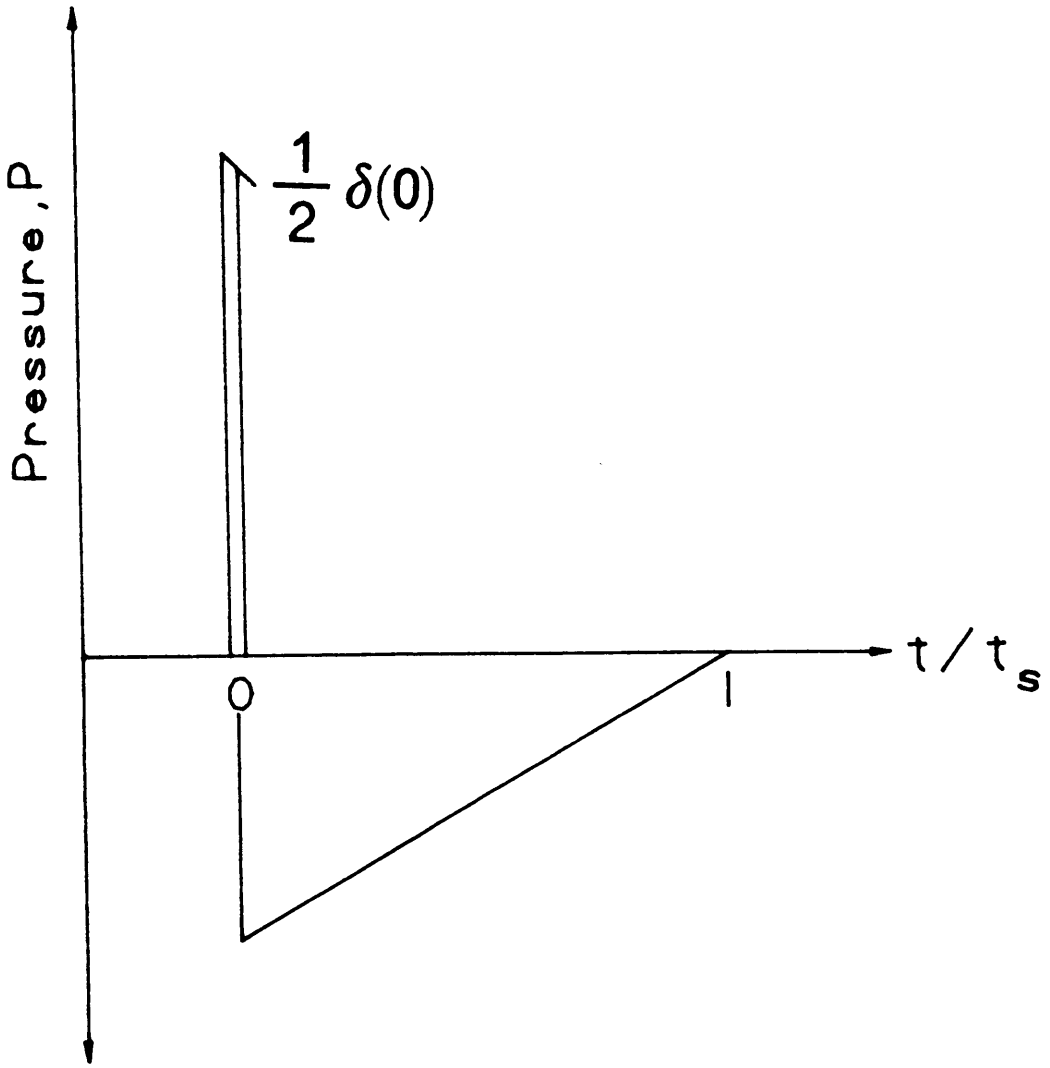

Fig. 12. Acoustic Pressure versus Time for a Surface Ignited Sphere.

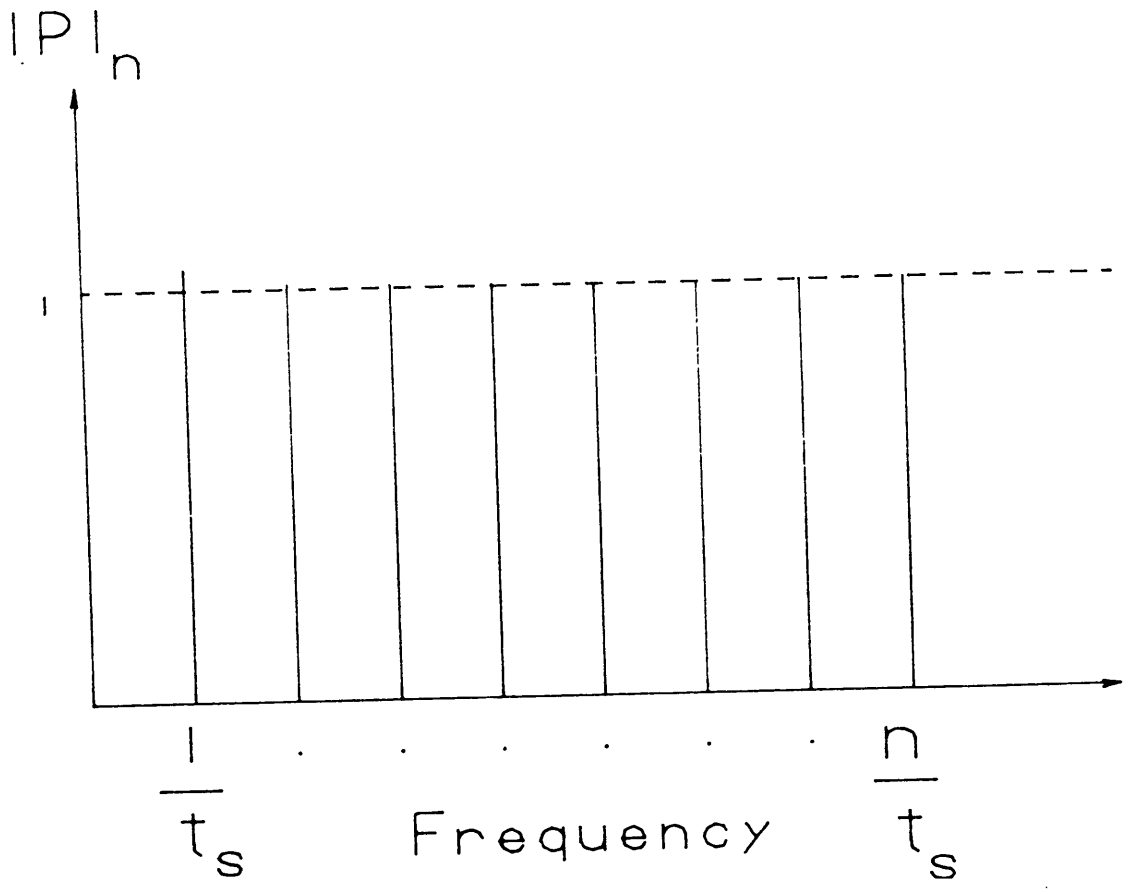

Fig. 13. Line Spectrum Due to a Surface Ignited Sphere.

3.4 *Improvements to Mahan's Original Model*

On analyzing his results, Mahan realized that his solution does not represent a realistic line spectra. It is known that real flames do not produce uniform line spectra. Realistically, a sound pressure spectrum from turbulent flames rolls off continuously with frequency after attaining a peak in the 500 Hz octave band. Addressing this problem, Mahan pointed out that the delta function can not be used in the form discussed above. In reality, the time rate of change of volume of a combustible sphere cannot jump from zero to some finite value in zero time; such behavior defies the basic laws of nature. In the same paper, Mahan [27] proposed a solution to this problem which involves introducing a *time delay* ε to account for a more gradual change in dV/dt from zero at time equal to zero to its initial value for surface ignition at some short (but finite) time later. The corresponding function of rate of change of volume for Mahan's improved model is shown in Fig. 14, the corresponding acoustic pressure is shown in Fig. 15, and the line spectrum for nondimensional pressure amplitude is shown in Fig. 16. As expected, the improved model does predict a spectral shape typical of those observed for actual open turbulent flames. However, no physical interpretation of the quantity ε is given in Ref. [27]. Again, Mahan's theory only accounts for the acoustic emission by a single continuous stream of burning cells. How the radii of the individual cells and the number of such continuous streams contributing to combustion noise are related to basic burner and fuel parameters is not given in either of his models.

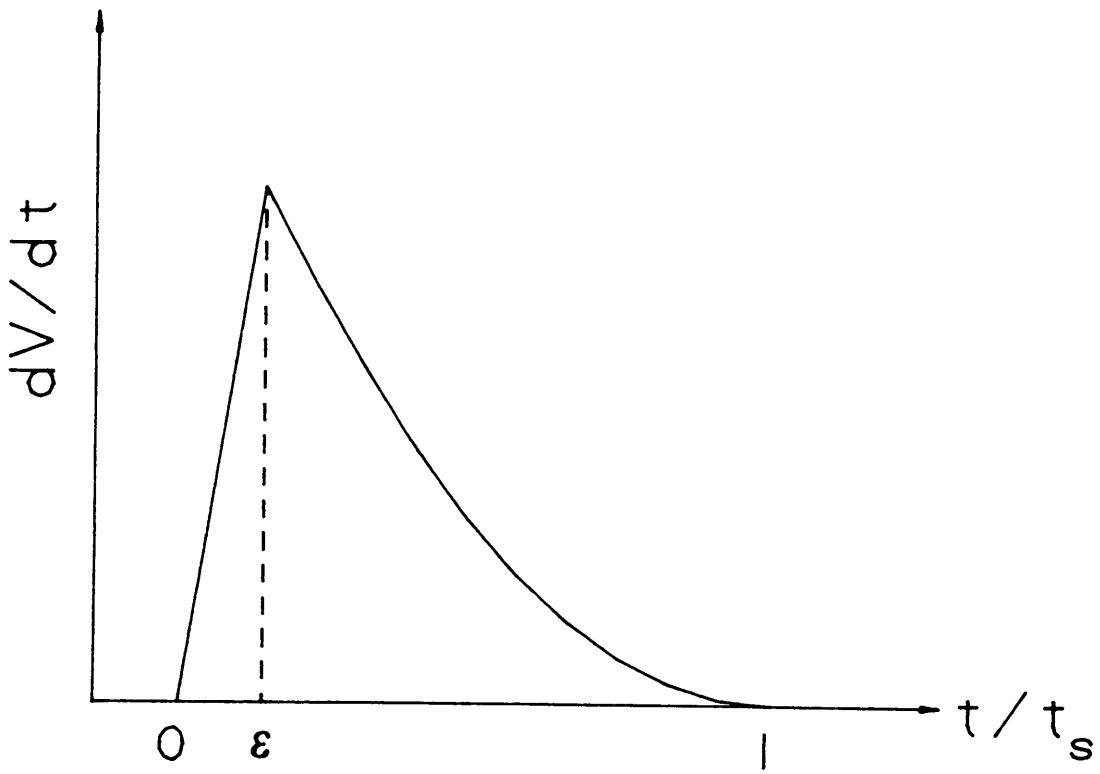

Fig. 14. The Quantity dV/dt Versus Time for a Surface Ignited Sphere (the improved model).

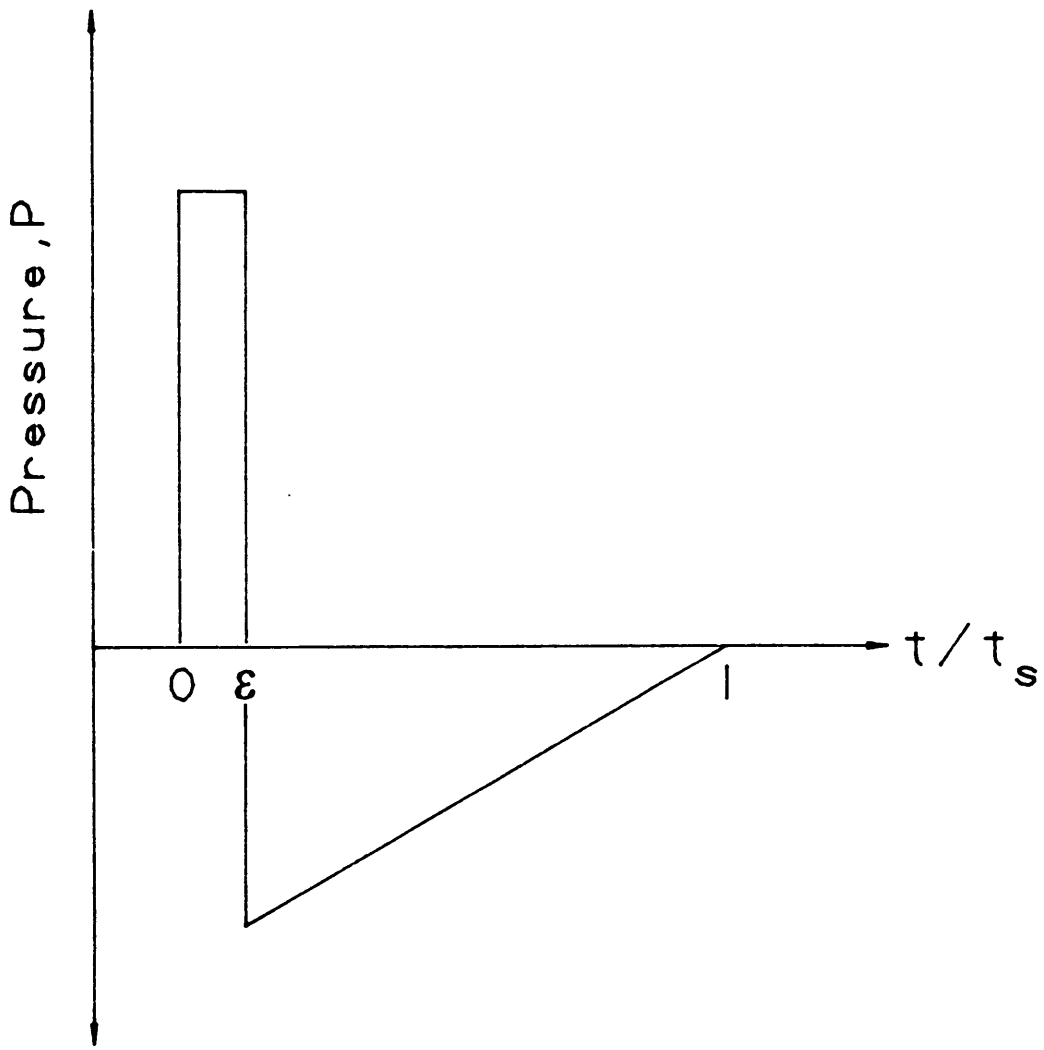

Fig. 15. Acoustic Pressure versus Time for a Surface Ignited Sphere (the improved model).

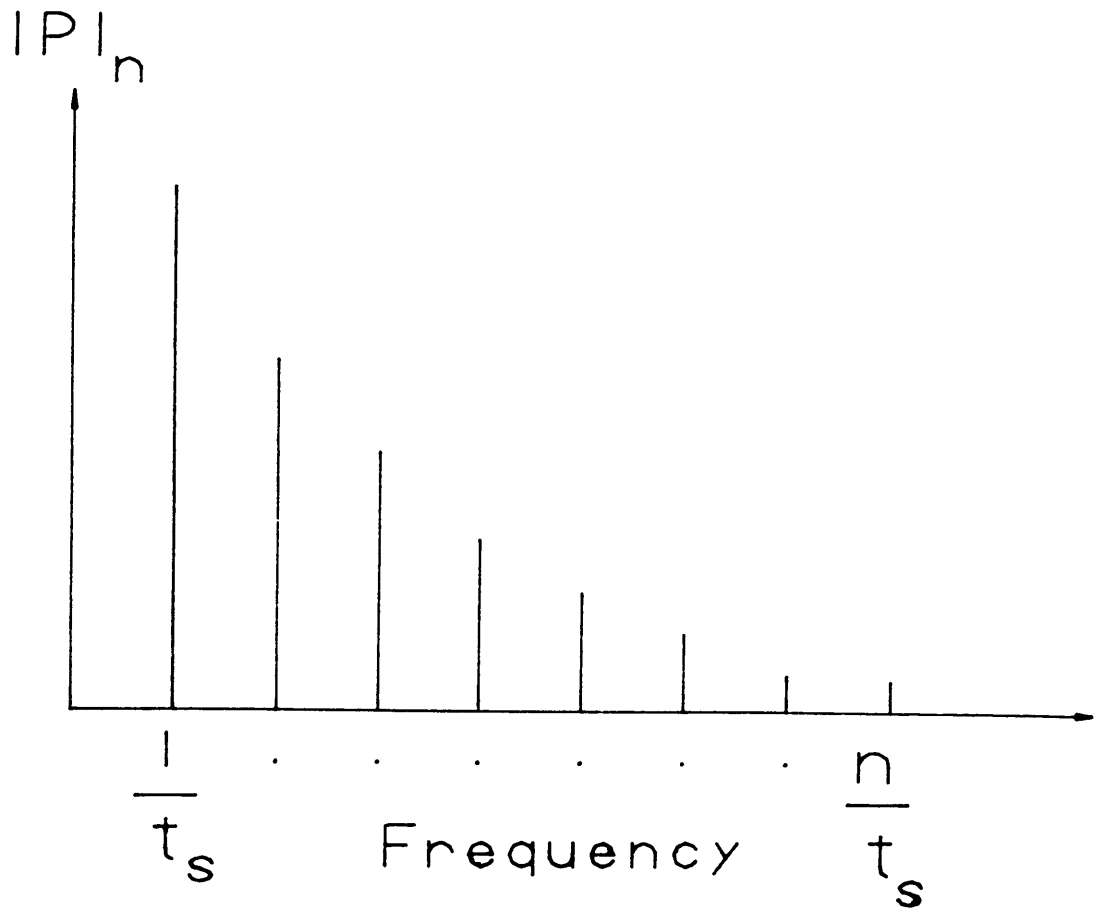

Fig. 16. Line Spectrum Due to a Surface Ignited Sphere (the improved model).

To summarize, the primary deficiencies of Mahan's model are:

1. A relationship between the initial radius R_s of the cell, and the burner variables is not developed.
2. The number of compact sources effective at any given instant is not given.
3. The delta function, or the parameter ε in the improved version, does not adequately define the begining of surface burning.

A more complete combustion noise model is developed in the subsequent chapters of this thesis. This model has its foundation in Mahan's improved turbulent combustion noise model presented in this chapter. Salient features of this new model are:

1. Several modifications and extensions, justified on the basis of physical arguments, will be introduced to Mahan's model.
2. The simplicity and generality of the parent model will be preserved.
3. All of the input parameters in this model are fundamental burner and fuel variables known to have an effect on the acoustic characteristics of the turbulent flame.
4. Finally, a direct combustion noise model on first principles is presented.

4.0 The New Model

4.1 The Ignition of a Turbulent Eddy

In reality, a turbulent jet of air-fuel mixture consists of a stream of turbulent eddies incident to the flame front. Upon entering the flame front, alternate layers of air-fuel and hot products are formed which subsequently are ignited and burn, as indicated by four stages of a turbulent eddy shown in Fig. 17 from Mahan [13]. In Stage (a), a turbulent eddy is shown approaching the flame front; in Stages (b) and (c), this eddy penetrates the flame front; and in Stage (d), the eddy is completely surrounded by hot products of combustion. In this thesis, Mahan's [27] suggestion to model the complex shapes of these eddies as spherical cells of air-fuel mixture has been followed. Figure 18 shows the ignition and burning of a spherical cell corresponding to the four stages of the entrainment and ignition of a turbulent eddy shown in Fig. 17.

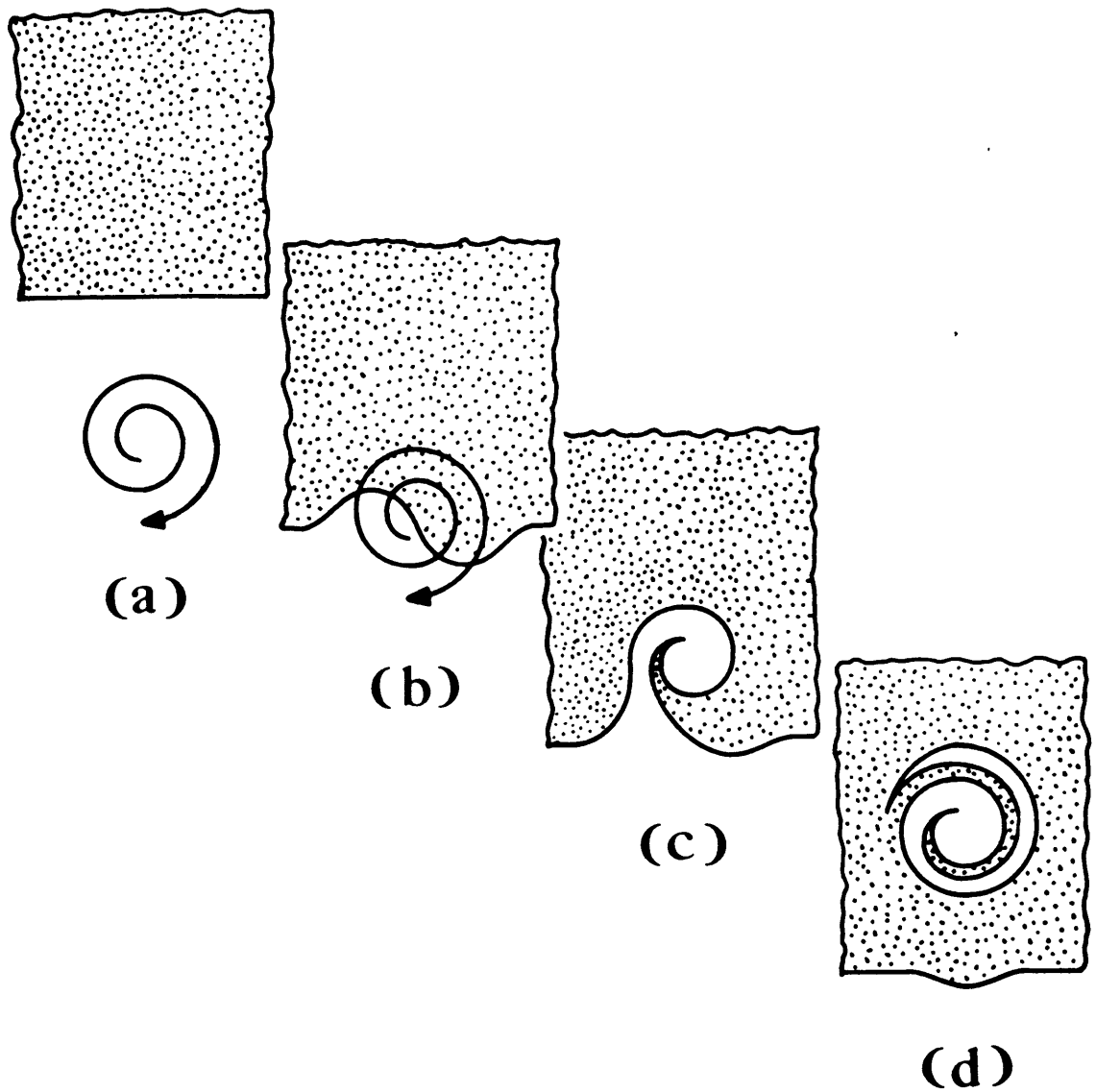

Fig. 17. Entrainment and Ignition of a Turbulent Eddy [13]

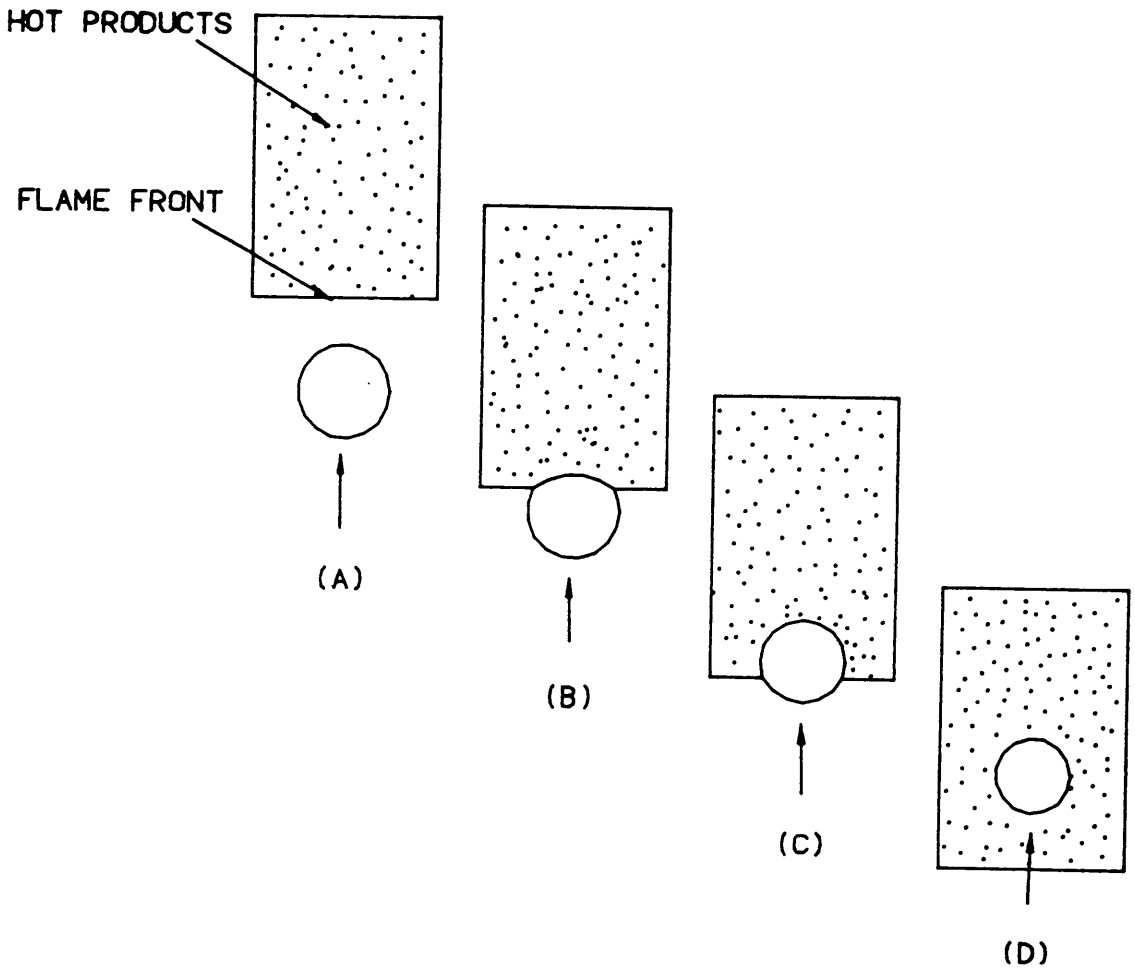

Fig. 18. Ignition and Burning of a Spherical Cell as it Crosses the Flame Front.

4.2 *The Radius of the Noise Source*

The volumetric flow rate, Q, of the reactant is given by

$$Q = \frac{\pi}{4} D^2 U \,, \tag{4.1}$$

where D is the burner diameter and U is the reactant's convective velocity. Let R_i be the initial radius of an individual noise source (i.e., a spherical cell). Then the initial volume of a single cell is

$$V_i = \frac{4}{3} \pi R_i^3 \,. \tag{4.2}$$

To evaluate R_i, an assumption about the turbulent structure needs to be made. Suppose a continuous stream of injected fuel breaks up uniformly into a single row of spherical cells. The "injection time", defined as the time in which a single cell is produced, is given by

$$t_i = \frac{2R_i}{U} \,. \tag{4.3}$$

Since there is only a single row of eddies, the volumetric flow rate, Q, becomes

$$Q = \frac{V_i}{t_i} \,. \tag{4.4}$$

Upon substituting Eq. (4.2) and Eq. (4.3) into Eq. (4.4), there results

$$Q = \frac{\frac{4}{3}\pi R_i^3}{\frac{2R_i}{U}} ,$$

or,

$$Q = \frac{2}{3}\pi R_i^2 U . \tag{4.5}$$

Equating Eqs. (4.1) and (4.5), there results

$$\frac{2}{3}\pi R_i^2 U = \frac{\pi}{4} D^2 U ,$$

or finally,

$$R_i = \sqrt{\frac{3}{8}}\, D . \tag{4.6}$$

It must be noted that Eq. (4.6) has been derived without any reference to the rich body of literature on turbulent flow. Its greatest weakness is also its greatest strength: its simplicity. Judgement on the correctness of Eq. (4.6) must await evaluation of the results to which it leads.

4.3 Burning Zones

In this section, different burning zones of a combustible cell are defined. These definitions are the result of a two step logic process discussed below.

4.3.1 Background Information

The flame front, as defined by Giammar and Putnam [19], is an isothermal surface of sufficiently high temperature to ignite a turbulent eddy when crossing it. The literature offers compelling evidence that the predominant noise generating mechanism in open turbulent flames is the turbulent velocity fluctuation at the flame front rather than the entrainment and subsequent combustion of individual turbulent eddies of mixture after they have penetrated into the combustion zone, as already stated in Section 2.0. In this new model, the above observations are interpreted as a predominant influence of the burning at the flame front on combustion generated noise as opposed to the noise contribution by the subsequent burning of turbulent eddies after they have penetrated into the combustion zone. The full impact of invoking this idea will become clear when the final results of this model are reached.

4.3.2 Intuitive reasoning

In the last chapter, turbulent eddies in the combustion zone were modeled as combustible spheres of mean initial radius R_S. According to Mahan's original hypothesis [27], the ignition of these spherical cells occurs instantaneously over the entire surface. It is here the concept of flame front discussed above needs to be introduced. The concept of instantaneous ignition over the entire surface of a spherical cell assumes that the cell is completely surrounded by hot products of combustion at time $t = 0$. However, common sense suggests that this is not possible. Before the cell can be completely surrounded by hot products, it must completely cross the flame front. This, then, means that instantaneous ignition of the entire surface of the cell does not occur, but rather those parts of the surface of the cell ignite first which first come into contact with the flame front. In other words, the surfaces are not ignited until after they are exposed to the hot products. Figure 18 models the turbulent eddy shown in Fig. 17 as a spherical cell which burns in the fashion discussed above.

Based on the above discussion, two burning processes of a spherical cell may be identified.

4.3.3 The Transition Process

The transition process occurs during the time period which begins when the cell first touches the flame front boundary, and ends when the cell is first completely surrounded by hot products of combustion, as indicated in Fig. 19. Since $2R_i$ is the initial diameter of the cell, and since it crosses the flame front at the convective velocity U, the transition time t_{tr} of a single cell is given by

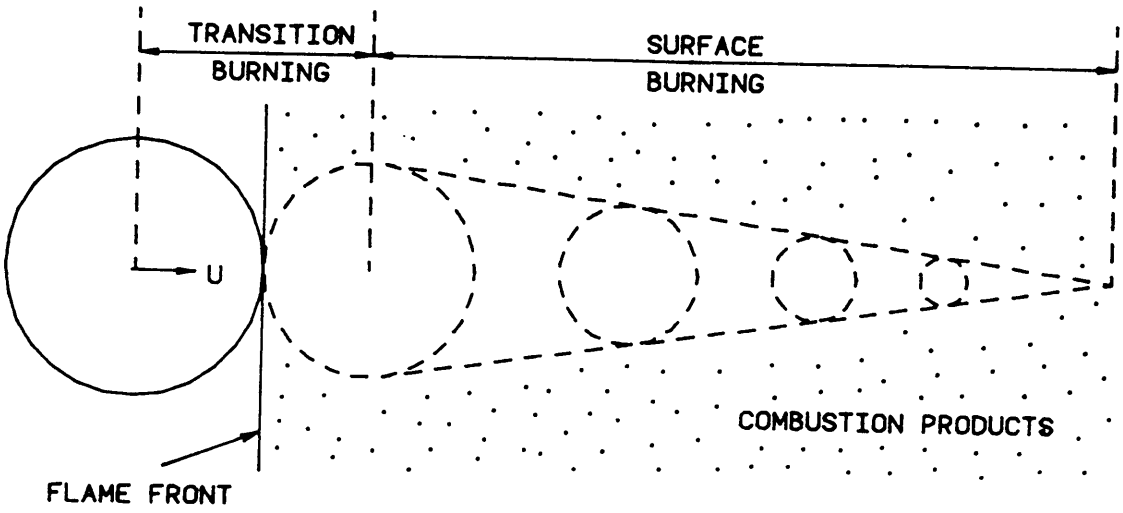

Fig. 19. Two Burning Processes of a Spherical Cell.

$$t_{tr} = \frac{2R_i}{U} \quad . \tag{4.7}$$

(Variables pertaining to the transition process are indicated by the subscript "tr".)

4.3.4 The Surface Burning Process

The surface burning process refers to that time period which begins when the cell is first completely surrounded by hot products of combustion; i.e., at the end of transition burning, and ends when the fuel in the cell is completely consumed, as indicated in Fig. 19. The spherical shape of radius R_S is assumed for the cell at the beginning of surface burning. Note that the radius R_S is not yet known, and consequently still has to be evaluated. Since burning occurs radially inwards at the flame speed, the surface burning time t_S is given by

$$t_S = \frac{R_S}{S_L} \quad . \tag{4.8}$$

(Variables pertaining to the surface burning process are indicated by the subscript "s".) The relationships established by Eqs. (4.7) and (4.8) are illustrated in Fig. 20. The total burning time, t_{tt}, of the cell is thus

$$t_{tt} = t_{tr} + t_S \, . \tag{4.9}$$

This completes the qualitative descriptions of the two burning processes. In the next two sections, quantitative definitions of the transition process and the surface burning process are developed.

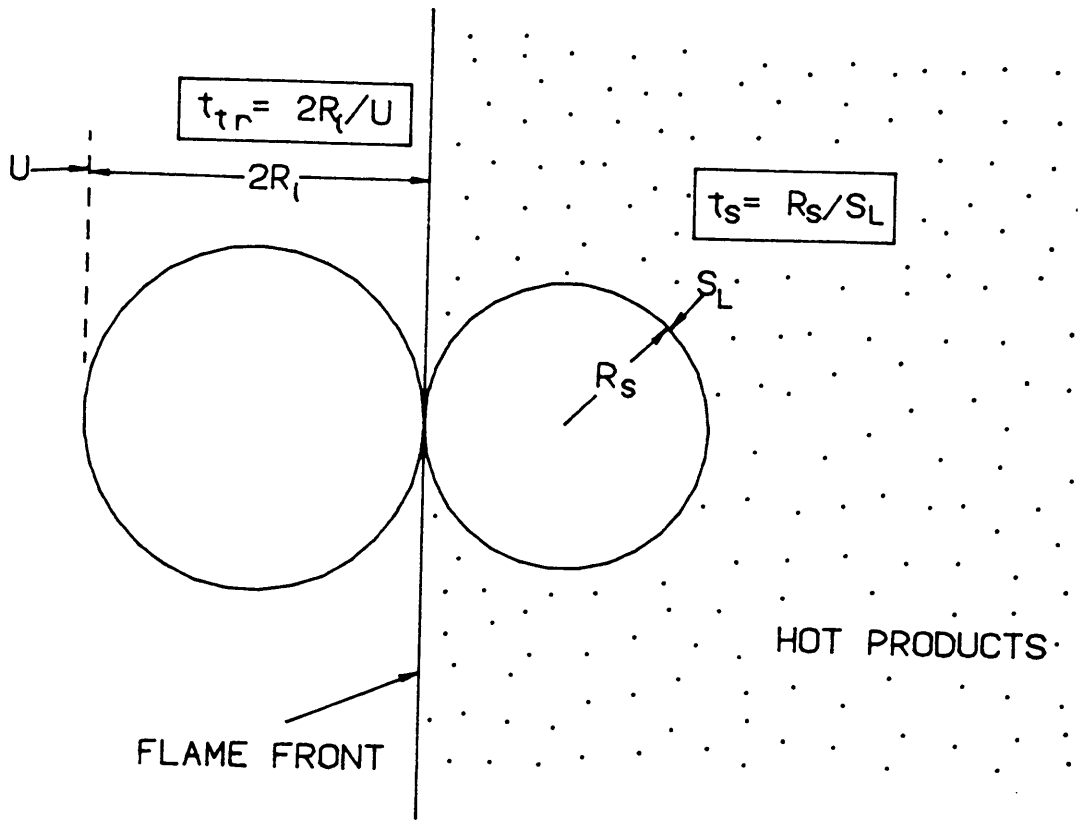

Fig. 20. Definition of Burning Times for the Two Processes.

4.4 *The Transition Process*

Since the objective of this modeling effort is to obtain an expression for acoustic pressure produced by the process of burning a turbulent eddy, or cell, the immediate task becomes that of evaluating expressions for dV/dt as a function of time for the transition and surface burning processes. Remember, because $p \propto d^2V/dt^2$, it is necessary to evaluate dV/dt as a function of time before the solution for the acoustic pressure can be obtained. Referring back to Fig. 18, a representative spherical cell of air-fuel mixture is shown approaching the flame front with convective velocity U. The moment this cell touches the flame front is identified as time $t = 0$. Now, this cell takes time $t = t_{tr}$ to fully enter the flame front. Thus, the transition process extends from $t = 0$ to $t = t_{tr}$, and the surface burning process extends from $t = t_{tr}$ to $t = t_{tt}$, where t_{tt} represents the moment when all of the fuel has been consumed.

Mahan's solution for dV/dt, and subsequently for acoustic pressure p, for the case of the surface burning process was developed in the previous chapter. Now, the problem is reduced to that of finding the correct equation for dV/dt, and subsequently for acoustic pressure p, during the transition process; i.e., during the time interval between $t = 0$ and $t = t_{tr}$. An elementary study of this problem indicates that to find a rigorous expression for dV/dt during the transition process would involve a prohibitively complicated mathematical formulation. The best approach would seem to be to first gather as much information about the transition process as possible, and then make the best

approximation for the expression for dV/dt during this period. Unfortunately, it does not take very long to realize that not much information is available for dV/dt during the transition period. However, there are some fundamental ideas that can be applied at the two ends of this period. Based on the reasoning that follows, conceptual curves for dV/dt and acoustic pressure p may be drawn, as shown in Fig. 21.

4.4.1 The Initial Conditions

The process of burning starts at time $t = 0$, suggesting that the rate of change of volume, and the corresponding acoustic pressure generated by the cell at this instant should be zero. Since acoustic pressure, p, is proportional to d^2V/dt^2, the time derivative of the rate of change in volume at $t = 0$ should also be zero. These two conditions may be stated mathematically as

$$\left.\frac{dV}{dt}\right|_{tr} = 0 \quad \text{and} \quad \left.\frac{d^2V}{dt^2}\right|_{tr} = 0\,, \quad \text{at} \quad t = 0\,. \tag{4.10}$$

4.4.2 The Final Conditions

Based on logic similar to that discussed above, the idea of continuity for the rate of change of volume and the acoustic pressure at time $t = t_{tr}$ should also be satisfied. Since the end of the transition period signifies the begining of the surface burning period, the final boundary conditions may be written

$$\left.\frac{dV}{dt}\right|_{tr} = \left.\frac{dV}{dt}\right|_{s} \quad \text{and} \quad \left.\frac{d^2V}{dt^2}\right|_{tr} = \left.\frac{d^2V}{dt^2}\right|_{s}\,, \quad \text{at} \quad t = t_{tr}\,. \tag{4.11}$$

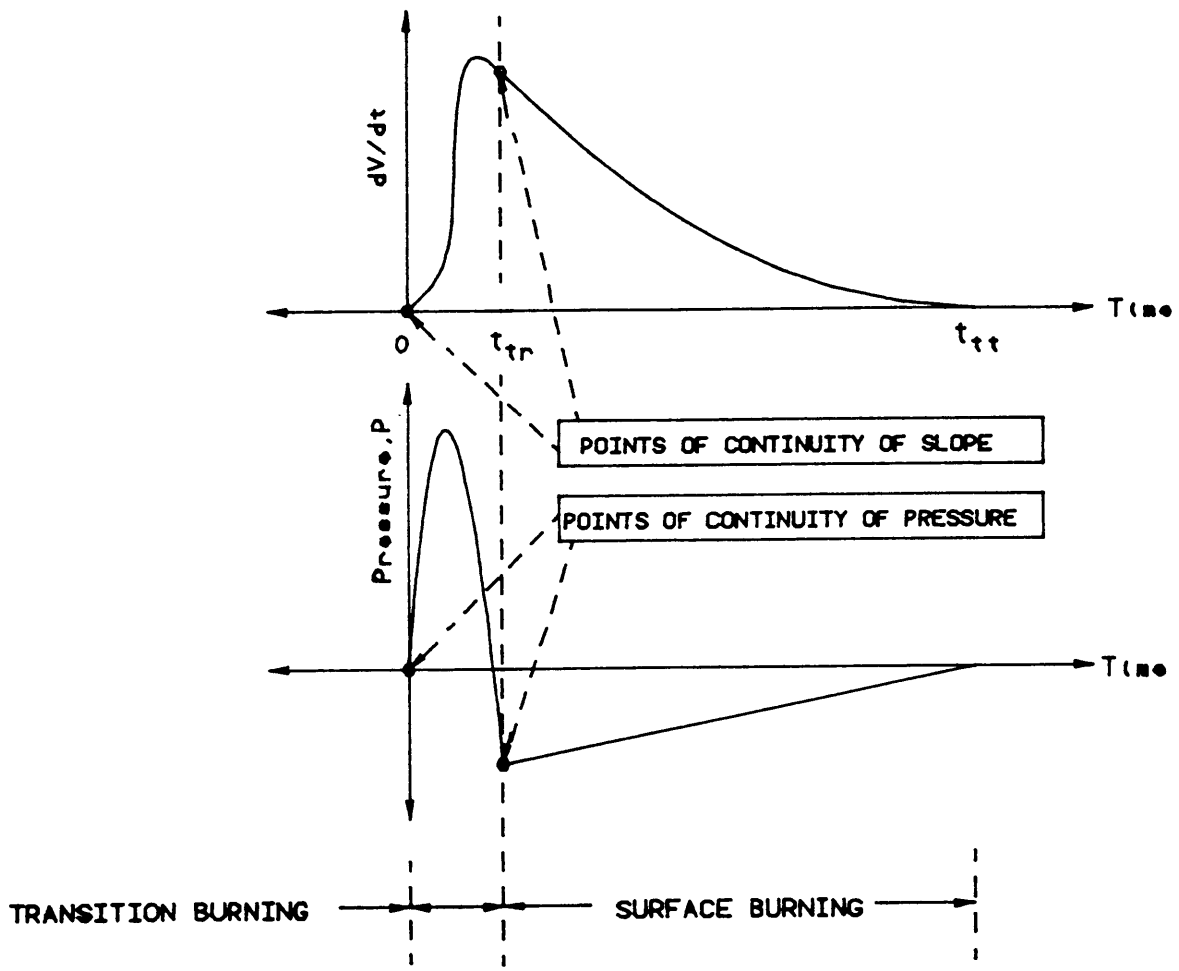

Fig. 21. Hypothetical Curves for (a) dV/dt Versus Time and (b) Acoustic Pressure Versus Time.

Thus, there are four boundary conditions which together can predict an approximate shape of the curve for dV/dt, and hence for acoustic pressure, during the transition period. When faced with similar boundary conditions, fluid mechanicians have traditionally chosen to represent an unknown function of a single variable as a polynomial expression of sufficiently low degree that all of the coefficients can be found by applying known boundary conditions. This approach is followed in the present thesis. Since there are four boundary conditions, a third-degree quadratic expression is assumed for dV/dt during the transition period; that is,

$$\left.\frac{dV}{dt}\right|_{tr} = at^3 + bt^2 + ct + d\,. \tag{4.12}$$

In the next section, the surface burning expressions discussed in Section (3.2.1) are modified in view of the changes in the time scales that have come up due to the introduction of the transition period.

4.5 *Modified Surface Burning Expressions*

Before applying the boundary conditions for the transition period, which also involve the initial conditions of surface burning at $t = t_{tr}$, the expressions for surface burning, developed in Section (3.2.1), need to be modified to account for the changes in the time scale that have been made. Earlier, in the absence of the transition process, surface burning was assumed to start at time $t = 0$. However, this is no longer true. Due to the introduction of the transition period, surface burning now starts at time $t = t_{tr}$. This means that the expressions developed previously for surface burning will hold true only if care is taken to initialize the begining of this process to time $t = t_{tr}$, instead of at $t = 0$. This is achieved by replacing all occurances of t by $t - t_{tr}$ in the surface burning expressions. As a result, the surface burning expression defined by Eq. (3.14) takes the form

$$\left.\frac{dV}{dt}\right|_s = 4\pi(E-1)[R_s - S_L(t-t_{tr})]^2 S_L$$

$$= 4\pi(E-1)[t_s - t + t_{tr}]^2 S_L^2$$

$$= 4\pi(E-1)(t_{tt} - t)^2 S_L^2 , \qquad (4.13)$$

where

$$t_{tt} = \text{ total combustion time } = t_{tr} + t_s . \qquad (4.14)$$

In this case Eq. (3.15) becomes

$$\frac{d^2V}{dt^2}\Big|_s = 8\pi R_s(E-1)\left(\frac{t-t_{tr}}{t_s}-1\right)S_L^2$$

$$= \frac{8\pi R_s(E-1)(t-t_{tr}-t_s)S_L^2}{t_s}$$

$$= 8\pi(E-1)(t-t_{tt})S_L^3 . \tag{4.15}$$

This completes the quantitative definitions of the transition and surface burning processes. However, it should be noted that while surface burning expressions are in an explicit form, the transition burning expressions are still defined in terms of unknown constants *a*, *b*, *c*, and *d*. In the next section, an attempt is made to evaluate the transition burning constants.

4.6 *Evaluation of the Transition Burning Process Constants*

Applying the first of the initial two boundary conditions, Eq. (4.10), to the expression for the transition process, Eq. (4.12), there results

$$\left.\frac{dV}{dt}\right|_{tr} = a0^3 + b0^2 + c0 + d = 0 \ , \ \text{at } t = 0 \ ,$$

which reduces to

$$d = 0 \ . \tag{4.16}$$

Applying the second of these boundary conditions, Eq. (4.10), to Eq. (4.12) results in

$$\left.\frac{d^2V}{dt^2}\right|_{tr} = 3a0^2 + 2b0 + c = 0 \ , \ \text{at } t = 0 \ ,$$

which reduces to

$$c = 0 \ . \tag{4.17}$$

Thus, the application of the two initial boundary conditions have reduced the cubic expression to

$$\left.\frac{dV}{dt}\right|_{tr} = at^3 + bt^2 \,. \tag{4.18}$$

Applying the first of the final two boundary conditions at $t = t_{tr}$, Eq. (4.11), to Eq. (4.12) it follows that

$$\left.\frac{dV}{dt}\right|_{tr} = \left.\frac{dV}{dt}\right|_{s} \text{ at } t = t_{tr} \,,$$

or

$$at_{tr}3 + bt_{tr}^2 = 4\pi(E-1)[t_{tt} - t_{tr}]^2 S_L^3 \,,$$

or finally,

$$b = -at_{tr} + \frac{4\pi(E-1)t_s^2 S_L^3}{t_{tr}^2} \,. \tag{4.19}$$

Finally, using the second of these boundary conditions at $t = t_{tr}$, Eq. (4.11), there results

$$\left.\frac{d^2V}{dt^2}\right|_{tr} = \left.\frac{d^2V}{dt^2}\right|_{s}, \quad \text{at} \quad t = t_{tr} \,,$$

or

$$3at_{tr}^2 + 2bt_{tr} = -8\pi(E-1)(t_{tt} - t_{tr})S_L^3 \,. \tag{4.20}$$

Substituting the value of b from Eq. (4.19) into Eq. (4.20), there results

$$3at_{tr}^2 + 2\left(-at_{tr} + \frac{4\pi(E-1)t_s^2 S_L^3}{t_{tr}^2}\right)t_{tr} = -8\pi(E-1)t_s S_L^3 \,.$$

Solving for a, one obtains

$$a = \frac{-8\pi(E-1)t_s t_{tt} S_L^3}{t_{tr}^3} \ . \tag{4.21}$$

Substituting this value of a into the expression for b, Eq. (4.19), there results

$$b = \frac{4\pi(E-1)t_s^2 S_L^3}{t_{tr}^2} + \frac{8\pi(E-1)t_s t_{tt} S_L^3}{t_{tr}^2} \ ,$$

or finally,

$$b = \frac{4\pi(E-1)t_s S_L^3}{t_{tr}^2}(t_s + 2t_{tt}) \ . \tag{4.22}$$

This completes the evaluation of all the unknown constants a, b, c and d, in the transition process in terms of known or previously defined parameters.

4.7 *Evaluation of the Radius at the Beginning of Surface Burning*

Now there only remains the task of finding the radius R_s of the cell at the beginning of the surface burning. It should be noted that R_s is implicitly contained in both the transition and surface burning expressions, and thus needs to be evaluated in terms of the basic fuel and burner parameters.

In the beginning (that is, at time $t = 0$), the volume of the unburned cell is given by V_i. Let V_s be the volume of the unburned portion of the gas at the end of the transition period. Then the decrease in volume of the unburned gas is given by

$$V_i - V_s = \frac{4}{3}\pi\left(R_i^3 - R_s^3\right) . \tag{4.23}$$

During the transition process, the volume of the cell changes at a rate dV/dt given by Eq. (4.12). It would be worthwhile to re-emphasize at this point that the expression for dV/dt for both burning periods accounts for the volume occupied together by the burned as well as the unburned portion of gases. The total change in volume ΔV during the transition process can be evaluated by integrating dV/dt over the entire transition process; that is,

$$\Delta V = \int_0^{t_{tr}} \frac{dV}{dt}\Big|_{tr} . \tag{4.24}$$

But the volume of gas that has been generated by burning during the transition process is given by $E(V_i - V_s)$. Thus, the total change in volume of the gas during the transition burning process is given by

$$\Delta V = (E-1)(V_i - V_s) . \tag{4.25}$$

Equations (4.24) and (4.25) may be combined to yield

$$\Delta V = \int_0^{t_{tr}} \frac{dV}{dt}\Big|_{tr} = (E-1)(V_i - V_s) . \tag{4.26}$$

Substituting the expression for $V_i - V_s$ from Eq. (4.23), and the expression for dV/dt from Eq. (4.18), there results

$$\int_0^{t_{tr}} (at^3 + bt^2)dt = \frac{4}{3}\pi(E-1)\left(R_i^3 - R_s^3\right) ,$$

or upon integration,

$$\frac{at_{tr}^4}{4} + \frac{bt_{tr}^3}{3} = \frac{4}{3}\pi(E-1)\left(R_i^3 - R_s^3\right) . \tag{4.27}$$

It is noted that the only unknown parameter on both sides is R_S. However, since a and b are both nonlinear functions of R_S (due to the involvement of the t_S and t_{tt} terms), it is not possible to obtain an explicit expression for R_S. Equation (4.27) must be solved iteratively with Eqs. (4.7), (4.8), (4.9), (4.21) and (4.22) to obtain R_S. This procedure not only allows evaluation of R_S, but as a consequence yields values of the constants a and b in terms of basic fuel and burner parameters. This section completes the evaluation of all the unknowns involved in the expressions for dV/dt and d^2V/dt^2 for both the transition and the surface burning processes. Figure 22(a) shows dV/dt as a function of time, and Fig. 22(b) shows the acoustic pressure as a function of time for a single burning turbulent eddy (modeled as a spherical cell).

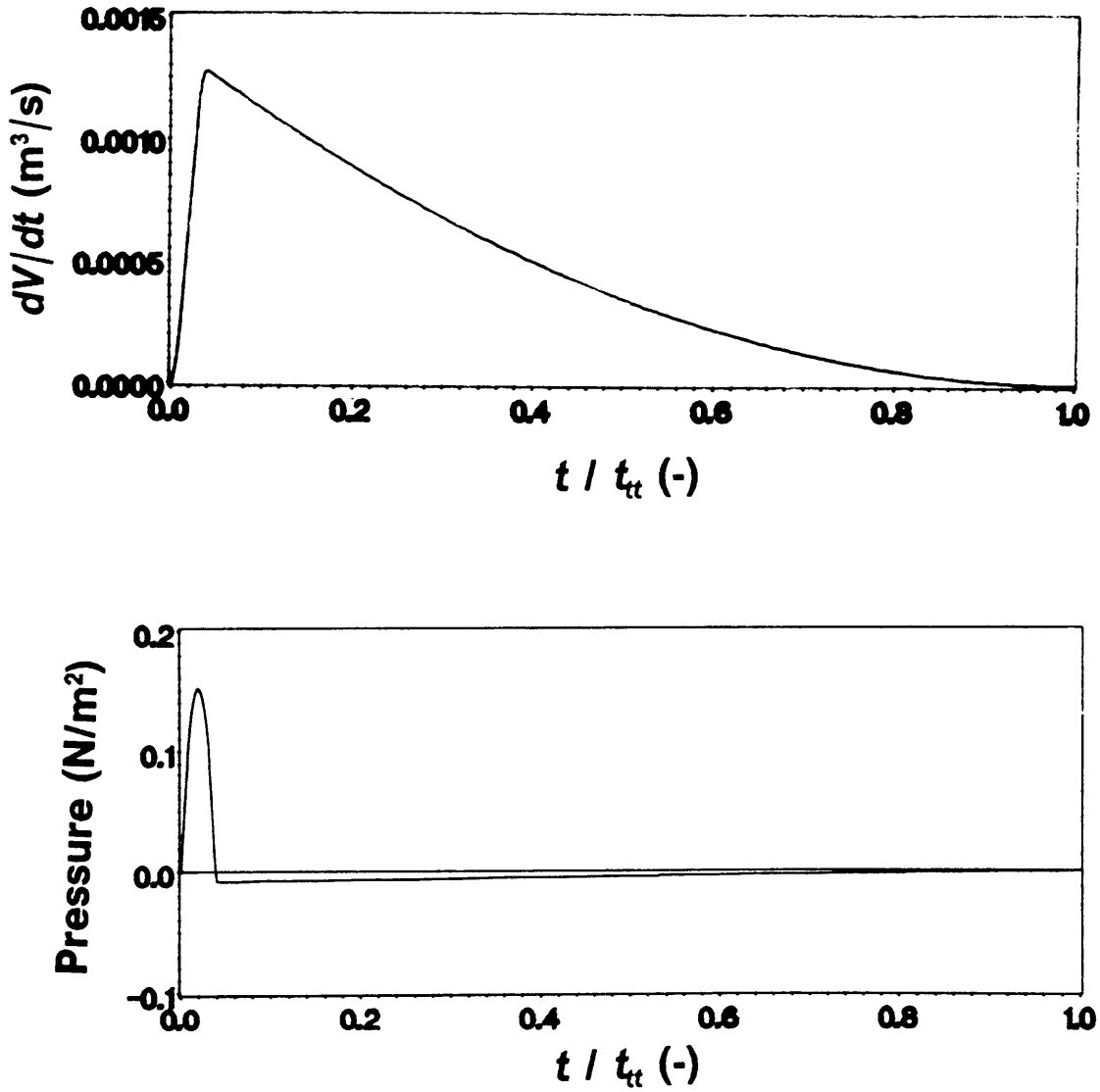

Fig. 22. (a) dV/dt Versus Time and (b) Acoustic Pressure Versus time: U = 20 m/s, D = 1 cm , SL = 40 cm/s, E = 8

4.8 *Development of the Acoustic Pressure Expression*

Acoustic pressure from a single burning cell in terms of fundamental burner and fuel variables can now be obtained. However, it is usual practice to nondimensionalize all of the quantities involved in a model. It is inconvenient to nondimensionalize the acoustic pressure during the transition process, because of the implicit solution for the constants a and b. Therefore, expressions for the surface burning process will be nondimensionalized first. Reintroducing the surface burning expression for the derivative of dV/dt from Eq. (4.15),

$$\left.\frac{d^2V}{dt^2}\right|_s = 8\pi(E-1)(t-t_{tt})S_L^3$$

$$= 8\pi(E-1)t_{tt}\left(\frac{t-t_{tt}}{t_{tt}}\right)S_L^3$$

$$= 8\pi t_{tt}(E-1)(\tau-1)S_L^3\,, \tag{4.28}$$

where

$$\tau = \text{ nondimensional time } = \frac{t}{t_{tt}}\,, \tag{4.29}$$

such that at $t = t_{tt}$,

$$\tau = \varepsilon = \frac{t_{tr}}{t_{tt}} \ . \tag{4.30}$$

Then, Eq. (4.28) can be written

$$\frac{d^2V}{dt^2}\Big|_s = \beta(\tau - 1) \ , \tag{4.31}$$

where

$$\beta = 8\pi t_{tt}(E-1)S_L^3. \tag{4.32}$$

The acoustic pressure for surface burning is defined from Eq. (3.13) as

$$p_s = \frac{\rho}{4\pi d}\frac{d^2V}{dt^2}\Big|_s$$

$$= \frac{\rho}{4\pi d}\beta(\tau - 1)$$

$$= \gamma(\tau - 1) \ , \tag{4.33}$$

where

$$\gamma = \frac{\rho}{4\pi d}\beta \ , \tag{4.34}$$

or finally,

$$P_s = \tau - 1 \ , \tag{4.35}$$

where P_s is the nondimensional acoustic pressure for surface burning, defined as

$$P_s = \frac{p_s}{\gamma} \ . \tag{4.36}$$

The nondimensional acoustic pressure for the transition process can now be written based on the above nondimensionalized pressure expressions for surface burning. The acoustic pressure during transition burning is given by

$$p_{tr} = \frac{\rho}{4\pi d} \frac{d^2V}{dt^2} \Big|_{tr} \ . \tag{4.37}$$

Substituting the value of $\rho/4\pi d$ from Eq.(4.34) into Eq. (4.37) yields

$$p_{tr} = \frac{\gamma}{\beta} \frac{d^2V}{dt^2} \Big|_{tr} \ . \tag{4.38}$$

The nondimensional acoustic pressure for the transition period can now be defined as

$$P_{tr} = \frac{p_{tr}}{\gamma} = \frac{1}{\beta} \frac{d^2V}{dt^2} \Big|_{tr} \ .$$

Finally, substitution of Eq. (4.18) into the above expression yields

$$P_{tr} = \frac{1}{\beta} (3at^2 + 2bt) \ .$$

or, replacing t by τt_{tt},

$$P_{tr} = \frac{1}{\beta} (3at_{tt}^2\tau^2 + 2bt_{tt}\tau) \ . \tag{4.39}$$

Equations (4.35) and (4.39) together give the solution of the nondimensional acoustic pressure as a function of time for the entire process of combustion and burning of one

cell. This completes the evaluation of the pressure time series produced by a single burning cell. In the next section, this solution is converted into the frequency domain for subsequent spectral analysis of the combustion-generated noise.

4.9 *Solution of the Acoustic Pressure Expression*

Assume that there is a continuous stream of combustible cells entering the combustion zone. "A continuous stream of combustible cells" means that only one cell burns at a time. After the fuel content of this cell is completely consumed, the next cell enters the combustion zone and so on. The line spectrum produced by this continuous train of burning eddies may be obtained by computing the Fourier series of the periodic function of period $\tau = 1$. The result is a line spectrum corresponding to the Fourier series

$$P = a_0 + \sum_{n=1}^{\infty} a_n \cos(2\pi n\tau)d\tau + \sum_{n=1}^{\infty} b_n \sin(2\pi n\tau)d\tau \ . \tag{4.40}$$

By "line spectrum" it is meant the variation of

$$|P_n| = \sqrt{a_n^2 + b_n^2} \tag{4.41}$$

with n. The time series corresponding to Eq. (4.40) is

$$P = P_{tr} = \frac{1}{\beta}(3at_{tt}^2\tau^2 + 2bt_{tt}\tau) \quad 0 \le \tau \le \varepsilon, \quad 1 \le \tau \le 1 + \varepsilon, \ldots \tag{4.42a}$$

and

$$P = P_s = \tau - 1, \quad \varepsilon < \tau < 1, \quad \varepsilon + 1 < \tau < 2, \ldots \tag{4.42b}$$

Coefficient a_0 is given by

$$\frac{a_0}{2} = \int_0^1 P d\tau \ .$$

Substituting Eq. (4.42) into the above expression and integrating yields

$$\frac{a_0}{2} = \frac{1}{\beta} \int_0^{\varepsilon} (3at_{tt}^2\tau^2 + 2bt_{tt}\tau) d\tau + \int_{\varepsilon}^1 (\tau - 1) d\tau \ ,$$

or,

$$\frac{a_0}{2} = \frac{1}{\beta} (at_{tt}^2\varepsilon^3 + bt_{tt}\varepsilon^2) - \frac{1}{2} + \varepsilon - \frac{\varepsilon^2}{2} \ . \tag{4.43}$$

Substituting values of a from Eq. (4.21), b from Eq. (4.22), β from Eq.(4.32), and ε from Eq.(4.30), and simplifying, there results

$$\frac{a_0}{2} = \frac{t_s^2}{2t_{tt}^2} - \frac{1}{2} + \frac{t_{tr}}{t_{tt}} - \frac{t_{tr}^2}{2t_{tt}^2}$$

$$= \frac{t_s^2 - (t_{tt} - t_{tr})^2}{2t_{tt}^2}$$

$$= \frac{t_s^2 - t_s^2}{2t_{tt}^2}$$

$$= 0 \,, \tag{4.44}$$

which is consistent with the expected value of a_0, since combustion noise would not be expected to have a steady component. It may be noticed that this is the first remarkable result given by this model, because no attempt *a priori* was made to influence this pleasing outcome. This is the natural outcome of the sound logic that has been followed in the development of this model.

Coefficients a_n and b_n in Eq. (4.40) are defined as

$$\frac{a_n}{2} = \int_0^1 P \cos(2\pi n\tau) d\tau \quad \text{and} \quad \frac{b_n}{2} = \int_0^1 P \sin(2\pi n\tau) d\tau \,.$$

Substituting Eq. (4.42) in the above expressions, there results

$$\frac{a_n}{2} = \frac{1}{\beta} \int_0^{\varepsilon} (3at_{tt}^2\tau^2 + 2bt_{tt}\tau) \cos(2\pi n\tau) d\tau + \int_{\varepsilon}^1 (\tau - 1) \cos(2\pi n\tau) d\tau \,, \tag{4.45a}$$

and

$$\frac{b_n}{2} = \frac{1}{\beta} \int_0^{\varepsilon} (3at_{tt}^2\tau^2 + 2bt_{tt}\tau) \sin(2\pi n\tau) d\tau + \int_{\varepsilon}^1 (\tau - 1) \sin(2\pi n\tau) d\tau \,. \tag{4.45b}$$

To solve for the above Fourier coefficients a_n and b_n, all the integrals are first evaluated separately; that is,

$$\int_0^{\varepsilon} \sin(2\pi n\tau)d\tau = \frac{1}{2n\pi}\left[1 - \cos(2n\pi\varepsilon)\right], \tag{4.46a}$$

$$\int_0^{\varepsilon} \cos(2\pi n\tau)d\tau = \frac{1}{2n\pi}\sin(2n\pi\varepsilon), \tag{4.46b}$$

$$\int_0^{\varepsilon} \tau \sin(2\pi n\tau)d\tau = \frac{1}{2n\pi}\left[-\varepsilon\cos(2n\pi\varepsilon) + \int_0^{\varepsilon}\cos(2\pi n\tau)d\tau\right], \tag{4.46c}$$

$$\int_0^{\varepsilon} \tau \cos(2\pi n\tau)d\tau = \frac{1}{2n\pi}\left[\varepsilon\sin(2n\pi\varepsilon) - \int_0^{\varepsilon}\sin(2\pi n\tau)d\tau\right], \tag{4.46d}$$

$$\int_0^{\varepsilon} \tau^2 \sin(2\pi n\tau)d\tau = \frac{1}{2n\pi}\left[-\varepsilon^2\cos(2n\pi\varepsilon) + 2\int_0^{\varepsilon}\tau\cos(2\pi n\tau)d\tau\right], \tag{4.46e}$$

$$\int_0^{\varepsilon} \tau^2 \cos(2\pi n\tau)d\tau = \frac{1}{2n\pi}\left[\varepsilon^2\sin(2n\pi\varepsilon) - 2\int_0^{\varepsilon}\tau\sin(2\pi n\tau)d\tau\right], \tag{4.46f}$$

$$\int_0^{\varepsilon} \tau^3 \sin(2\pi n\tau)d\tau = \frac{1}{2n\pi}\left[-\varepsilon^3\cos(2n\pi\varepsilon) + 3\int_0^{\varepsilon}\tau^2\cos(2\pi n\tau)d\tau\right], \tag{4.46g}$$

$$\int_0^{\varepsilon} \tau^3 \cos(2\pi n\tau)d\tau = \frac{1}{2n\pi}\left[\varepsilon^3 \sin(2n\pi\varepsilon) - 3\int_0^{\varepsilon} \tau^2 \sin(2\pi n\tau)d\tau\right], \tag{4.46h}$$

$$\int_{\varepsilon}^{1} \sin(2\pi n\tau)d\tau = = \frac{1}{2n\pi}\left[\cos(2n\pi\varepsilon) - 1\right], \tag{4.46i}$$

$$\int_{\varepsilon}^{1} \cos(2\pi n\tau)d\tau = = -\frac{1}{2n\pi}\sin(2n\pi\varepsilon), \tag{4.46j}$$

$$\int_{\varepsilon}^{1} \tau \sin(2\pi n\tau)d\tau = \frac{1}{2n\pi}\left[-1 + \varepsilon\cos(2n\pi\varepsilon) + \int_{\varepsilon}^{1} \cos(2\pi n\tau)d\tau\right], \tag{4.46k}$$

and

$$\int_{\varepsilon}^{1} \tau \cos(2\pi n\tau)d\tau = \frac{1}{2n\pi}\left[-\varepsilon\sin(2n\pi\varepsilon) - \int_{\varepsilon}^{1} \sin(2\pi n\tau)d\tau\right]. \tag{4.46l}$$

Substituting Eqs. (4.46) into Eqs. (4.45), there results

$$\begin{aligned} a_n = &\left[\frac{3at_{tt}^2\varepsilon}{(n\pi)^2\beta} + \frac{bt_{tt}}{(n\pi)^2\beta} - \frac{1}{2(n\pi)^2}\right]\cos(2n\pi\varepsilon) \\ &+ \left[\frac{3at_{tt}^2\varepsilon^2}{n\pi\beta} - \frac{3at_{tt}^2}{2(n\pi)^3\beta} + \frac{2bt_{tt}\varepsilon}{n\pi\beta} - \frac{\varepsilon}{n\pi} - \frac{1}{n\pi}\right]\sin(2n\pi\varepsilon) \\ &+ \left[-\frac{bt_{tt}}{(n\pi)^2\beta} + \frac{1}{2(n\pi)^2}\right] \end{aligned} \tag{4.47a}$$

and

$$b_n = \left[-\frac{3at_{tt}^2\varepsilon^2}{n\pi\beta} + \frac{3at_{tt}^2}{2(n\pi)^3\beta} - \frac{2bt_{tt}\varepsilon}{n\pi\beta} + \frac{\varepsilon}{n\pi} + \frac{1}{n\pi} \right] \cos(2n\pi\varepsilon)$$

$$+ \left[\frac{3at_{tt}^2\varepsilon}{(n\pi)^2\beta} + \frac{bt_{tt}}{(n\pi)^2\beta} - \frac{1}{2(n\pi)^2} \right] \sin(2n\pi\varepsilon)$$

$$+ \left[\frac{-3at_{tt}^2}{2(n\pi)^3\beta} - \frac{2}{n\pi} \right]. \qquad (4.47b)$$

Finally, the pressure amplitude at a distance d can be given in nondimensional form as

$$|P_0| = a_0 \quad \text{when} \quad n = 0, \quad \text{and} \quad |P_n| = \sqrt{a_n^2 + b_n^2}\ , \quad n = 1,2,3,....\infty. \qquad (4.48)$$

The frequencies corresponding to these pressure amplitudes are given by

$$f_n = n/t_{tt}\ . \qquad (4.49)$$

This completes the evaluation of the line spectrum produced by a single continuous train of combustible cells passing into the flame zone. These results were first given by Mahan and Nathani [28]. However a hypothetical value of initial radius R_i was assumed in the development of that model. The line spectra generated by such a train of burning cells for a variety of conditions are shown in Figs. 23 through 27. In each case the line spectrum is for a condition typical of a turbulent hydocarbon-air premixed flame. Figure 23 shows the line spectrum generated by a methane-air premixed flame. The reactants are injected from a burner of exit diameter 1 cm with the convective velocity 20 m/s. The approximate values of the laminar flame speed and the expansion ratio for a methane-air flame are approximately 40 cm/s and 6 respectively. In Figs. 24, 25, 26 and

27, each of the basic burner and fuel parameters are doubled in turn while the other parameters are held constant at their initial values of Fig. 23. The objective of this analysis is to study the influences of different parameters on combustion noise spectra.

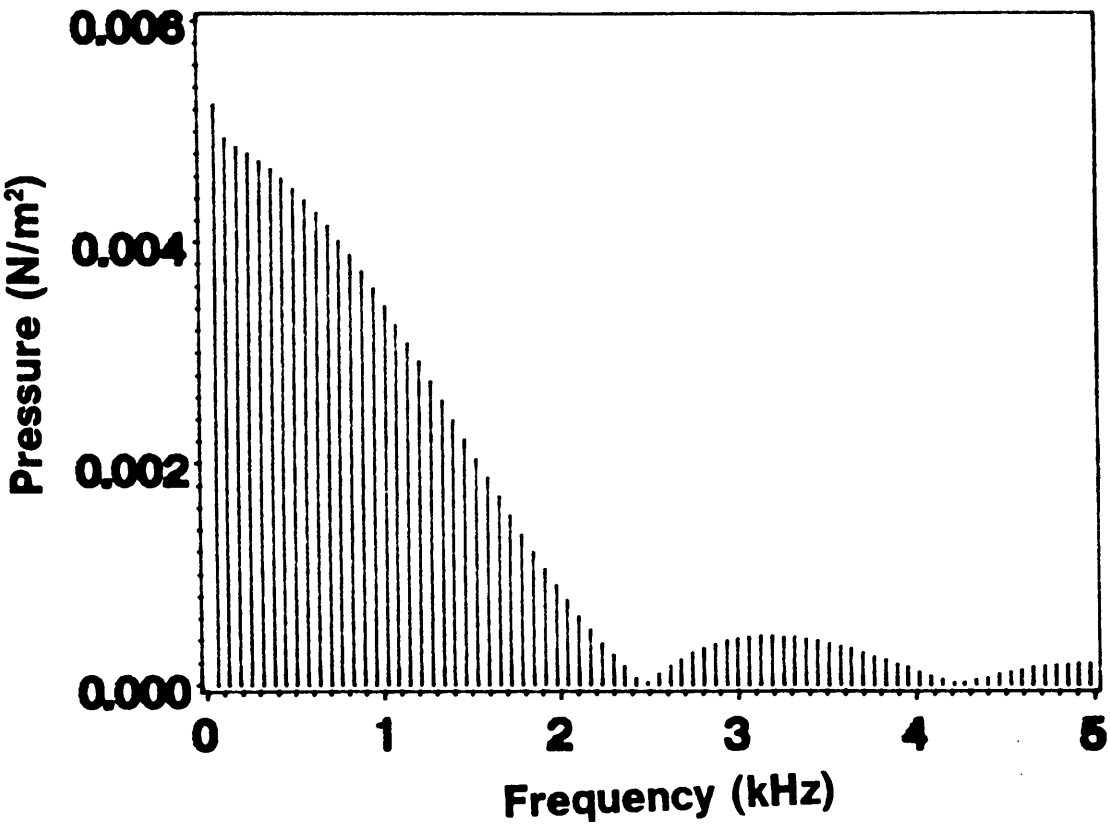

Fig. 23. Line Spectrum due to a Single Burning Cell: U = 20 m/s, D = 1 cm , SL = 40 cm/s, E = 6

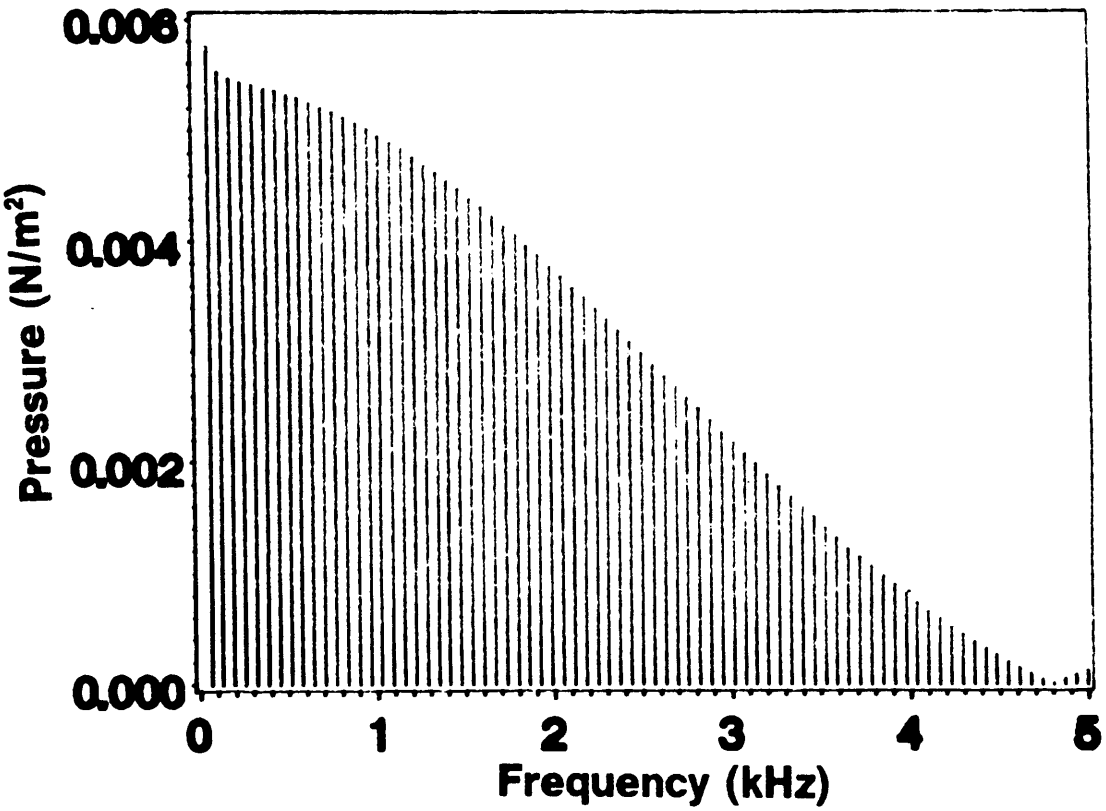

Fig. 24. Line Spectrum due to a Single Burning Cell: U = 40 m/s, D = 1 cm , SL = 40 cm/s, E = 6

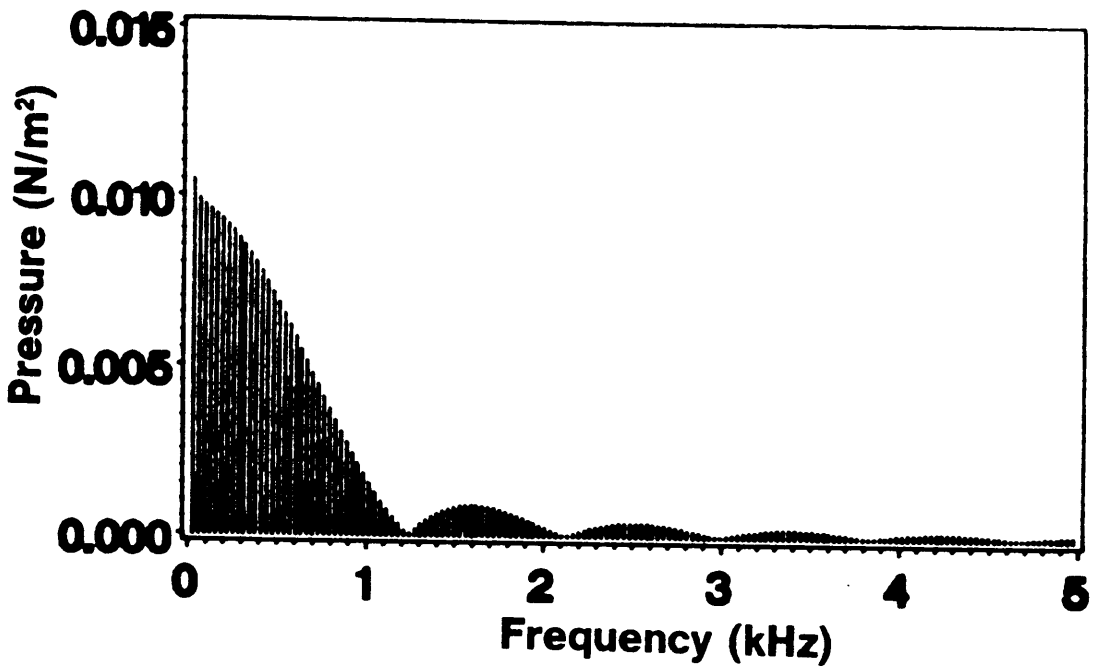

Fig. 25. Line Spectrum due to a Single Burning Cell: U = 20 m/s, D = 2 cm , SL = 40 cm/s, E = 6

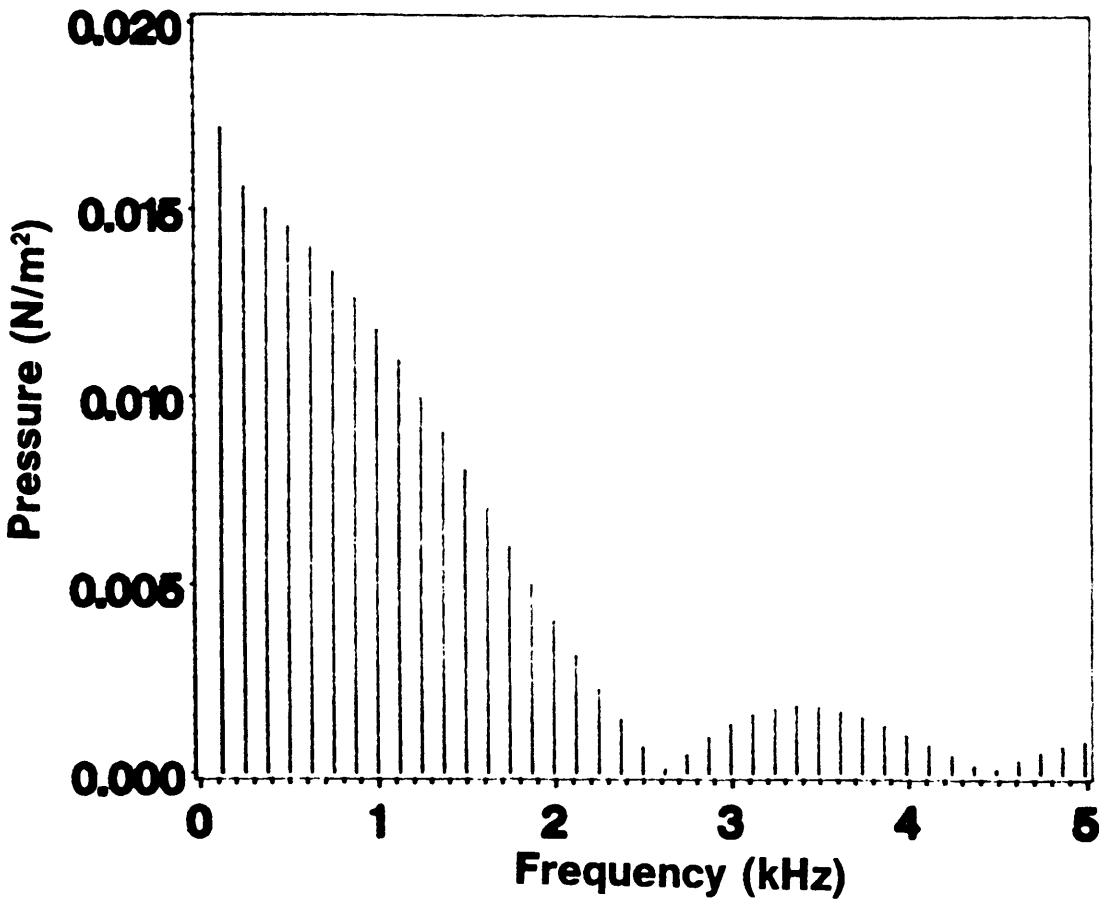

Fig. 26. Line Spectrum due to a Single Burning Cell: U = 20 m/s, D = 1 cm , SL = 80 cm/s, E = 6

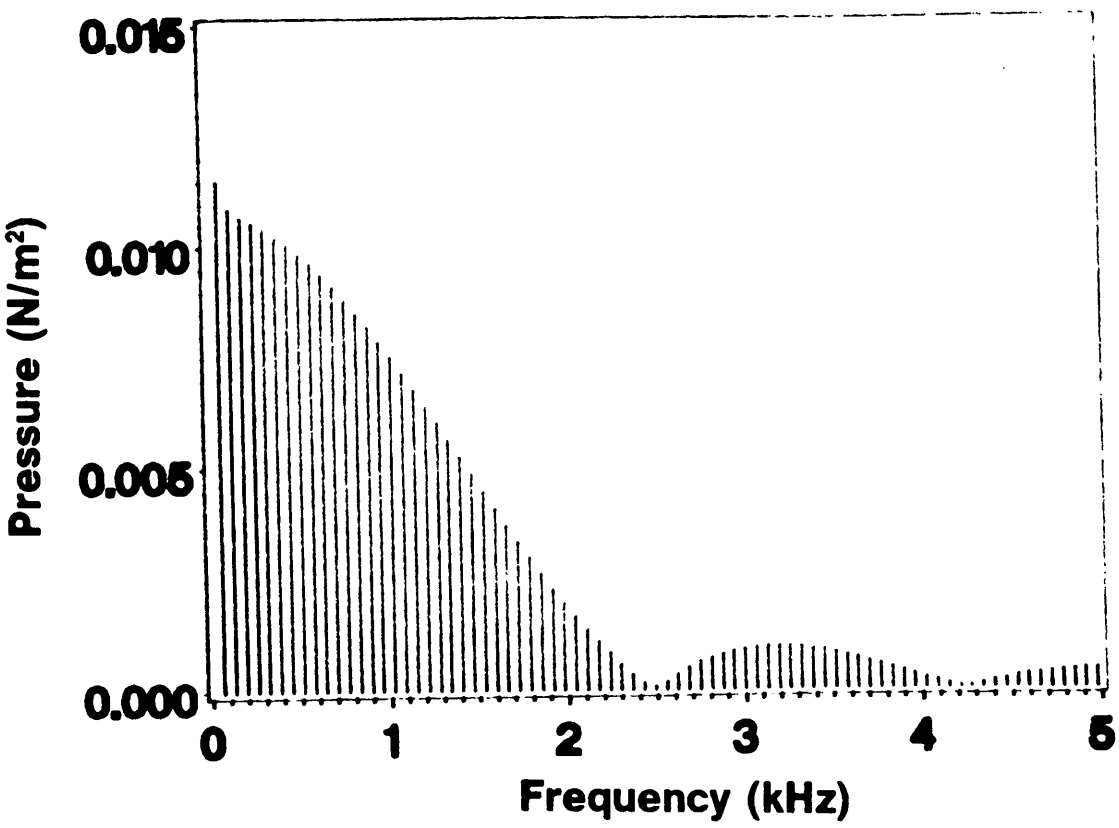

Fig. 27. Line Spectrum due to a Single Burning Cell: U = 20 m/s, D = 1 cm , SL = 40 cm/s, E = 12

4.10 1/3-Octave Band Spectra

A line spectrum due to the burning of a single continuous train of burning cells was obtained in terms of fundamental burner and fuel variables in the previous section. However, one should remember that most of the experimental work on combustion noise was done in 1970's when fast Fourier transform analysers were not in common use. It was the usual practice in those days to present experimental results in terms of 1/3 octave band spectra. Because of this, the line spectra developed in the previous section are converted into 1/3-octave band spectra in this section. This allows direct comparisons between predicted spectral shapes and spectra obtained from literature.

The first 1/3-octave band extends from 0 to 45 Hz. The center frequency of this band is 20 Hz. The above definition may be stated symbolically as

$$0 < f_1 < 45 \text{ Hz}, \text{ and } f_{1c} = 20 \text{ Hz} . \tag{4.50}$$

Having defined the lowest 1/3-octave band, the remaining bands are given by

$$f_{bl} < f_b < f_{bu} , \quad b = 2,3,4.....\infty, \tag{4.51}$$

where the lower frequency of the b^{th} band is given by

$$f_{bl} = 45 \text{ x } 2^{(b-2)/3}, \tag{4.52}$$

the upper frequency of the b^{th} band is given by

$$f_{bu} = 45 \text{ x } 2^{(b-1)/3}, \tag{4.53}$$

and the center frequency of this band is given by

$$f_{bc} = 45 \text{ X } 2^{(2b-3)/6}. \tag{4.54}$$

The above definitions give the boundaries and center frequencies of each band in a 1/3-octave analysis. The next task is to convert the pressure amplitudes from the line spectra, $|P_n|$, to the corresponding amplitudes in 1/3-octave bands, $|P_b|$. This is achieved by taking the root mean square of all the pressure amplitudes that lie inside each 1/3-octave band. In other words, the pressure amplitudes whose frequencies are given by $f_{bl} < f_n < f_{bu}$ lie in the same 1/3-octave band. Since $f_n = n/t_{tt}$, Eq.(4.49) the above explanation can be summarized as

$$|P_b| = \sqrt{\sum_{n=f_{bl}t_{tt}}^{n=f_{bu}t_{tt}} |P_n|^2} \quad , \; b = 1,2,....\infty. \tag{4.55}$$

This completes the evaluation of the 1/3-octave band spectra corresponding to the line spectra produced by a single continuous train of the combustible cells described in Section 4.9. The 1/3-octave bands generated corresponding to the line spectra of Figs. 23 through 27 are shown in Figs. 28 through 32 respectively. The corresponding 1/3-octave band spectra in decibels are shown in Figs. 33 through 37.

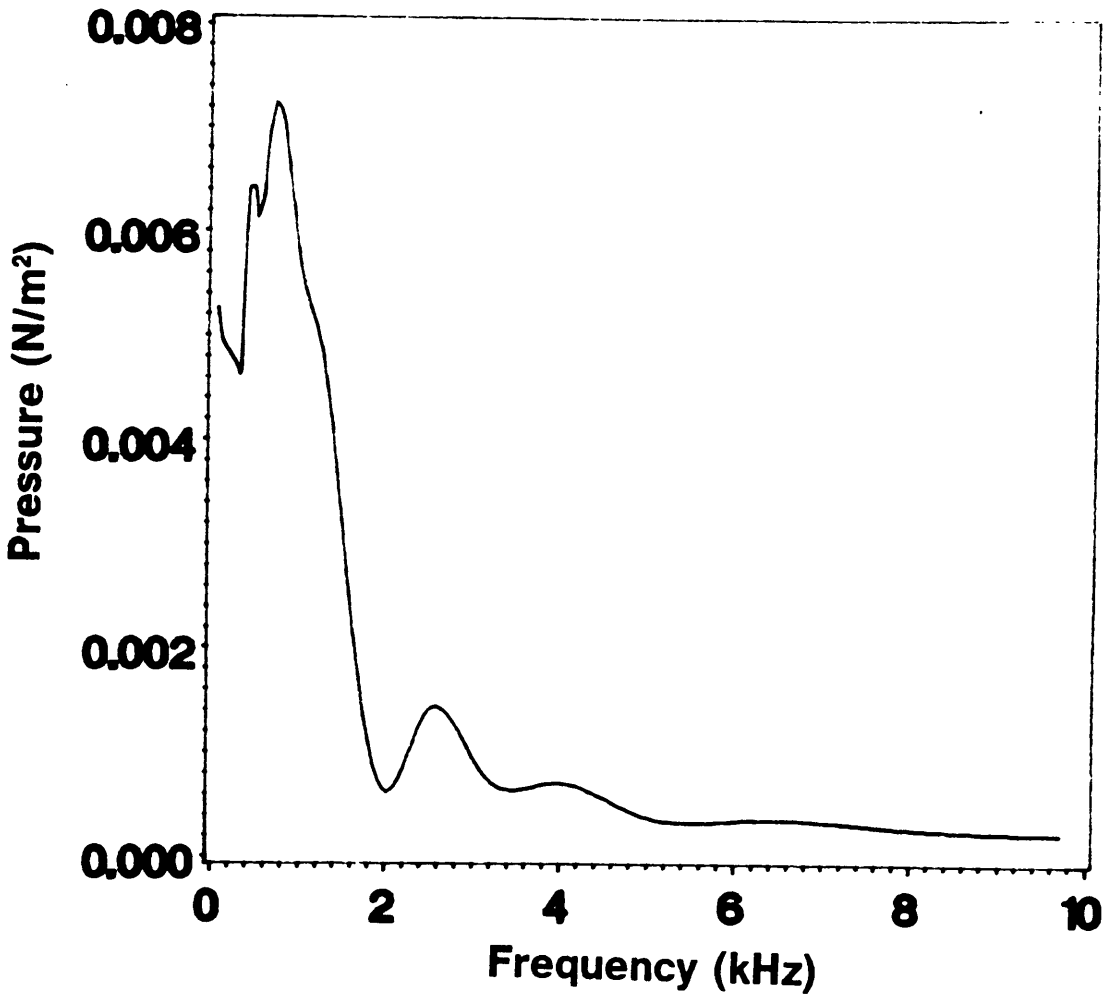

Fig. 28. 1/3-Octave due to a Single Burning Cell: U = 20 m/s, D = 1 cm , SL = 40 cm/s, E = 6

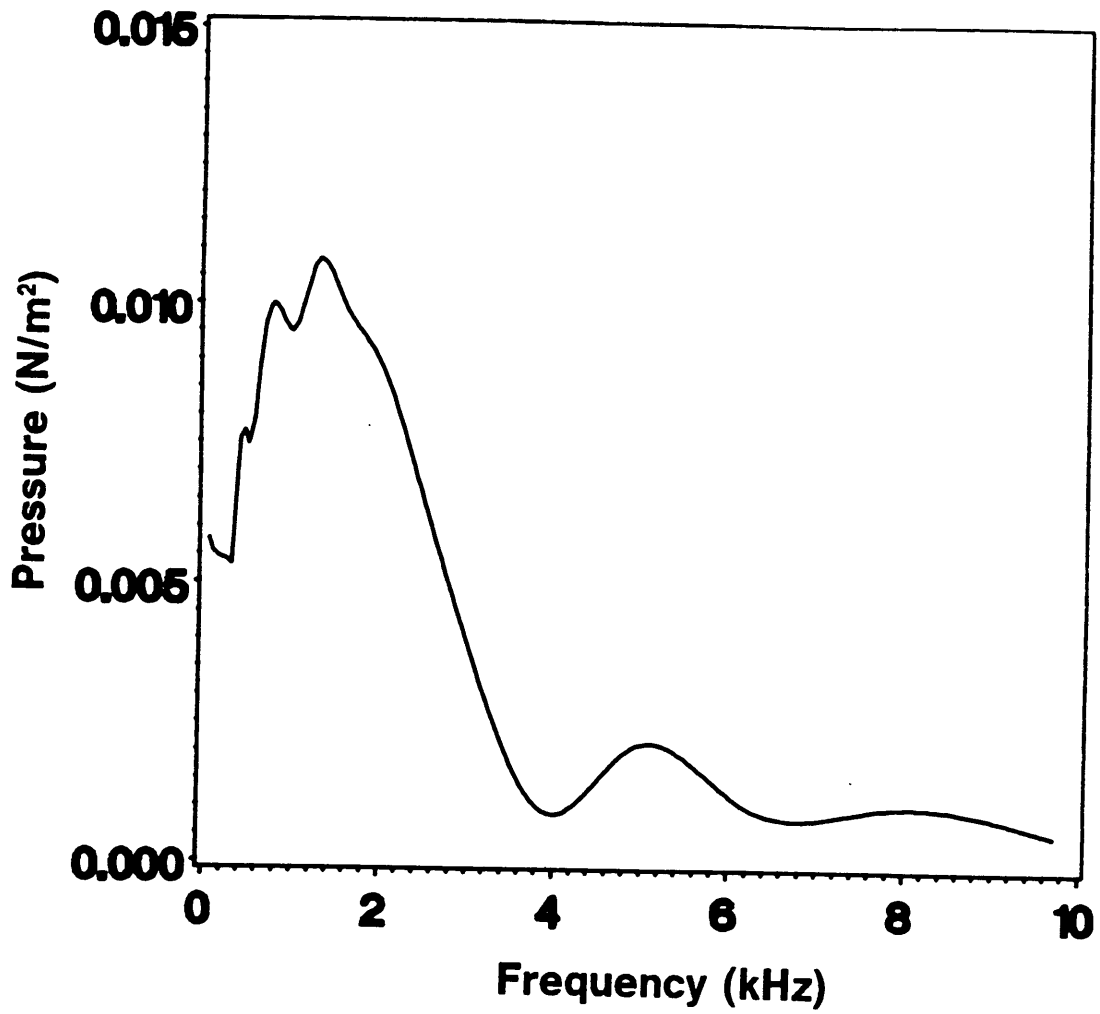

Fig. 29. 1/3-Octave due to a Single Burning Cell: U = 40 m/s, D = 1 cm , SL = 40 cm/s, E = 6

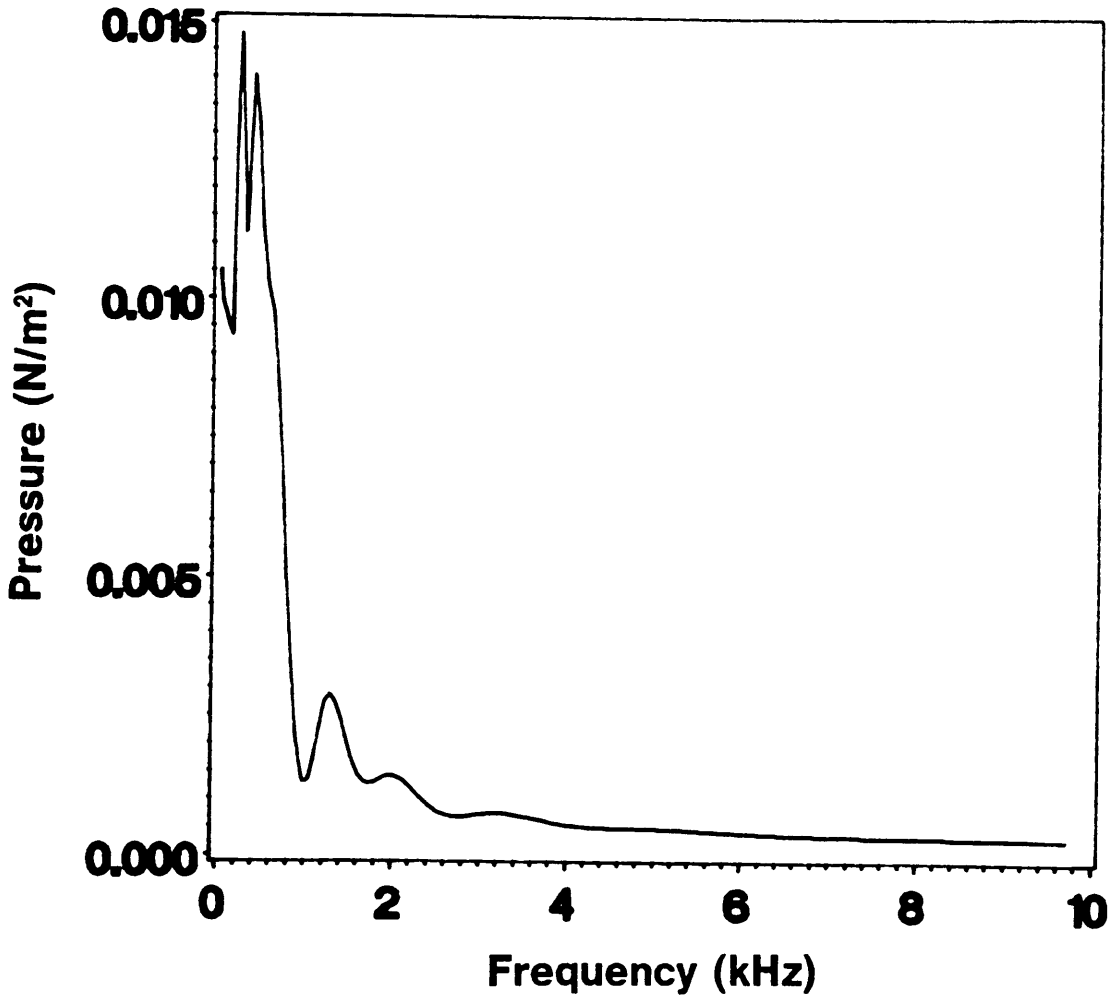

Fig. 30. 1/3-Octave due to a Single Burning Cell: U = 20 m/s, D = 2 cm , SL = 40 cm/s, E = 6

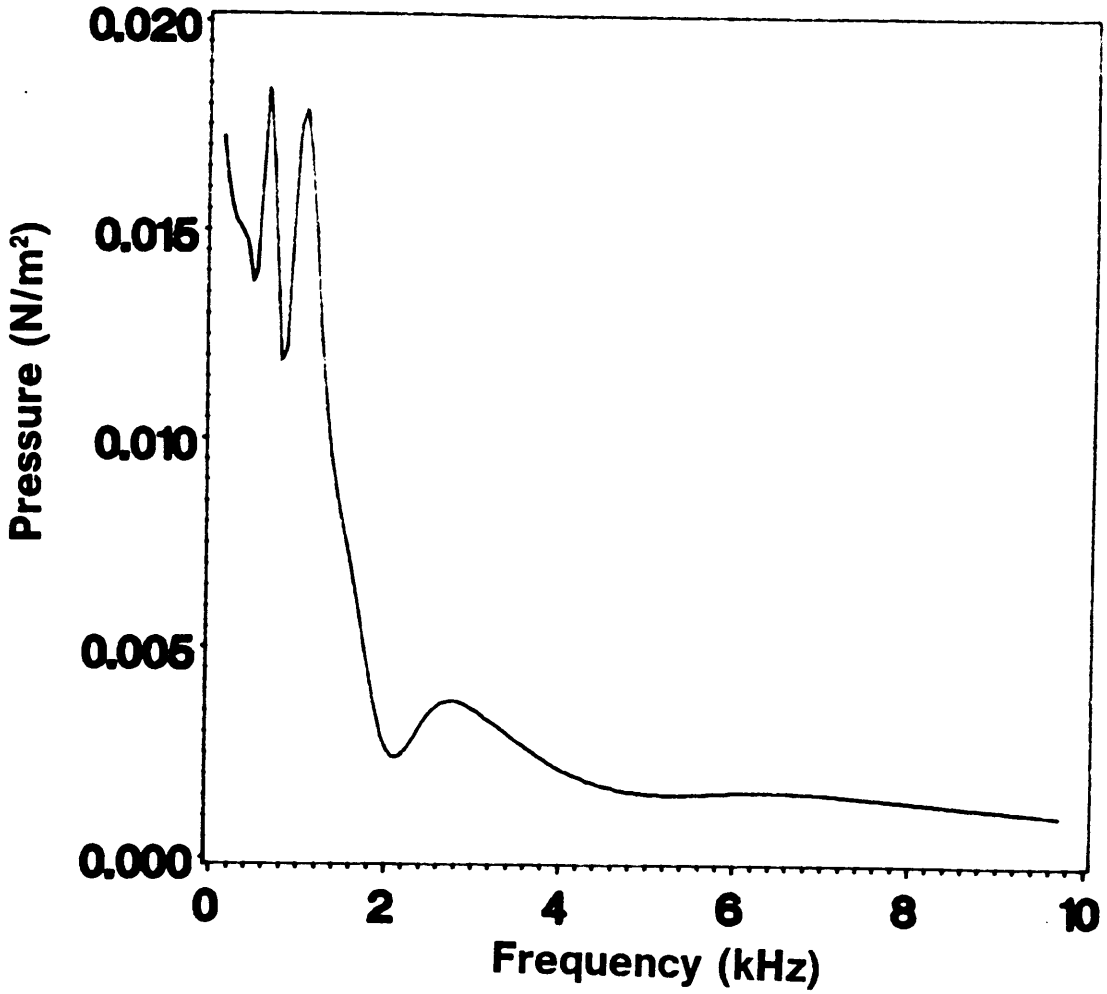

Fig. 31. 1/3-Octave due to a Single Burning Cell: U = 20 m/s, D = 1 cm , SL = 80 cm/s, E = 6

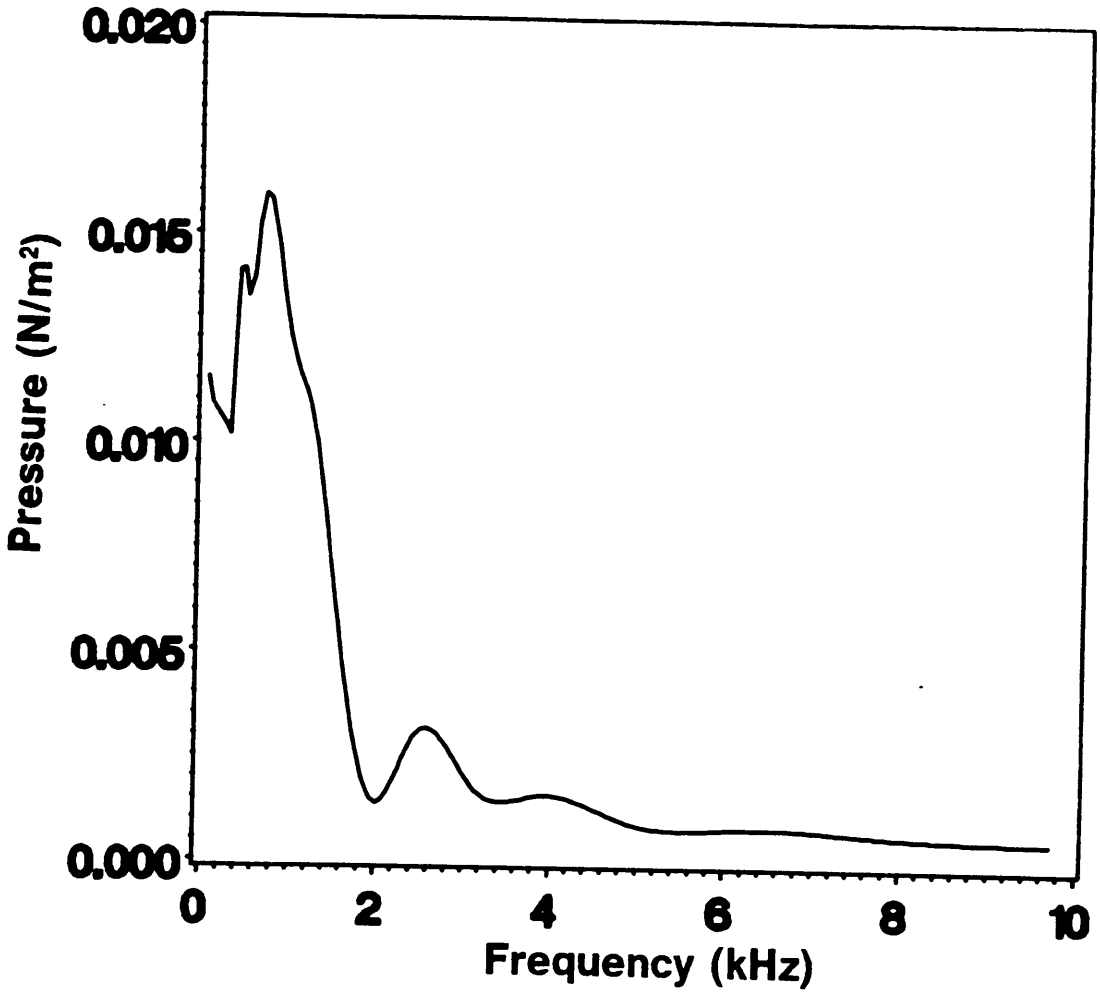

Fig. 32. 1/3-Octave due to a Single Burning Cell: U = 20 m/s, D = 1 cm , SL = 40 cm/s, E = 12

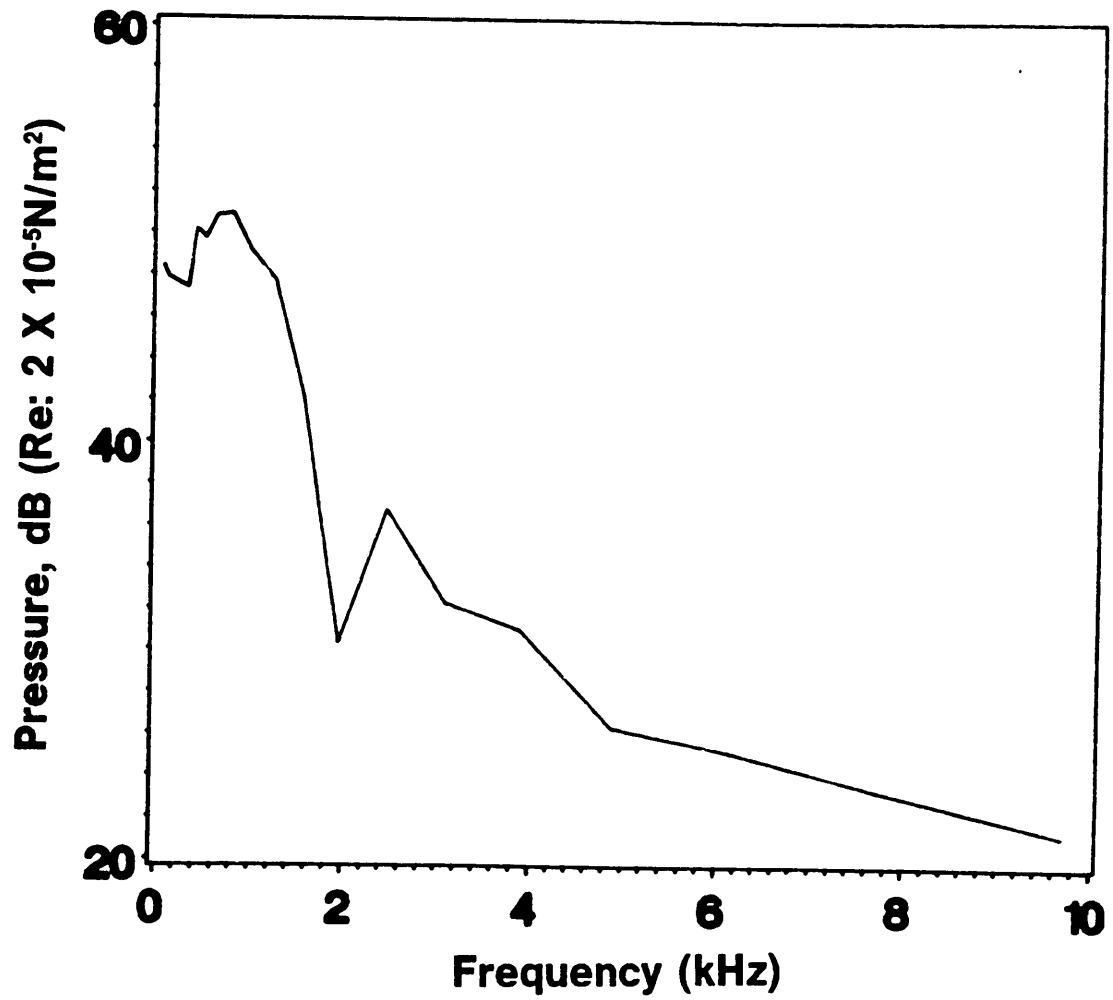

Fig. 33. 1/3-Octave (in dB) due to a Single Burning Cell: U = 20 m/s, D = 1 cm , SL = 40 cm/s, E = 6

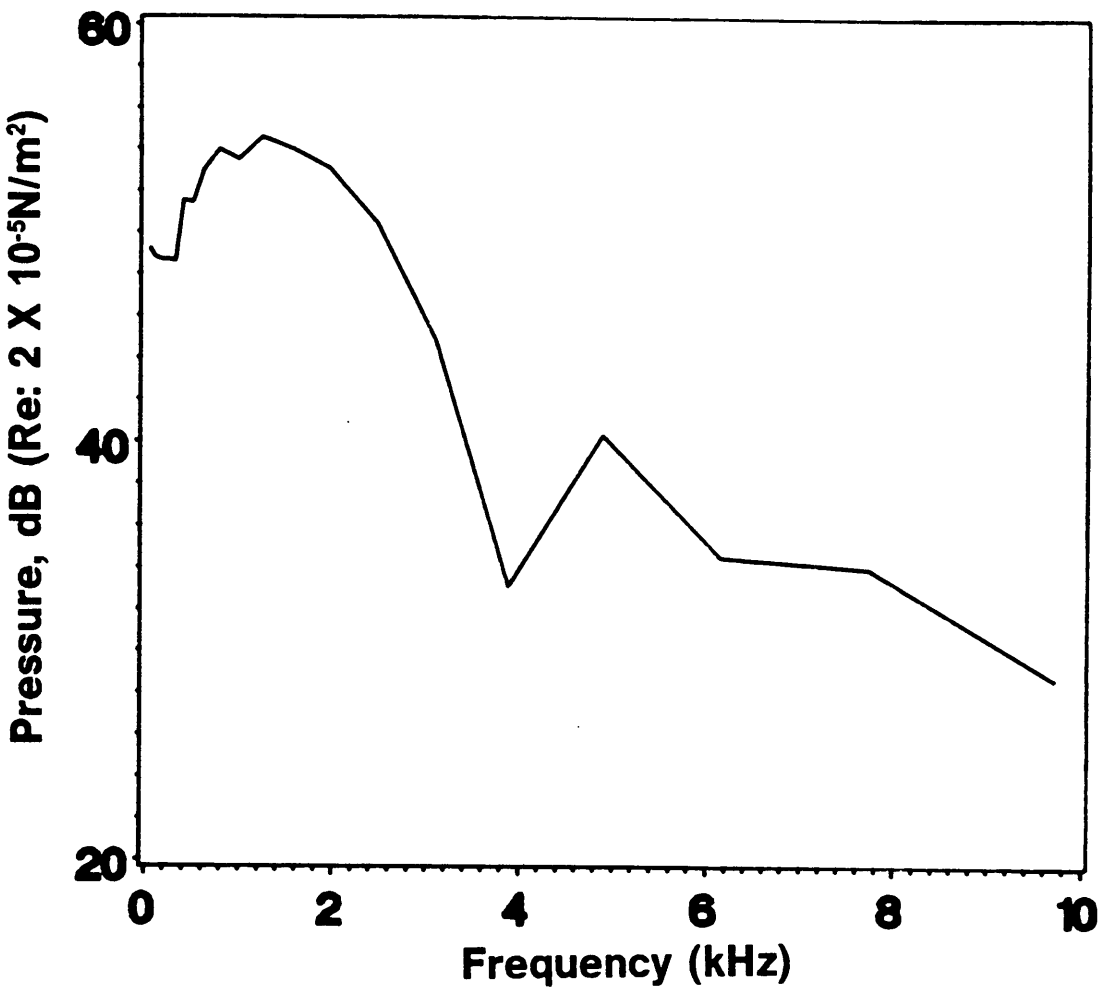

Fig. 34. 1/3-Octave (in dB) due to a Single Burning Cell: U = 40 m/s, D = 1 cm , SL = 40 cm/s, E = 6

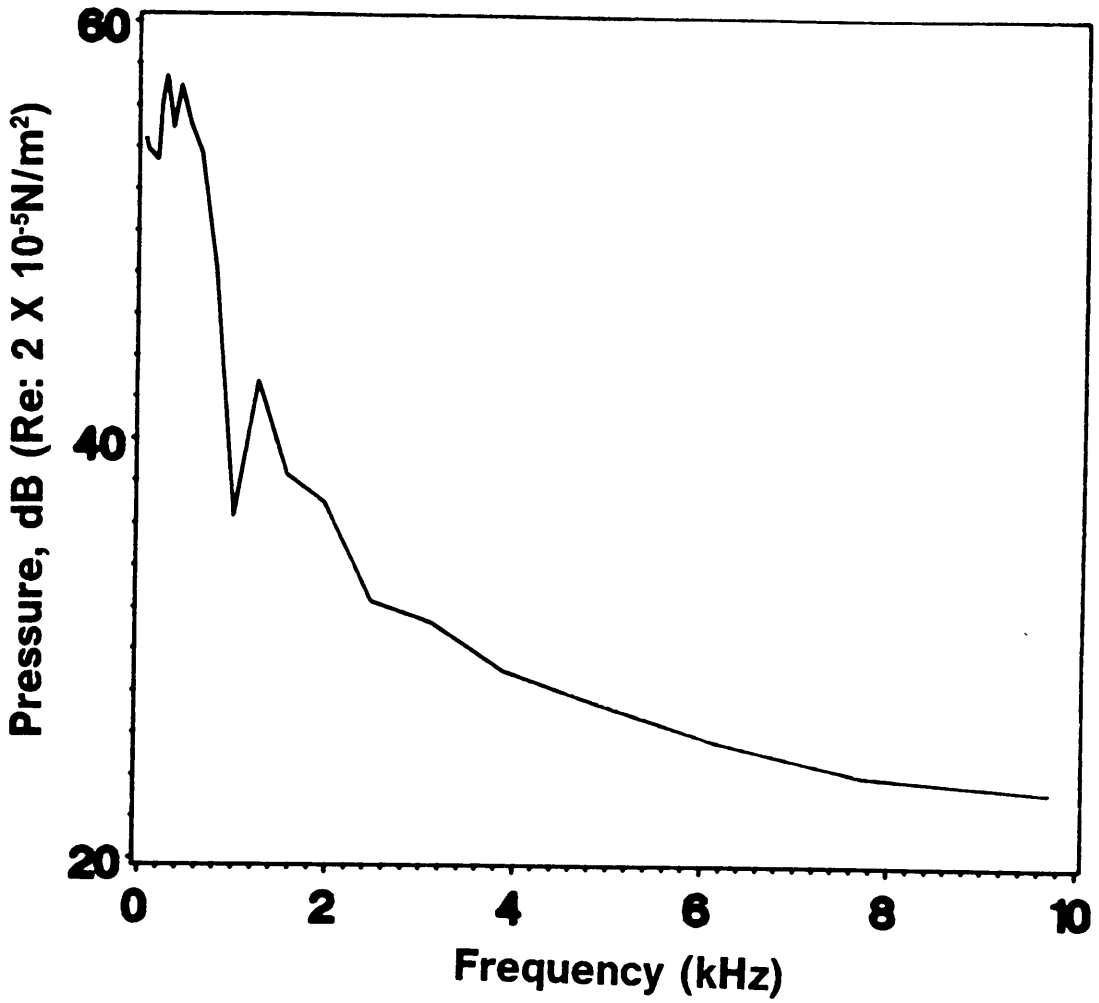

Fig. 35. 1/3-Octave (in dB) due to a Single Burning Cell: U = 20 m/s, D = 2 cm , SL = 40 cm/s, E = 6

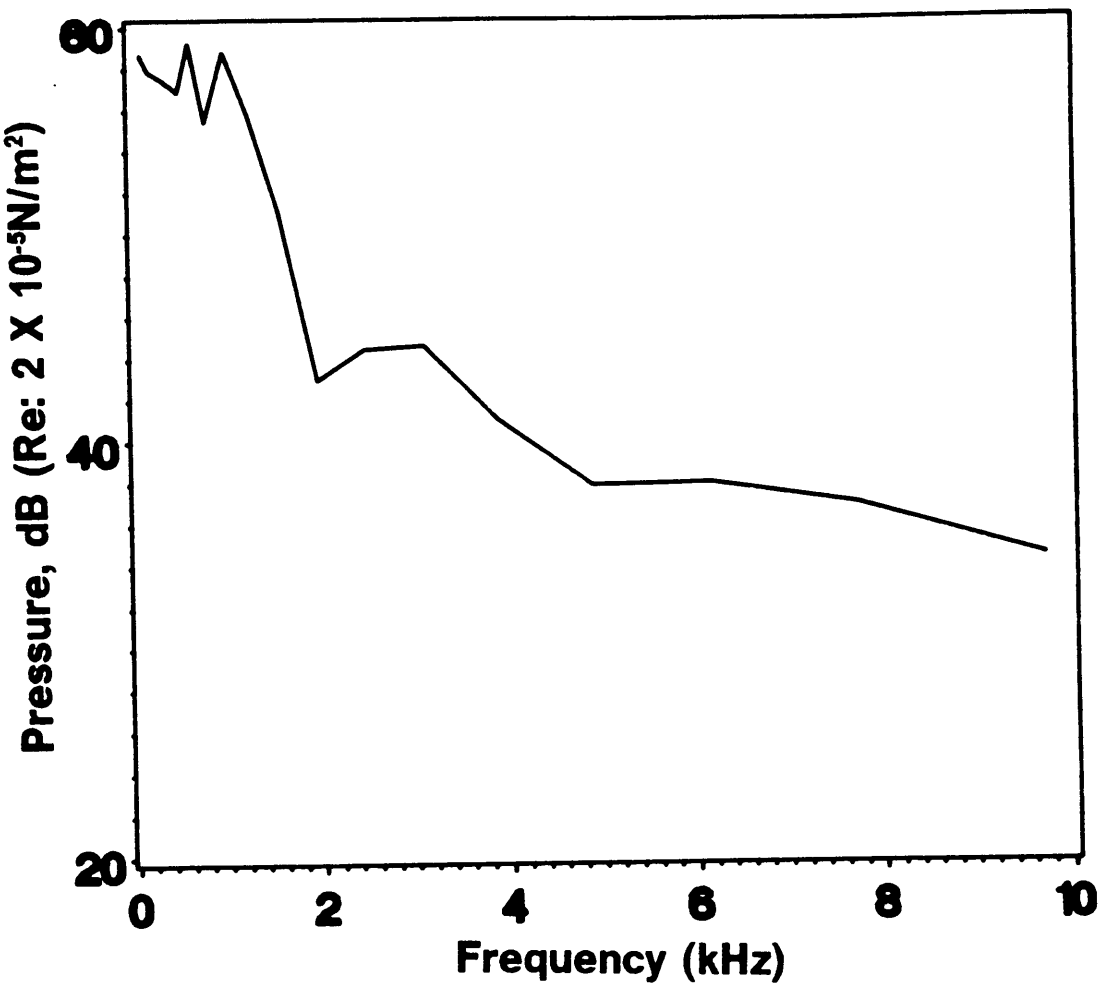

Fig. 36. 1/3-Octave (in dB) due to a Single Burning Cell: U = 20 m/s, D = 1 cm , SL = 80 cm/s, E = 6

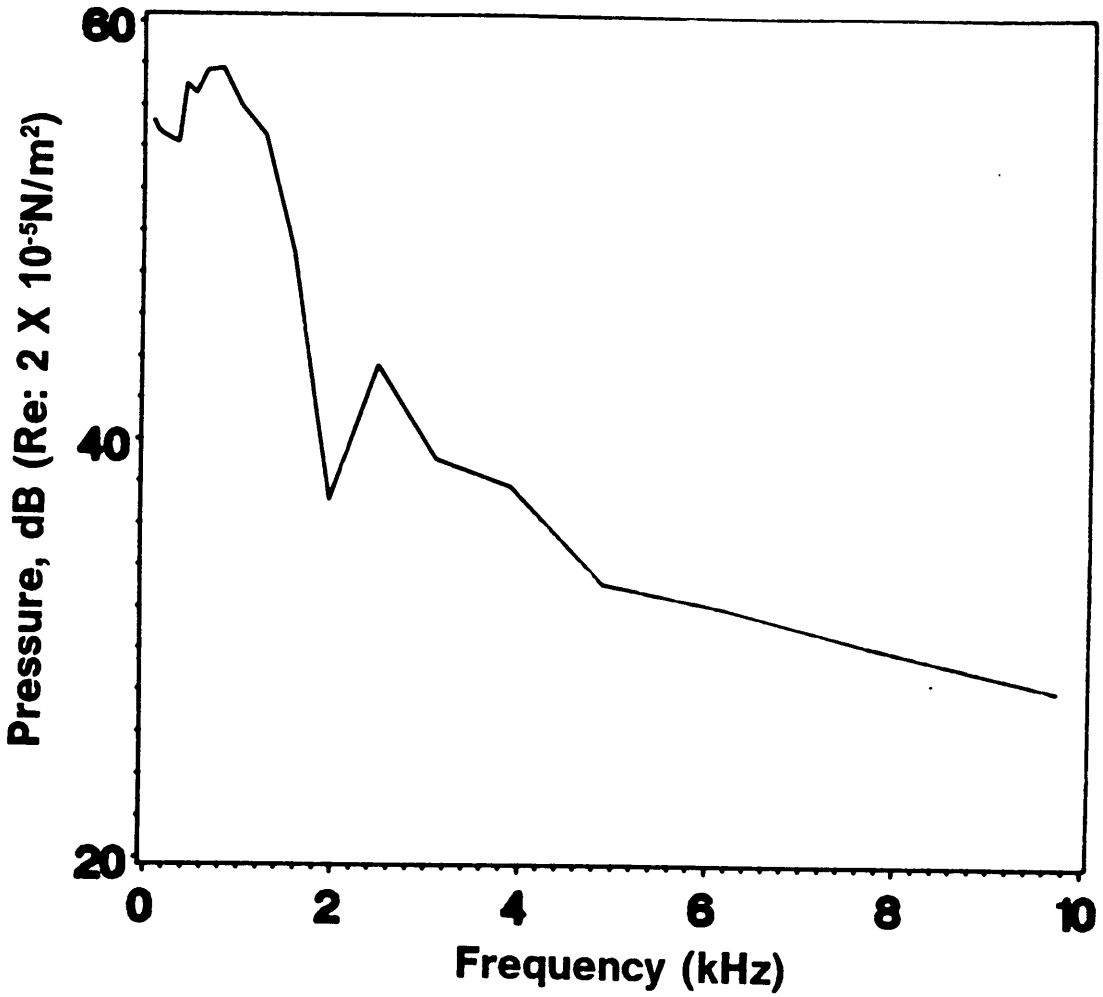

Fig. 37. 1/3-Octave (in dB) due to a Single Burning Cell: U = 20 m/s, D = 1 cm , SL = 40 cm/s, E = 12

4.11 *The Effective Number of the Noise Sources*

It should be noted that the solution for the acoustic pressure developed in the previous sections represents only a single continuous train of burning cells. In this section an expression will be developed for the number of such continuous trains of cells in terms of the fundamental burner and fuel parameters.

The volumetric flow rate, Q, is given by

$$Q = \frac{\pi}{4} D^2 U \,. \tag{4.1}$$

Suppose $\dot{n}$ is the production rate of the spherical cells of initial volume V_i in the combustion zone. Then

$$Q = \dot{n} V_i \,,$$

or,

$$Q = \dot{n}\left(\frac{4}{3} \pi R_i^3 \right) . \tag{4.56}$$

Equating Eqs. (4.56) and (4.1), there follows

$$\frac{\pi}{4} D^2 U = \dot{n}\left(\frac{4}{3} \pi R_i^3 \right) \quad ;$$

and, solving for the number of cells created per unit time,

$$\dot{n} = \frac{3 D^2 U}{16 R_i^3} \,. \tag{4.57}$$

Since the combustion time of each cell is t_{tt}, the number of effective noise sources at any instant is given by

$$n = \dot{n} t_{tt} = \frac{3D^2 U t_{tt}}{16 R_i^3} \quad . \tag{4.58}$$

Upon substitution of the value of R_i from Eq. (4.26), Eq.(4.58) reduces to

$$n = \sqrt{\frac{2}{3}} \frac{U t_{tt}}{D} \quad . \tag{4.59}$$

Thus an expression for the total sound power can be obtained by multiplying the power expressions for the noise generated by a single cell by the instantaneous number of cells in the combustion zone.

4.12 Evaluating Pressure, Power and Thermoacoustic Efficiency

4.12.1 Sound Pressure

The sound pressure amplitude generated by a single cell is obtained by taking the root-mean square of the pressure amplitudes in each band, that is,

$$P_{sl} = \sqrt{|P_1|^2 + |P_2|^2 + |P_3|^2 + ... + |P_b|^2 + ... + |P_{\infty|}{}^2} \ . \tag{4.60}$$

The over-all sound pressure produced by n continuous streams of the burning cells is given by

$$P = \sqrt{n}\, P_{sl} \ . \tag{4.61}$$

The Over-All Sound Pressure Level (OASPL) is given by

$$OASPL = 20 \log\left(\frac{P}{P_{ref}} \right), \tag{4.62}$$

where

$$P_{ref} = 2 \text{ x } 10^{-5} \ \text{N/m}^2 \ . \tag{4.63}$$

4.12.2 Sound Power

The sound power is the product of the pressure amplitude produced by a single cell and the instantaneous number of the combustible cells; that is,

$$S_P = 4\pi d^2 n\left(\frac{P_{si}^2}{2\rho c}\right), \tag{4.64}$$

where ρ is the density of air and c is the velocity of sound. The Over-All Sound Power Level (OAPWL) is expressed as

$$OAPWL = 10\log\left(\frac{S_P}{S_{Pref}}\right), \tag{4.65}$$

where,

$$S_{Pref} = 10^{-13}\ \text{W}. \tag{4.66}$$

4.12.3 Thermoacoustic Efficiency

As defined earlier, the thermoacoustic efficiency, η, is the fraction of the chemical heat release in the combustion process which appears as acoustic energy in the far field of burner. Thus, if H is the rate of heat release in combustion zone, the thermoacoustic efficiency is given by

$$\eta = \frac{S_P}{H}\ . \tag{4.67}$$

If q is the calorific value (heat released per unit volume consumption) of the fuel, and if F is the stochiometric fuel volume fraction in air, then the heat released per unit time in the flame is given by

$$H = qFQ \ . \tag{4.68}$$

Substituting Eqs. (4.68) and (4.1) into Eq. (4.65), there results

$$\eta = \frac{4S_P}{q\pi FUD^2} \ . \tag{4.69}$$

5.0 Results and Discussion

5.1 Pressure Time Series

The pressure time series produced by the burning of a single methane-air mixed turbulent eddy is shown in Fig. 22(b). The convective velocity is 20 m/s, the burner diameter is 1 cm, the laminar flame speed is 40 cm/s, and the expansion ratio is 8. Figure 22(b) exhibits two distinct characteristics of combustion generated noise which are consistent with the experimental observations:

1. The area enclosed by the positive pressure curve and the time-axis is equal to the area enclosed by the negative pressure curve and the time-axis. Since combustion noise should not have a steady component, this characteristic of the predicted pressure time series seems consistent with real world expectations. While this result strengthens the foundation of the model, its greater significance lies in the fact that no *a priori* attempt was made to influence this pleasing outcome. This is a natural outcome of the sound logic that has been followed in the development of Eq. (4.44).

2. In analyzing Fig. 22(b), a distinct dominant spike is observed corresponding to positive values of pressure for a very short time interval corresponding to the transition burning process, while a relatively flat curve is observed at negative values of pressure for a longer time interval corresponding to the surface burning process. The frequency spectrum corresponding to the time series of Fig. 22(b) is dominated by components generated by the "spike" representing transition burning. This, then, is consistent with the experimental observations of Roberts and Leventhall [21], as discussed in Sections 2.0 and 4.2.1, that the predominant noise generating mechanism in open turbulent flames is the "complex" burning phenomena at the flame front as opposed to the subsequent burning of turbulent eddies after they are completely surrounded by hot products.

5.2 Sound Power

In practice, the results for sound power are given in the form of a simple expression involving only the burner and fuel characteristics. Since the literature mostly gives the experimental results expressed in terms of sound power, a regression analysis is performed to evaluate the relationship of the sound power to the fundamental burner and fuel variables.

5.2.1 Regression Analysis of the Sound Power

The subroutine RGIVN is invoked from the International Mathematical Subroutine Library (IMSL) to perform the regression. RGIVN performs an orthogonal reduction of the matrix of regressors to upper triangular form. The reduction is based on fast Givens transformations [29]. This analysis gives the empirical correlation for sound power

$$S_P = 2.46 \text{ x } 10^{-4} U^{2.43} D^2 S_L^{1.58} E^{2.3} \quad \text{W} . \tag{5.1}$$

This regression supercedes the one given earlier by Nathani and Mahan [30]; the primary difference between this improved model and the one given earlier is the different way in which the radius of a noise source and the number of noise sources are calculated. In Eq. (5.1), U is the convective velocity, D is the burner diameter, S_L is the laminar flame speed, and E is the expansion ratio. The velocity of sound and the density of air are assumed to be 343 m/s and 1.21 Kg/m^3, respectively. To obtain this regression, the program was run for 81 sets of burner and fuel parameters, with U varying from 15 to 45 m/s, D varying from 1 to 5 cm, S_L varying from 40 to 80 cm/s, and E varying from 6 to 10, as shown in Table 1. For this set of burner and fuel parameters, the lowest predicted sound power is 0.0003 W, and the highest predicted sound power is 0.989 W. The results of the regression are shown in Fig. 38. The standard deviation of the above results is six percent.

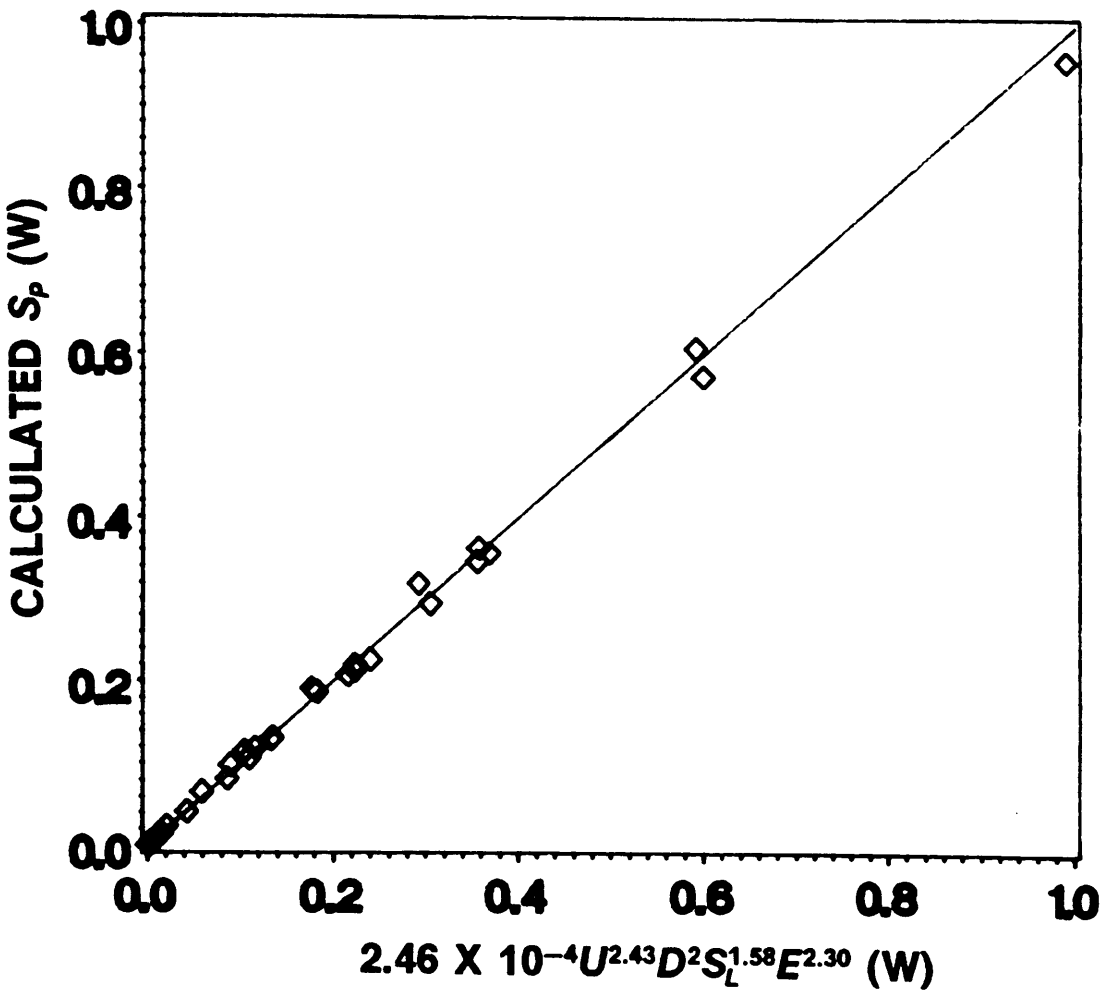

Fig. 38. Results of the Regression Analysis

Table 1. Model Predictions for Various Sets of Fuel and Burner Parameters

Fuel and Burner Parameters				Predicted Parameters			
U (m/s)	D (cm)	E (-)	S_L (cm/s)	S_P (W)	η x 10^8	OASPL (dB)	f_c (Hz)
15	1	6	40	.0003	8	70	496
15	1	6	60	.0005	15	73	496
15	1	6	80	.0007	20	74	100
15	1	8	40	.0006	16	73	496
15	1	8	60	.0010	29	76	496
15	1	8	80	.0014	40	77	100
15	1	10	40	.0010	27	76	496
15	1	10	60	.0017	49	78	496
15	1	10	80	.0024	67	79	100
15	3	6	40	.0026	8	80	17
15	3	6	60	.0048	15	82	158
15	3	6	80	.0066	20	84	17
15	3	8	40	.0050	15	83	17
15	3	8	60	.0093	29	85	158
15	3	8	80	.0129	40	87	17
15	3	10	40	.0083	26	85	17
15	3	10	60	.0154	49	88	158
15	3	10	80	.0213	67	89	17
15	5	6	40	.0071	8	84	17
15	5	6	60	.0132	15	87	79
15	5	6	80	.0183	20	88	17
15	5	8	40	.0139	15	87	17
15	5	8	60	.0259	29	90	79
15	5	8	80	.0358	40	91	17
15	5	10	40	.0231	26	89	17
15	5	10	60	.0429	49	92	79
15	5	10	80	.0592	67	93	17

Table 1 contd.

U (m/s)	D (cm)	E (-)	S_L (cm/s)	S_P (W)	η x 10^8	OASPL (dB)	f_c (Hz)
30	1	6	40	.0015	21	77	785
30	1	6	60	.0030	42	80	986
30	1	6	80	.0048	68	82	986
30	1	8	40	.0030	42	80	785
30	1	8	60	.0058	82	83	986
30	1	8	80	.0094	134	85	986
30	1	10	40	.0049	70	83	785
30	1	10	60	.0096	137	85	986
30	1	10	80	.0156	222	88	986
30	3	6	40	.0136	21	87	395
30	3	6	60	.0267	42	90	250
30	3	6	80	.0410	65	92	250
30	3	8	40	.0267	42	90	395
30	3	8	60	.0523	83	93	250
30	3	8	80	.0803	127	95	250
30	3	10	40	.0442	70	92	395
30	3	10	60	.0864	137	95	250
30	3	10	80	.1328	210	97	250
30	5	6	40	.0360	20	91	158
30	5	6	60	.0741	42	94	199
30	5	6	80	.1139	65	96	158
30	5	8	40	.0706	40	94	158
30	5	8	60	.1452	83	97	199
30	5	8	80	.2232	127	99	158
30	5	10	40	.1167	66	96	158
30	5	10	60	.2400	137	99	199
30	5	10	80	.3689	210	101	158

Table 1 contd.

U (m/s)	D (cm)	E (-)	S_L (cm/s)	S_P (W)	η x 10^8	OASPL (dB)	f_c (Hz)
45	1	6	40	.0036	34	81	1240
45	1	6	60	.0077	73	84	1559
45	1	6	80	.0122	116	87	1559
45	1	8	40	.0071	67	84	1240
45	1	8	60	.0150	143	87	1559
45	1	8	80	.0239	227	89	1559
45	1	10	40	.0117	111	86	1240
45	1	10	60	.0248	236	90	1559
45	1	10	80	.0395	376	92	1559
45	3	6	40	.0325	34	91	395
45	3	6	60	.0690	73	94	496
45	3	6	80	.1099	116	96	395
45	3	8	40	.0637	67	94	395
45	3	8	60	.1352	143	97	496
45	3	8	80	.2154	228	99	395
45	3	10	40	.1052	111	96	395
45	3	10	60	.2235	236	99	496
45	3	10	80	.3561	377	101	395
45	5	6	40	.0902	34	95	250
45	5	6	60	.1823	69	98	250
45	5	6	80	.3053	116	101	314
45	5	8	40	.1768	67	98	250
45	5	8	60	.3573	136	101	250
45	5	8	80	.5985	228	103	314
45	5	10	40	.2923	111	100	250
45	5	10	60	.5906	225	103	250
45	5	10	80	.9894	377	106	314

5.2.2 Discussion of the Predicted Sound Power

Referring back to the literature review (Section 2.0) the most widely accepted formula for the prediction of sound power is the one given by Strahle [23], which is

$$S_P \propto U^{2.67} D^{2.81} S_L^{1.83} F^{-0.26} \quad \text{for fuel-lean premixed flames,} \tag{5.2a}$$

and

$$S_P \propto U^3 D^2 \quad \text{for fuel-rich premixed flames.} \tag{5.2b}$$

On inspecting Eqs. (5.1) and (5.2), it becomes clear that the direct comparison of the effects of all the parameters on the predicted sound power with the results from the literature is not possible at this stage. The reason for this is that each of the three expressions above have at least one parameter different from the others; the expansion ratio E has been used in the current model, while Strahle's relation for fuel-lean premixed flames contains the fuel ratio F and his model for fuel-rich premixed flames accounts only for the burner characteristics U and D without taking into consideration the influence of fuel parameters. However, the exponents of the three fundamental combustion noise parameters; U, D and S_L; can be compared. The comparisons are made below in terms of the percentage variation of the exponents for the predicted and observed experimental values.

1. In the case of fuel-lean premixed flames, the agreements between the exponents of U (9.2 percent difference), and S_L (13.7 percent difference) are excellent, while the exponent of D exhibits a fairly significant disagreement (28.8 percent). However, it is noted that the disagreements for all three exponents discussed above are well

within the range of the standard deviation of Strahle's results (43.2 percent) and the predicted results (six percent).

2. For the case of fuel-rich premixed flames, while the exponent of D agrees exactly with the observed values, the exponent of U exhibits moderate disagreement (19 percent). The agreement between the results for fuel-rich premixed flames is remarkable; however, it should be remembered that the characteristics of fuel-rich premixed flames approach those of pure diffusion flames as the percentage volume of air in the reactants becomes substantially lower than the stochiometric percentage of air. While the foundation of the model appears general enough, its physics can be associated more closely with the structure of fuel-lean premixed flames as compared to diffusion flames. Thus, although the results predicted for fuel-rich premixed flames are very encouraging, their verification will have to await certain modifications to the existing model to more adequately account for the structure of diffusion flames.

5.3 Pressure Spectra

Figures 23 through 27 show the line spectra, Figs. 28 through 32 show the 1/3-octave band spectra, and Figs. 33 through 37 show the 1/3-octave spectra in decibels predicted by this model for the burning of a single continuous stream of turbulent eddies. To obtain the above spectra, two variables for each of the burner and fuel parameters are used. The two values for convective velocity are 20 and 40 m/s, for burner diameter are 1 and 2 cm, for laminar flame speed are 40 and 80 cm/s, and for expansion ratio are 6 and 12, respectively. Neglecting the possible effect of destructive interference between

different continuous streams of the turbulent eddies, it can be conveniently assumed that the spectra of Figs. 23 through 37, while accounting for the burning of a single continuous stream of burning eddies, do adequately represent the over-all shape of the combustion noise spectra.

5.3.1 Discussion of the Predicted Pressure Spectra

Referring back to Section 2.0, the influences of basic fuel and burner parameters on the 1/3 octave band spectra for fuel-lean premixed flames has been shown in Figs. 2 and 3. Figure 4 shows the various pressure spectra obtained by Seshan [26] for the case of diffusion (or fuel-rich premixed) flames. The similarities between the experimental and the predicted spectra are remarkable as are obvious from the following comparisons:

1. As observed experimentally, the predicted spectra are typical of the type associated with jet noise, extend over about 10 octaves, and exhibit no sharp peaks. The "universal shape" of the combustion noise spectra, as shown by Seshan in Fig. 6, is in excellent agreement with the predicted shapes shown in Figs. 33 through 37.
2. The predicted spectra exhibit a predominately low frequency (300-500 octave band) content which is consistent with the experimental observations of various researchers including the ones which are reproduced in Figs. 2, 3 and 6. Table 1 shows the central frequency of the peak 1/3-octave band for the 81 sets for which the regression for sound power was performed. The mean peak frequency for these conditions is 450 Hz.
3. The observed shifts in the peak frequency in relation to the convective velocity, the burner diameter and the laminar flame speed are shown in Figs. 2 and 3. It is noted

from Fig. 2 that the peak frequency increases with the increasing convective velocity and the laminar flame speed. Figure 3 shows that the peak frequency decreases with the increasing burner diameter. Similar trends are observed in the predicted results, as may be seen in Figs. 28 through 37, and in Table 1.

5.4 *Over-All Sound Pressure Level*

The expressions for the overall sound power level have been developed in Section 4.12.1. Since the sound pressure is reflective of the sound power generated, no separate correlation has been given for OASPL. The Over-All Sound Pressure Levels predicted using the model for the 81 sets of burner and fuel parameters are shown in Table 1. For the above set of parameters, the lowest predicted OASPL is 70 dB and the highest predicted OASPL is 106 dB. For the given values of burner and fuel variables, this range of OASPL looks very reasonable and consistent with the experimental observations.

5.5 *Thermoacoustic Efficiency*

For the same set of conditions as stated in Section 5.2, the lowest predicted thermoacoustic efficiency is 8×10^{-8}, and the highest is 3.8×10^{-6}. This range of η is very consistent with the experimentally observed values reported in Refs. [17], [18], [22] and [23]. Indeed, that thermoacoustic efficiencies for all hydro-carbon fuels burning in an

open turbulent flame range from 10^{-8} to 10^{-6} seems to be an unanimously accepted conclusion in the combustion-noise research community.

6.0 Conclusions

This thesis is an attempt to develop a first-principle model to predict the direct combustion noise characteristics of an open turbulent flame from the basic burner and fuel parameters. The fundamental burner and fuel parameters used are (1) convective velocity of the fuel-air mixture (2) burner diameter (3) laminar flame speed of the fuel, and (4) expansion ratio (ratio of volume occupied by burned gases to that of unburned gases at the same pressure). The model allows the following combustion noise characteristics to be predicted:

1. The pressure time series; which shows consistency with reality in that (1) it has no steady component, and (2) it recovers the experimental conclusion that the predominant noise generating mechanism in open turbulent flames is the "complex burning" phenomenon at the flame front.
2. The pressure spectra; which derive support from the observations of several experimentalists in that (1) they are typical of the type associated with jet noise, extend over about ten octaves and exhibit no sharp peaks, (2) exhibit a predominately low frequency (300-500 Hz) content, and (3) demonstrate the exper-

imentally observed shifts in the peak frequency with varying burner and fuel parameters.

3. The sound power; which is exceedingly close to reality in that the exponents of the convective velocity, the burner diameter and the laminar flame speed in the sound power expression are well within the standard deviation of the empirical correlations for sound power present in the literature.
4. Over-All Sound Pressure Level (OASPL); which, being directly related to the sound power, agrees equally well with the experimental observations as do the predicted results for the sound power.
5. Thermoacoustic efficiency; which is in total agreement with the experimental observations of all hydrocarbon fuels burning in an open turbulent flame in that it ranges from 10^{-8} to 10^{-6}, a unanimously accepted conclusion in the combustion-noise research community.

In conclusion, this model shows remarkable agreement between the predicted and the experimentally observed characteristics of open flame combustion noise. It is believed that the availability of this first principle model will subsequently facilitate:

- Development of technology that may be applied to suppress engine core noise in gas turbine power plants,
- Development of acoustic diagnostic techniques characterizing burner combustion performance.

7.0 Recommendations for Further Research

The model presented in this thesis gives excellent results while using a straightforward, intuitive approach. However, it should be remembered that this is a simplified first-principle model, which does not take fully into account all of the numerous complex phenomena going on in a turbulent flame. By predicting exceedingly realistic results while using only four burner and fuel variables, this model exhibits tremendous potential for further research. It is anticipated that further research and extensions to this model may finally offer a solution to the complex problem of predicting combustion noise from first principles. Suggested areas of further research are:

1. To maintain the simplicity of the model, a simple assumption about the way a turbulent jet breaks up into a single row of spherical cells has been made. This assumption does not take into account the possibility of more than one parallel continuous stream of cells entering the combustion zone. Realistically, this is at best a questionable assumption. It is a well-known fact that the sizes and the number of turbulent eddies in the combustion zone are affected by numerous complex turbulent parameters which are variable both in time and space. Perhaps, Mahan's

suggestion [27] to model the complex shapes of these eddies as a statistical distribution of unburned spheres about some mean initial value of cell radius $\overline{R_i}$ will be useful here. The exact evaluation of the cell radius and the number of parallel continuous streams of cells should, in principle, further improve the agreement between the various predicted and observed parameters. However, to achieve this the simplicity of the model would have to be sacrificed.

2. The model accounts for the complete combustion of a turbulent eddy. How the expression for acoustic pressure will be modified in the case of incomplete combustion is not considered. Extensions to the present model to account for the incomplete combustion of turbulent eddies will not only reflect the more realistic case of turbulent combustion, but may even exhibit the potential of predicting various combustion characteristics through far-field acoustic measurements.
3. The model does not take into account fuel fraction F in the case of premixed flames; that is, stoichiometric combustion is assumed. Consideration of fuel fraction could lead to significant changes.
4. Destructive interference effects between the various streams of burning turbulent eddies are not accounted for by the theory developed in this thesis. Modifications to the existing model to account for these interference effects may explain the slight directivity observed experimentally in combustion noise.

References

1. Strahle, W. C., "A Review of Combustion Generated Noise", AIAA Paper No. 75, 1975.

2. Lighthill, M. J., "On Sound Generated Aerodynamically. 1. General Theory,", Proceedings of the Royal Society of London, Series A, Vol. 211, 1952, pp. 564-587.

3. Legendre, R., La Recherche Aerospatiale, 1985, pp. 145-150.

4. Goldstein, M. E., Aeroacoustics, McGraw-Hill, New York, 1976.

5. Candel, S. M., Ph.D. Dissertation, California Institute of Technology, 1972.

6. Putnam, A. A., "Combustion Roar of Seven Industrial Gas Burners", Jounal of the Institute of Fuel, September 1976, pp. 135-138.

7. Putnam, A. A., "Combustion Noise in Industrial Burners", Noise Control Engineering, July-August 1976, pp. 24-34.

8. Mahan, J. R., and J. M. Kasper, "Influence of Heat Release Distribution on the Acoustic Response of Long Burners", ASME Paper No. 79-DET-31, Design Engineering Technical Conference, St. Louis, MO, September 10-12, 1979.

9. Valk, M., "Acoustic Power Measurements of Oscillating Flames", Combustion and Flame, Vol. 41, 1981, pp. 251-260.

10. Mahan, J. R., and J. D. Jones, "Recovery of Acoustic Source Structure in a Long Turbulent Burner from far-field Sound Spectra", Paper No. 83-0763, AIAA 8th Aeroacoustics Conference, Atlanta, GA, April 11-13, 1983.

11. Mahan, J. R., "Experimental Study of the Thermo-Acoustic Efficiency in a Long, Turbulent Diffusion-Flame Burner", NASA Contractor Report-3725, August 1983.

12. Mahan, J. R., and S.-Y. Yeh, "Anomalous Recovery of Damped Radial Modes in a Circular-Sector Duct with Locally Heated Flow", 107th meeting of the Acoustical Society of America, Norfolk, VA, May 7-10, 1984.

13. Mahan, J. R., "A Critical Review of Noise Production Models for Turbulent, Gas-Fueled Burners", NASA Contractor Report 3803, June 1984.

14. Gayden, A. G., and H. G. Wolfhard, Flames, 1st ed., Chapman and Hall, London, 1953, p. 158.

15. Bragg, S. L., "Combustion Noise," Journal of the Institute of Fuel, Vol. 35, No. 264, January 1963, pp. 12-16.

16. Discussion of Ref. [16], Journal of the Institute of fuel, Vol. 36, No. 271, August 1963, pp. 344-346.

17. Smith, T. J. B., and J. K. Kilham, "Noise Generation by Open Turbulent Flames," Journal of the Acoustical Society of America, Vol. 35, No. 5, May 1963, pp. 715-724.

18. Thomas, A., and G. T. Williams, "Flame Noise: Sound Emission from Spark-Ignited Bubbles of Combustible Gas," Proceedings of the Royal Society of London, Series A, Vol. 294, 1966, pp. 449-466.

19. Giammar, R. D., and A. A. Putnam, "Combustion Roar of Turbulent Diffusion Flames," ASME Transactions, Series A, Jounal of Engineering for Power, Vol. 92, No. 2, April 1970, pp. 157-165.

20. Arnold, J. S., "Generation of Combustion Noise," Journal of the Acoustical Society of America, Vol. 5A 2, No. 1, 1972, pp. 5-12.

21. Roberts, J. P., and H. G. Leventhall, "Noise Sources in Turbulent Premixed Flames," Applied Acoustics, Vol. 6, 1973, pp. 301-308.

22. Shivashankara, B. N., W. C. Strahle, and J. C. Handley, "Combustion Noise Radiation by Open Turbulent Flames," AIAA Paper No. 73-1025, AIAA Aeroacoustics Conference, Seattle, WA, October 15-17, 1973.

23. Strahle, W. C., "Convergence of Theory and Experiment in Direct Combustion-Generated Noise," AIAA Paper No. 75-522, Second AIAA Aeroacoustics Conference, Hampton, VA, March 24-26, 1975.

24. Ramohalli, K., "Acoustic Diagnostics of the Nonpremixed Turbulent Jet Flames," AIAA Paper No. 79-0591, 1979.

25. Ramachandra, M. K., and W. C. Strahle, "Acoustic Signature from Flames as a Combustion Diagnostic Tool," AIAA Journal, Vol. 21, No. 8, August 1983.

26. Seshan, P. K., "Reynolds Number Effects in Combustion Noise," Combustion Science and Technology, Vol. 49, pp.1986, pp. 263-275.

27. Mahan, J. R., "A New Turbulent Combustion Noise Model," Proceedings of NOISE-CON 87, The Pennsylvania State University, PA, June 8-10, 1987, pp. 201-206.

28. Mahan, J. R., and A. Nathani, "An Improved Turbulent Combustion Noise Model," Proceedings of INTER-NOISE 88, International Conference on Noise Control Engineering, Avignon, France, August 30 - September 1, 1988, pp. 891-894.

29. Draper, N. R., and H. Smith, Applied Regression Analysis, 2nd edition, John Wiley and Sons, New York, 1981.

30. Nathani, A., and J. R. Mahan, "Prediction of Direct Combustion Noise in Open Turbulent Flames" Proceedings of Combustion Institute: The Eastern Section, Clearwater Beach, FL, December 5-7, 1988.

Appendix

FORTRAN PROGRAM

FOR CALCULATIONS

```
C              FORTRAN PROGRAM FOR
C
C         "A TURBULENT COMBUSTION NOISE MODEL"
C
C                 (THESIS)
C
C                 SUBMITTED TO
C
C         DEPARTMENT OF MECHANICAL ENGINEERING
C
C     VIRGINIA POLYTECHNIC INSTITUTE AND STATE UNIVERSITY
C
C              BLACKSBURG, VIRGINIA
C
C                   BY
C
C                 ARUN NATHANI


C         THE FOLLOWING PROGRAM EVALUATES CURVES FOR
C         DV/DT AND ACOUSTIC PRESSURE GENERATED BY A
C         SINGLE BURNING CELL IN THE COMBUSTION ZONE.
C         IT ALSO GENERATES LINE SPECTRA, 1/3 OCTAVE BAND
C         SPECTRA FOR THE TOTAL SOUND PRESSURE PRODUCED IN
C         THE COMBUSTION ZONE.  IN ADDITION, THIS PROGRAM
C         GIVES THERMOACOUSTIC EFFICIENCY, SOUND POWER,
C         PEAK FREQUENCY AND OVER-ALL SOUND PRESSURE LEVEL.
C         FINALLY, THE PROGRAM DEVELOPS A EMPIRICAL
C         CORRELATION FOR THE SOUND POWER PRODUCED IN
C         TERMS OF FUNDAMENTAL BURNER AND FUEL PARAMETERS


C              INPUT BURNER PARAMETERS
C
C         U ..... CONVECTIVE VELOCITY OF FUEL INJECTION (M/S)
C         D ..... BURNER DIAMETER (M)


C              INPUT FUEL PARAMETERS
C
C         SL ..... LAMINAR FLAME SPEED (M/S)
C         E ..... EXPANSION RATIO  (RATIO BETWEEN THE VOLUME
C                 OCCUPIED BY BURNT GASES TO UNBURNT GASES
C         QQ ..... CALORIFIC VALUE OF THE FUEL (J/M**3)
C         FR ..... AIR-FUEL VOLUMETRIC RATION
C         FLTP..... FLAME TEMPERATURE (KELVINS)


C              EXPERIMENTAL PARAMETERS
C
C         DOP,DP... DISTANCE OF OBSERVATION POINT FROM SOURCE (M)
C         RHO ..... DENSITY OF AIR (KG/M**3)
C         CSOU..... VELOCITY OF SOUND IN AIR (M/S)
C         FLIN..... PREIGNITION REACTANT TEMPERATURE


C              PARAMETERS EVALUATED
C
C         DVT  .... DV/DT (M**3/S), (RATE OF CHANGE OF VOLUME
C                 FOR A SINGLE BURNING CELL AS A FUNCTION
C                 OF TIME)
C         D2VT .... D**V/DT**2 (M**3/S**2), (DERIVATIVE  OF
C                 DV/DT AS A FUNCTION OF TIME)
C         PST..... ACOUSTIC PRESSURE (N/M**2) AS A FUNCTION
C                 OF TIME FOR A SINGLE BURNING CELL
C         SPL..... SOUND PREESSURE LEVEL SPECTRUM, (NONDIMEN
C                 -SIONAL LINE SPECTRUM AS A FUNCTION
C                 OF FREQUENCY)
C         OASPL ... OVER-ALL SOUND PRESSURE LEVEL, (NONDIMEN
C                 SIONAL)
```

```
C       ETA ..... THERMOACOUSTIC EFFICIENCY
C       POWW  ... ACOUSTIC POWER (WATTS)


C       INTERMEDIATE PARAMETERS
C
C       RI ..... INITIAL RADIUS OF THE CELL (M)
C       RS ..... CELL RADIUS AT THE BEGINING OF
C            SURFACE BURNING (M)
C       NI ..... INSTANTANEOUS NUMBER OF CELLS
C       A,B ..... CONSTANTS IN THE DV/DT EXPRESSION
C       TTR ..... TRANSITION TIME (S)
C       TS ..... SURFACE BURNING TIME (S)
C       TTT ..... TOTAL BURNING TIME (S)
C       AN,BN ... FREQUENCY DEPENDENT VARIABLES USED TO
C            EVALUATE SPL SPECTRUM
C       H ..... HEAT PRODUCTION RATE


C          INDEPENDENT PARAMETERS
C
C       CF ..... CENTRAL FREQUENCIES IN 1/3 OCTAVE BAND (HZ)
C       F ..... FREQUENCY (HZ)
C       T ..... TIME (S)
C       PR ..... REFERENCE ACOUSTIC PRESSURE (N/M**2)
C       BF ..... FREQUENCIES ENVELOPING THE 1/3 OCTAVE BANDS
C       PI ..... 22./7.
C       NN ..... NUMBER OF HARMONICS WHERE CALCULATIONS STOP
C       IA,IB,IC,ID,IE..... INTEGERS TO IDENTIFY THE USER PROMTS

C          REGRESSION ARRAYS INVOLVED
C
C       UUU,UU....ARRAYS FOR CONVECTIVE VELOCITY
C       DDD,DD....ARRAYS FOR BURNER DIAMETER
C       EEE,EE....ARRAYS FOR EXPANSION RATIO
C       SLLL,SLL..ARRAYS FOR FLAME SPEED
C       PPP .....ARRAY OF PREDICTED POWER
C       PRWW.....ARRAY OF REGRESSION POWER
C       BB.....SOLUTION OF REGRESSION
C       X,DBD,R,SCPE,XMAX,XMIN...EXTERNAL ARRAYS FOR RGIVN


C       THIS PART OF THE PROGRAM WILL GIVE DIMENSIONS TO ALL
C       ARRAYS INVOLVED IN THE SOLUTION

      DIMENSION DV(500),PST(500)
      DIMENSION FN(900),AN(900),BN(900)
      DIMENSION PF(900),PSF(900),PAF(900)
      DIMENSION BF(900),CF(900),CFK(900),PBAND(900),DB(900)
      DIMENSION POWER(200),BCF(200),UN(200),UA(200)
      DIMENSION POGIL(200)
      DIMENSION DDD(6,6,6,6),UUU(6,6,6,6),SLLL(6,6,6,6),EEE(6,6,6,6)
      DIMENSION PPP(6,6,6,6),FFF(6,6,6,6),POWR(6,6,6,6)
      DIMENSION UU(4),EE(4),SLL(4),DD(4)
      DIMENSION X(81,5),BB(5,1),DBD(5),R(5,5),SCPE(1,1),XMAX(5),XMIN(5)

c       FOLLOWING STEP DEFINES THE EXTERNAL SUBROUTINES
C       WHICH SUBSEQUENTLY WILL BE USED TO EVALUATE THE
C       REGRESSION FIT FOR SOUND POWER

      EXTERNAL AMACH,RGIVN,UMACH,WRRRN

C       FOLLOWING STEPS PROMPT THE USER TO FEED IN THE NECESSARY
C       INFORMATION FOR WHICH THE PROGRAM IS DESIRED TO RUN.
C       ACCORDING TO THE INFORMATION FED IN, THESE STEPS TAKE
C       AN EXIT TO EXECUTE THE DESIRED ACTIONS OR FURTHER PROMPT
C       THE USER FOR MORE INFORMATION.

 10   CONTINUE
      STDE=0.
      CFFP=0.
      WRITE(6,*)
```

```
      WRITE(6,*)'       DO YOU WANT TO...'
      WRITE(6,*)'       DEVELOP REGRESSION FIT FOR SOUND POWER?'
      WRITE(6,*)
      WRITE(6,*)'       ENTER: <1> FOR YES, <2> FOR NO'
      READ(5,*)IA
      RHO = 1.21
      FR = 9.47
      DP = 1.
      CSOU = 343.
      QQ = 3.58*10.**7
      WRITE(6,*)
      IF (IA .EQ. 1) GO TO 11
      WRITE(6,*)'       DO YOU WANT TO...'
      WRITE(6,*)'       EVALUATE POWER, THERMOACOUSTIC EFFICIENCY'
      WRITE(6,*)'       PEAK FREQUENCY AND OASPL FOR A SINGLE CASE'
      WRITE(6,*)
      WRITE(6,*)'       ENTER: <1> FOR YES, <2> FOR NO'
      READ(5,*)IB
      WRITE(6,*)
      WRITE(6,*)'       DO YOU WANT TO...'
      WRITE(6,*)'       OBTAIN LINE SPECTRUM FOR A SINGLE'
      WRITE(6,*)'       BURNING CELL?'
      WRITE(6,*)
      WRITE(6,*)'       ENTER: <1> FOR YES, <2> FOR NO'
      READ(5,*)IC
      WRITE(6,*)
      WRITE(6,*)'       DO YOU WANT TO...'
      WRITE(6,*)'       OBTAIN 1/3 OCTAVE BAND FOR A SINGLE'
      WRITE(6,*)'       BURNING CELL?'
      WRITE(6,*)
      WRITE(6,*)'       ENTER: <1> FOR YES, <2> FOR NO'
      READ(5,*)ID
      WRITE(6,*)
      WRITE(6,*)'       DO YOU WANT TO...'
      WRITE(6,*)'       OBTAIN DV/DT VS. TIME, AND PRESSURE'
      WRITE(6,*)'       VS. TIME PLOTS FOR A SINGLE BURNING CELL?'
      WRITE(6,*)
      WRITE(6,*)'       ENTER: <1> FOR YES, <2> FOR NO'
      READ(5,*)IE
      WRITE(6,*)
      IF (IA .EQ. 2) GO TO 12
   11 CONTINUE
      WRITE(6,*)'       PLEASE ENTER U(MIN),U(MAX) '
      WRITE(6,*)'  (BOUNDARY VALUES OF CONVECTIVE VELOCITY (IN M/S))'
      READ(5,*)UMIN,UMAX
      WRITE(6,*)
      UU(1) = UMIN
      UU(2) = (UMIN + UMAX)/2.
      UU(3) = UMAX
      DO 13 K = 1,3
      DO 14 L = 1,3
      DO 15 M = 1,3
      DO 16 N = 1,3
      UUU(K,N,M,L) = UU(N)
   16 CONTINUE
   15 CONTINUE
   14 CONTINUE
   13 CONTINUE

      WRITE(6,*)'       PLEASE ENTER D(MIN),D(MAX)'
      WRITE(6,*)'  (BOUNDARY VALUES OF BURNER DIAMETER, (IN CM))'
      READ(5,*)DMIN,DMAX
      WRITE(6,*)
      DD(1) = DMIN/100.
      DD(2) = (DMIN + DMAX)/(2.*100.)
      DD(3) = DMAX/100.
      DO 17 K = 1,3
      DO 18 L = 1,3
      DO 19 N = 1,3
      DO 20 M = 1,3
      DDD(K,N,M,L) = DD(M)
   20 CONTINUE
```

```
19  CONTINUE
18  CONTINUE
17  CONTINUE

    WRITE(6,*)'       PLEASE ENTER SL(MIN),SL(MAX)'
    WRITE(6,*)'     (BOUNDARY VALUES OF FLAME SPEED (IN CM/S))'
    READ(5,*)SLMIN,SLMAX
    WRITE(6,*)
    SLL(1)=SLMIN/100.
    SLL(2)=(SLMIN+SLMAX)/(2.*100.)
    SLL(3)=SLMAX/100.
    DO 21 K=1,3
    DO 22 M=1,3
    DO 23 N=1,3
    DO 24 L=1,3
    SLLL(K,N,M,L)=SLL(L)
24  CONTINUE
23  CONTINUE
22  CONTINUE
21  CONTINUE

    WRITE(6,*)'       PLEASE ENTER E(MIN),E(MAX)'
    WRITE(6,*)'   (BOUNDARY VALUES OF EXPANSION RATIO)'
    READ(5,*)EMIN,EMAX
    WRITE(6,*)
    EE(1)=EMIN
    EE(2)=(EMIN+EMAX)/2.
    EE(3)=EMAX
    DO 25 M=1,3
    DO 26 N=1,3
    DO 27 L=1,3
    DO 28 K=1,3
    EEE(K,N,M,L)=EE(K)
28  CONTINUE
27  CONTINUE
26  CONTINUE
25  CONTINUE

    WRITE(6,*)' U   D   E   SL    SP    ETA  OSPL   FREQP'
    WRITE(6,*)

    MM=1
    DO 29 L=1,3
    DO 30 M=1,3
    DO 31 K=1,3
    DO 32 J=1,3

C       THIS PART OF THE PROGRAM WILL GIVE VALUES TO ALL
C       THE EXPERIMENTAL PARAMETERS USED
C
    U=UUU(K,L,M,J)
    D=DDD(K,L,M,J)
    SL=SLLL(K,L,M,J)
    E=EEE(K,L,M,J)


C       THIS PART OF THE PROGRAM WILL GIVE INPUT VALUES OF
C       THE BURNER AND FUEL PARAMETERS

    IF (IA .EQ. 1)THEN
    GO TO 33
    ENDIF
12  WRITE(6,*)'       ENTER CONVECTIVE VELOCITY U (M/S)'
    READ(5,*)U
    WRITE(6,*)
    WRITE(6,*)'       ENTER BURNER DIAMETER D (CM)'
    READ(5,*)D
    D=D/100.
    WRITE(6,*)
    WRITE(6,*)'       PLEASE ENTER INITIAL REACTANT TEMP. IN KELVINS'
    WRITE(6,*)'       (ENTER <1> FOR DEFAULT (298 K))'
    READ(5,*)GG
```

```
WRITE(6,*)

IF (GG .EQ. 1) THEN
FLIN = 298.
ELSE
FLIN = GG
ENDIF

WRITE(6,*)'      PLEASE ENTER SOUND VELOCITY IN MEDIUM'
WRITE(6,*)'      (ENTER <1> FOR DEFAULT (343 M/S))'
READ(5,*)HH
WRITE(6,*)

IF (HH .EQ. 1) THEN
CSOU = 343.
ELSE
CSOU = HH
ENDIF

WRITE(6,*)'      PLEASE ENTER MEDIUM DENSITY'
WRITE(6,*)'      (ENTER <1> FOR DEFAULT (1.21 KG/M**3))'
READ(5,*)RR
WRITE(6,*)

IF (RR .EQ. 1.) THEN
RHO = 1.21
ELSE
RHO = RR
ENDIF

WRITE(6,*)'      PLEASE ENTER DISTANCE OF OBSERVATION POINT'
WRITE(6,*)'      (ENTER <1> FOR DEFAULT (1 M))'
READ(5,*)DOP
WRITE(6,*)

IF (DOP .EQ. 1.) THEN
DP = 1.
ELSE
DP = DOP
ENDIF

WRITE(6,*)'      ENTER FUEL TYPE FROM THE FOLLOWING OPTIONS...'
WRITE(6,*)'      ENTER <1> FOR METHANE'
WRITE(6,*)'      ENTER <2> FOR CARBON MONOXIDE'
WRITE(6,*)'      ENTER <3> FOR HYDROGEN'
WRITE(6,*)'      ENTER <4> FOR ACETYLENE'
WRITE(6,*)'      ENTER <5> FOR OTHER THAN ABOVE'
READ(5,*)IF
IF (IF .EQ. 1) THEN
SL = .5
FR = 9.47
FLTP = 2210.
QQ = 3.58*10.**7
ENDIF

IF (IF .EQ. 2) THEN
SL = .4
FR = 2.38
FLTP = 2400.
QQ = 5.86*10.**6
ENDIF

IF (IF .EQ. 3) THEN
SL = 2.5
FR = 2.88
FLTP = 2400.
QQ = 1.08*10.**7
ENDIF

IF (IF .EQ. 4) THEN
SL = 1.4
FR = 11.9
```

```
      FLTP = 2600.
      QQ = 5.61*10.**7
      ENDIF

      IF (IF .EQ. 5) THEN
      WRITE(6,*)' PLEASE ENTER THE FOLLOWING INFORMATION ABOUT THE FUEL'
      WRITE(6,*)
      WRITE(6,*)'       LAMINAR FLAME SPEED? (IN CM/S)'
      READ(5,*)SL
      SL = SL/100.
      WRITE(6,*)
      WRITE(6,*)'       STOCHIOMETRIC AIR-FUEL RATIO (VOLUMETRIC)?'
      READ(5,*)FR
      WRITE(6,*)
      WRITE(6,*)'       FLAME TEMPERATURE? (IN KELVINS)'
      READ(5,*)FLTP
      WRITE(6,*)
      WRITE(6,*)'       HEAT OF REACTION (IN J/M**3) X 10 ** -7 ?'
      READ(5,*)QQ
      QQ = QQ*10.**7
      WRITE(6,*)
      ENDIF

      E = FLTP/FLIN

      WRITE(6,*)
      WRITE(6,*)'OUTPUT.....'
      WRITE(6,*)
   33 CONTINUE
      NN = 500
      NNN = 50.
      PI = 22./7.

C          THIS PART OF THE PROGRAM EVALUATES THE INTERMEDIATE
C          PARAMETERS WHICH ARE DIRECTLY RELATED TO FUNDAMENTAL
C          BURNER AND FUEL VARIABLES

      RI = SQRT(3./8.)*D
      TTR = 2.*SQRT(3./8.)*D/U
      H = (PI/4.)*U*D**2*QQ/FR
      CN = U/(2.*SL)


C        1. IN THIS FIRST PHASE OF PROGRAMMING, THE
C           RADIUS "RS" AT THE BEGINING OF SURFACE
C           BURNING IS EVALUATED.

C       1.1  IN THE FIRST STEP THE INITIAL VALUES OF
C            HIGHEST POSSIBLE RS (RSH) AND LOWEST
C            POSSIBLE RS (RSL) ARE GIVEN.  ALSO A
C            INITIAL VALUE OF RS (RSG) IS GUESSED.

      RSH = RI
      RSL = 0.
      RSG = RI

C       1.2  LOOP FOR THE CALCULATION OF "RS" BEGINS
C            IN THIS STEP.  THE FIRST STEP IS TO CHECK
C            THE CONVERGENCE OF GUESSED VALUE OF "RS".

   34 IF (RSG .GT. RI .OR. RSG .LT. 0.1*RI) THEN
      WRITE(6,*)'PROGRAM NOT CONVERGING. INPUT DATA UNREASONABLE?'
      GO TO 35
      ENDIF

C       1.3  SURFACE BURNING TIME AND TOTAL BURNING TIME
C            ARE EVALUATED IN TERMS OF THE GUESSED VALUE
C            OF RADIUS AT THE BEGINING OF SURFACE BURNING

      TS = RSG/SL
      TTT = TTR + TS
      EPS = TTR/TTT
```

```
C     1.4  CONSTANTS A AND B ARE EVALUATED.

      A=-8.*PI*(E-1.)*TS*TTT*SL**3/(TTR**3)
      B=4.*PI*(E-1.)*TS*SL**3*(TS+2.*TTT)/(TTR**2)

C     1.5  THE DIFFERNCE "RSD" BETWEEN THE GUESSED VALUE OF RS
C          AND THE CALCULATED VALUE OF RS (FROM THE GUESS)
C          IS EVALUTED.  THIS DIFFERENCE IS CHANGED INTO
C          PERCENTAGE DEVIATION FROM THE GUESS.  IF THE CHANGE
C          IS LESS THAN 1%, THEN EXIT IS TAKEN FROM THE LOOP
C          AND THE CURRENT GUESS OF "RS" IS ACCEPTED AS THE
C          FINAL VALUE OF "RS".

      RSD=RSG-(RI**3-3.*TTR**3*(A*TTR/4.+B/3.)/(4.*(E-1.)*PI))**.333
      PD=RSD/RSG
      IF (PD .LT. 0.)THEN
      PD=-1.*PD
      ENDIF
      IF (PD .LE.  .01) THEN
      RS=RSG
      GO TO 36
      ENDIF

C     1.6  IF THE GUESSED VALUE OF "RS" IS LESS THAN THE
C          CALCULATED VALUE, THEN
C     1.6.1  LOWEST POSSIBLE VALUE OF "RS" IS EQUATED TO
C            THE GUESS,
C     1.6.2  A NEW GUESS IS MADE AS A MEAN OF PREVIOUS
C            GUESS AND THE HIGHEST ACCEPTABLE VALUE OF "RS".

      IF (RSD .LT. .0) THEN
      RSL=RSG
      RSG=(RSG+RSH)/2.
      ENDIF

C     1.7  IF THE GUESSED VALUE OF "RS" IS GREATER THAN THE
C          CALCULATED VALUE, THEN
C     1.7.1  HIGHEST POSSIBLE VALUE OF "RS" IS EQUATED TO
C            THE GUESS,
C     1.7.2  A NEW GUESS IS MADE AS A MEAN OF PREVIOUS
C            GUESS AND THE LOWEST POSSIBLE VALUE OF "RS".
C     1.7.3  GO BACK TO THE START OF LOOP

      IF (RSD .GT. .0) THEN
      RSH=RSG
      RSG=(RSG+RSL)/2.
      ENDIF
      GO TO 34
   36 CONTINUE
      BETA=8.*PI*TTT*(E-1.)*SL**3

C          THE FOLLOWING STEPS EVALUATE DV/DT AND RATE
C          OF CHANGE OF DV/DT AS A FUNCTION OF TIME
C          FOR A SINGLE BURNING EDDY

      IF (IA .EQ. 1) GO TO 37
      IF (IE .EQ. 2) GO TO 37
      GB=RHO/(4.*PI*DP)
      IF (IE .EQ. 1) THEN
      WRITE(6,*) 'DV/DT AND PRESSURE VS TIME FOR A SINGLE BURNING EDDY'
      WRITE(6,*)
      WRITE(6,*) 'NONDIMEN. TIME     DV/DT (M**3/S)    PRESS. (N/M**2)'
      WRITE(6,*)
      ENDIF
      DO 38 I=1,NNN
      TAU=FLOAT(I-1)/(NNN-1)
      T=TAU*TTT
      IF(TAU.LT.EPS)THEN
      DV(I)=A*T**3+B*T**2
      PST(I)=GB*(3.*A*T**2+2.*B*T)
      ENDIF
```

```
      IF(TAU.GT.EPS)THEN
      DV(I)=4.*PI*(E-1.)*(TTT-T)**2*SL**3
      PST(I)=GB*8.*PI*(E-1.)*(T-TTT)*SL**3
      ENDIF
      III=1
      IF (IA .EQ. 1) GO TO 39
      IF (IE .EQ. 1) THEN
      WRITE(6,1000) TAU,DV(I),PST(I)
      WRITE(6,*)
 1000 FORMAT(1X,3(F15.6,3X))
      ENDIF
   39 CONTINUE
   38 CONTINUE
   37 CONTINUE
      IF (IA .EQ. 1) GO TO 40
      IF (IB .EQ. 2 .AND. IC .EQ. 2 .AND. ID .EQ. 2 ) GO TO 35
      IF (IC .EQ. 1) THEN
      WRITE(6,*)
      WRITE(6,*)'  LINE SPECTRUM DUE TO A SINGLE BURNING EDDY'
      WRITE(6,*)
      WRITE(6,*)'  FREQ. (KHZ)    PRESS (N/M**2)'
      WRITE(6,*)
      ENDIF
   40 CONTINUE

C       2. THIS PART OF THE PROGRAM OBTAINS LINE SPECTRUM
C          PRODUCED BY A SINGLE CONTINUOUS TRAIN OF EDDIES.

C       2.1 A LOOP IS STARTED FOR THE ORDER N OF THE LINE
C          SPECTRUM. ALL THE VARIABLES DEPENDENT ON "N"
C          TO BE USED FOR THE EVALUATION OF CONSTANTS "AN"
C          AND "BN" ARE EVALUATED.

    41 CONTINUE
      PSUM=0.
      DO 42 N=1,NN
      XX=N
      Q=XX*PI
      TH=Q*EPS
      S=SIN(2.*TH)
      C=COS(2.*TH)
      FN(N)=N/TTT
      IF (FN(N) .GT. 13000.) GO TO 43

C       2.2 "AN" AND "BN" FOR THE GIVEN VALUE OF
C          N ARE EVALUATED.

      AN(N)=3.*A*TTT**2/BETA*((EPS**2/(2.*Q)-1./(4.*Q**3))*S
     1 +EPS/(2.*Q**2)*C)
     1 +2.*B*TTT/BETA*(EPS/(2.*Q)*S-1./(4.*Q**2)+1./(4.*Q**2)*C)
     1 -EPS/(2.*Q)*S-1./(4.*Q**2)*C+1./(4.*Q**2)
     1 -1./(2.*Q)*S

      BN(N)=3.*A*TTT**2/BETA*((-(EPS)**2/(2.*Q)+1./(4.*Q**3))*C
     1 +EPS/(2.*Q**2)*S-1./(4.*Q**3))
     1 +2.*B*TTT/BETA*(-EPS/(2.*Q)*C+1./(4.*Q**2)*S)
     1 +EPS/(2.*Q)*C-1./(2.*Q)-1./(4.*Q**2)*S
     1 -1./(2.*Q)+1./(2.*Q)*C

C          THIS STEP CALCULATES ACOUSTIC PRESSURE
C          AMPLITUDE AT EACH OF THE FREQUENCIES
C          ORDER "N" FOR A SINGLE BURNING CELL. THESE
C          PRESSURE AMPLITUDES ARE THEN MULTIPLIED BY
C          THE NUMBER OF COMPACT NOISE SOURCE REGIONS
C          TO OBTAIN THE TOTAL ACOUSTIC PRESSURE AT EACH
C          HARMONIC FREQUENCY. FINALLY THE LINE SPECTRUM FOR THE
C          SOUND PRESSURE VERSUS FREQUENCY IS PLOTTED.

      PF(N)=2.*SQRT(AN(N)**2+BN(N)**2)
      PSF(N)=RHO*PF(N)*BETA/(4.*PI*DP)
      YYY=0.00
      ZZZ=FN(N)/1000.
```

```
      IF (IA .EQ. 1) GO TO 44
      IF (IC .EQ. 1) THEN
      WRITE(6,2000)ZZZ,PSF(N)
 2000 FORMAT(2X,F7.3,10X,F8.6)
      ENDIF
   44 CONTINUE

C           SUM OF THE SQUARES OF THE PRESSURE AMPLITUDES
C           AT EACH FREQUENCY

      PSUM = PSUM + PSF(N)**2
   42 CONTINUE
   43 CONTINUE
      IF (IB .EQ. 2 .AND. ID .EQ. 2 .AND. IA .EQ. 2) GO TO 35

C           THE FOLLOWING STEPS EVALUATE PRESSURE AMPLITUDE
C           OVERALL SOUND PRESSURE LEVEL, SOUND POWER
C           PRODUCED, AND THERMOACOUSTIC EFFICIENCY

      PAMP = SQRT(PSUM)
      PDB = 20.*LOG10(PAMP/.00002)
      ASPL = 20.*LOG10(PAMP* SQRT(CN)/.00002)
      PRW = 4.*PI*DP**2*PAMP*PAMP*CN/(2.*RHO*CSOU)
      TAE = PRW/H
      IF (IA .EQ. 1) GO TO 45
      IF (IB .EQ. 1 .OR. ID .EQ. 1) GO TO 46
   45 CONTINUE

C           THIS SECTION COVERTS THE ARRAYS OF PREDICTED POWER
C           AND INPUT PARAMETERS INTO CORRESPONDING ARRAYS TO
C           BE USED LATER AS INPUT FOR IMSL SUBROITINE RGIVN

      PPP(K,L,M,J) = PRW
      X(MM,1) = LOG10(UUU(K,L,M,J))
      X(MM,2) = LOG10(DDD(K,L,M,J))
      X(MM,3) = LOG10(SLLL(K,L,M,J))
      X(MM,4) = LOG10(EEE(K,L,M,J))
      X(MM,5) = LOG10(PPP(K,L,M,J))
      MM = MM + 1
      NNNN = 1
   46 CONTINUE

C           THIS PART OF THE PROGRAM CONVERTS THE LINE SPECTRUM
C           GIVEN EARLIER INTO 1/3 OCTAVE BANDS.

C           IN THIS PART BOUNDARY FREQUENCIES OF THE
C           1/3 OCTAVE BANDS ARE DEFINED

      BF(1) = 16.
      BF(2) = 20.
      DO 47 N = 3,32
      BF(N) = 45.*2.**(.33*(N-3))
   47 CONTINUE

C           EVALUATION OF CENTRAL FREQUENCIES OF 1/3 OCTAVE BANDS

      CF(1) = 8.
      DO 48 N = 2,32
      CF(N) = SQRT(BF(N-1)*BF(N))
   48 CONTINUE
      CFP = 0.
      PMAX = 0.

C           INITIALIZATION OF PRESSURE AMPLITUDES IN EACH BAND

      DO 49 N = 1,32
      PBAND(N) = 0.
   49 CONTINUE

C           IN THIS SECTION NET PRESSURE AMPLITUDE IN EACH
C           1/3 OCTAVE IS EVALUATED AS THE MEAN SQUARE
C           ROOT OF THE PRESSURES LYING INSIDE EACH OCTAVE
```

```
C         ALSO THIS AMPLITUDE IS NONDIMENSIONALIZED
C         EXPRESSED IN DECIBELS

      DO 50 I=1,31
      DO 51 N=1,500
      IF(FN(N).GE.BF(I) .AND. FN(N).LE.BF(I+1)) THEN
      PBAND(I)=PBAND(I)+PSF(N)**2
      ENDIF
   51 CONTINUE
   50 CONTINUE
      IF (IA .EQ. 1) GO TO 52
      IF (ID .EQ. 1) THEN

C         THIS SECTION GIVES HEADINGS TO THE 1/3 OCTAVE RESULTS

      WRITE(6,*)
      WRITE(6,*)'      1/3 OCTAVE.....'
      WRITE(6,*)
      WRITE(6,*)' FREQ (KHZ)   PRESS (DB)   PRESS (N/M**2)'
      WRITE(6,*)
      ENDIF
   52 CONTINUE
      DO 53 N=1,31
      PBAND(N)=SQRT(PBAND(N))
      IF(PBAND(N).EQ.0.)THEN
      GO TO 53
      ENDIF
      DB(N)=20.*LOG10(PBAND(N)/.00002)

C         THIS SECTION PLOTS THE 1/3 OCTAVE BAND
C         FOR 1) PRESSURE AMPLITUDES 2) PRESSURE
C         AMPLITUDES IN DECIBELS VERSUS THE
C         CORRESPONDING CENTRAL FREQUENCIES

      CFK(N)=CF(N)/1000.
      IF (IA .EQ. 1) GO TO 54
      IF (ID .EQ. 1) THEN
      WRITE(6,3000)CFK(N),DB(N),PBAND(N)
      WRITE(6,*)
 3000 FORMAT(2X,F7.4,6X,F6.2,6X,F6.4)
      ENDIF
   54 CONTINUE

C         THIS SECTION EVALUATES THE PEAK FREQUENCY AND
C         THE CORRESPONDING PRESSURE AMPLITUDE

      IF(PBAND(N).GE.PMAX)THEN
      PMAX=PBAND(N)
C     PCF=CF(N)
C     CFP=1./TTT
      CFP=CF(N)
      ENDIF
   53 CONTINUE

C         THIS SECTION WRITES DOWN THE OVERALL SOUND PRESSURE
C         LEVEL, TOTAL SOUND PRESSURE, THE ACOUSTIC
C         POWER AND PEAK FREQUENCY FOR A SINGLE RUN.

      IF (IA .EQ. 1) GO TO 55
      IF (IB .EQ. 1) THEN
      WRITE(6,*)
      WRITE(6,*)'SOUND POWER =',PRW,'W'
      WRITE(6,*)
      WRITE(6,*)'THERMOACOUSTIC EFFICIENCY =',TAE
      WRITE(6,*)
      WRITE(6,*)'OVER-ALL SOUND PRESSURE LEVEL =',ASPL,'DB'
      WRITE(6,*)
      WRITE(6,*)'PEAK FREQUENCY =',CFP,'HZ'
      ENDIF
   55 CONTINUE
```

```
C          THIS SECTION WRITES DOWN THE OVERALL SOUND PRESSURE
C          LEVEL, TOTAL SOUND PRESSURE, THE ACOUSTIC
C          POWER AND PEAK FREQUENCY FOR MULTIPLE RUNS

      IF (IA .EQ. 1) THEN
      TAE=TAE*10.**8
      D=D*10.**2+.5
      SL=SL*10.**2+.5
      CFFP=CFP+CFFP
      NU=U
      ND=D
      NSL=SL
      NE=E
      NC=CFP
      NA=ASPL
      NT=TAE
      NP=PRW
      WRITE(6,4000)NU,ND,NE,NSL,PRW,NT,NA,NC
 4000 FORMAT(2X,I2,4X,I1,4X,I2,4X,I2,4X,F6.4,4X,I3,4X,I3,4X,I4)
      WRITE(6,*)
      ENDIF
C     FFF(K,L,M,J)=CFP
C     X(MM,5)=LOG10(FFF(K,L,M,J))
C     MM=MM+1
      IF (IA .EQ. 2) GO TO 35
      PMAX=0.
   32 CONTINUE
   31 CONTINUE
   30 CONTINUE
   29 CONTINUE

C          THIS SECTION PERFORMS THE REGRESSION FOR THE
C          SOUND POWER FOR 81 RUNNING SETS AS SPECIFIED
C          IN THE INPUT.  SUBROUTINE RGIVN FROM IMSL
C          PERFORMS THE REGRESSION

      IDO=0
      NROW=81
      NCOL=5
      LDX=81
      INTCEP=1
      IIND=-4
      IDEP=-1
      IFRQ=0
      IWT=0
      ISUB=1
      TOL=100.0*AMACH(4)
      LDB=5
      LDR=5
      LDSCPE=1
      NDEP=1
      CALL RGIVN (IDO, NROW, NCOL, X, LDX, INTCEP, IIND, INDIND, IDEP,
     1          INDDEP, IFRQ, IWT, ISUP, TOL, BB, LDB, R, LDR, DBD,
     1          IRANK, DFE, SCPE, LDSCPE, NRMISS, XMIN, XMAX)

C          THIS SECTION COMPARES THE PREDICTED RESULTS WITH THE
C          LITERATURE.  IT ALSO GIVES THE MEAN PEAK FREQUENCY
C          OF THE PREDICTED REGRESSION.  FINALLY IT GIVES THE
C          ACTUAL PREDICTED RESULTS AND THE CORRESPONDING
C          REGRESSION RESULTS FOR SOUND POWER

      BB(1,1)=10.**BB(1,1)
      WRITE(6,*)
      WRITE(6,*)'CONSTANT MULTIPLIER =',BB(1,1)
      WRITE(6,*)
      WRITE(6,*)'EXPONENT OF VELOCITY =',BB(2,1)
      IUR=(BB(2,1)-3.)*100./3.
      IUL=(BB(2,1)-2.67)*100./2.67
      WRITE(6,*)'% DIFF. FROM LITER. FOR FUEL-LEAN PREMIXED FLAME =',IUL
      WRITE(6,*)'% DIFF. FROM LITER. FOR FUEL-RICH PREMIXED FLAME =',IUR
      WRITE(6,*)
      WRITE(6,*)'EXPONENT OF BURNER DIAMETER =',BB(3,1)
```

```
      IDR = (BB(3,1)-2.00)*100./2.00
      IDL = (BB(3,1)-2.81)*100./2.81
      WRITE(6,*)'% DIFF. FROM LITER. FOR FUEL-LEAN PREMIXED FLAME = ',IDL
      WRITE(6,*)'% DIFF. FROM LITER. FOR FUEL-RICH PREMIXED FLAME = ',IDR
      WRITE(6,*)
      WRITE(6,*)'EXPONENT OF FLAME SPEED = ',BB(4,1)
      ISL = (BB(4,1)-1.83)*100./1.83
      WRITE(6,*)'% DIFF. FROM LITER. FOR FUEL-LEAN PREMIXED FLAME = ',ISL
      WRITE(6,*)
      WRITE(6,*)'EXPONENT OF EXPANSION RATIO = ',BB(5,1)
      WRITE(6,*)
      CFFP = (CFFP)/81.
      WRITE(6,*)'MEAN PEAK FREQUENCY = ',CFFP
      WRITE(6,*)
      WRITE(6,*)' CALCULATED SP    REGRESSION SP'
      WRITE(6,*)
      DO 56 L = 1,3
      DO 57 M = 1,3
      DO 58 K = 1,3
      DO 59 J = 1,3
      U = UUU(K,L,M,J)
      D = DDD(K,L,M,J)
      SL = SLLL(K,L,M,J)
      E = EEE(K,L,M,J)
      IJ = 1
      POWR(K,L,M,J) = BB(1,1)*U**BB(2,1)*D**BB(3,1)*SL**BB(4,1)*E**BB(5,1)
      WRITE(6,5000)PPP(K,L,M,J),POWR(K,L,M,J)
      WRITE(6,*)
 5000 FORMAT(2X,F10.6,6X,F10.6)
      STDE = (PPP(K,L,M,J)/POWR(K,L,M,J)-1.)**2 + STDE
   59 CONTINUE
   58 CONTINUE
   57 CONTINUE
   56 CONTINUE

C          THIS SECTION GIVES THE STANDARD DEVIATION IN THE
C          LITERATURE, AND THAT GIVEN BY THIS MODEL

      STDE = SQRT(STDE/81.)*100.
      WRITE(6,*)'STANDARD DEVIATION = ',STDE,'PERCENT'
      WRITE(6,*)
      WRITE(6,*)'STANDARD DEVIATION IN LITERATURE = 43 PERCENT'
   35 WRITE(6,*)

C          THIS SECTION PROMPTS THE USER FOR A SECOND RUN

      WRITE(6,*)'    DO YOU WANT TO RUN AGAIN'
      WRITE(6,*)
      WRITE(6,*)'    ENTER <1> FOR YES, <2> FOR NO'
      READ(5,*)IRUN
      IF(IRUN .EQ. 1) GO TO 10
      STOP
      END
```

The vita has been removed from the scanned document